RUSSIAN GEOGRAPHICAL SOCIETY

FACULTY OF GEOGRAPHY,
LOMONOSOV MOSCOW STATE UNIVERSITY

INSTITUTE OF GEOGRAPHY,
RUSSIAN ACADEMY OF SCIENCES

No. 03 (v. 08)
2015

GEOGRAPHY
ENVIRONMENT
SUSTAINABILITY

EDITORIAL BOARD

CONTENTS

Graziella Ferrara
Professor at Suor Orsola Benincasa of Naples

EUROPEAN TRANSPORT NETWORK EFFECTS ON REGIONAL GEOGRAPHY

ABSTRACT. The transport network policy aims to create a network of roads, railways, airlines, inland waterways and maritime transport and intermodal platforms extended to all European States. It has to improve connections between different modes of transport establishing a European network by 2050. When it will be completed the great majority of Europe's businesses will be no more than 30 minutes' travel time from this comprehensive network.

KEY WORDS: Economic Geography, Firms Strategies, Management, Europe

INTRODUCTION

In 1990s EU Member States decided to realize a trans-European network policy in the transport sector (TEN-T) in order to promote and strengthen transport chains for passenger and freight. The need of such network has been enhanced by the geographical extension of EU as a result of four enlargements, Europe's increasing responsibility at global level and revolutions in the field of Information and Communication Technologies.

The first guidelines for the development of TEN-T established a master plan connecting national networks of all transport modes. These guidelines constituted a reference framework for Member States infrastructure policy. In 2009 the European Commission launched a new policy framework, established as a result of several reviews, with several progress in the areas of governance, legal and network. In 2011 the European Commission adopted a package for a new transport infrastructure policy that comprises a proposal for the revision of the TEN-T guidelines and a proposal for a Connecting Europe Facility (CEF). Since 2014, the European Union has a new transport infrastructure policy that connects the continent between East and West, North and South. This policy aims to close the gaps between Member States' transport networks, remove bottlenecks that hamper the smooth functioning of the internal market and overcome technical barriers such as incompatible standards for

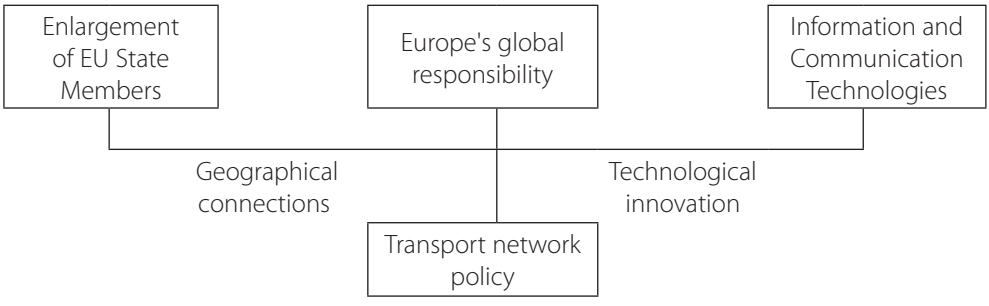

Fig. 1. Factors affecting European Transport Network Policy

railway traffic. It has several effects on regional geography and firms strategies. However, despite of the relevance of such topic few articles have been developed from researchers. At the aim to fill this literature gap next sections evidence European Transport Network effects on regional geography and firms strategies.

REGIONAL GEOGRAPHY

In the 80's, transport systems in Europe was developed along national lines with poor interconnections among Regions (Abraham and Roumpuy van, 1995; Barker and Kohler 1998, Beaverstock 2002). It affected economic growth of both regions and firms. Since the 90s, Transport European (TEN-T) Network policy was aimed to support the development of key European infrastructure projects. This projects aims at fostering the social, economic and territorial cohesion of the EU and inure to the benefit of its population [Alderighi et al. 2007, Camagni 1997, Allen 1999, Antonelli 1995, Aydalot 1986, Bakis 1981]. The policy fosters the implementation of a comprehensive network to be completed by 2050 and a core network to be completed by 2030 [Ashworth and Voogd 1995, Bathelt and Glukler 2003, ASSOCIAZIONE ITALIANA GEOMARKETING 2005]. The first one aims to ensure full coverage of the EU and accessibility of all regions, while the second one aims to prioritize the most important links and nodes of the TEN-T. Both of them include road, rail, air, inland waterways and maritime transport, as well as intermodal platforms [Batowski and Pastuszak 2008, Capello 2004, Batten 1995, Bramanti and Ratti 1997]. They will affect 83 main European seaports, by rail and road links, 37 airports by rail links to major cities, 15000 km of rail lines converted to high speed and 35 large cross-border projects to reduce bottlenecks.

The Core Network has been intended to eliminate bottlenecks, to modernize infrastructure and to streamline cross-border operations of passenger and freight transport throughout the EU, in order to improve the links between the different modes of transport. The implementation of the core network can be facilitated using a corridor approach. Corridors provide the basis for the co-ordinated development of infrastructure that bring together the Member States as well as the users. Each corridor must include three modes, three Member States and two cross-border sections [Beckmann and Thisse 1986, Benner 2003, Berry 1976, Berry et al., 1993]. Specifically, the Scandinavian-Mediterranean Corridor is the largest of the TEN-T core network corridors. It covers seven EU Member States and Norway linking the major urban centres of Germany, Italy and Scandinavia that represent the nodes of a crucial axis for the European economy. The regions along this corridor constitute an important socio-economic area within the European Union. Linear modes of transport that are assigned to the corridor are mainly rail and road while the connections Finland and Italy cross the sea. The other dimension of the corridor is composed of airports, seaports and rail-road terminals of the core network. For modal interconnection as well as the connection of the trans-European transport network with infrastructure for local and regional traffic, urban nodes are of specific importance. The North Sea–Baltic Corridor is 3.200 km long. With 16 airports, 13 seaports, 18 inland ports, and 17 railroad terminals, it has the potential of becoming one of the most economically diverse Corridors in the European Union. It connects Helsinki, Tallinn, Riga, Vilnius, Warsaw, Berlin, Brussels and Amsterdam. It connects also Europe's leading seaports in the west to the fastest developing region in the EU–the Baltic Sea Macro Region in the north/east. It has an effective inland waterways network stretching from the North Sea ports to Berlin and includes several of the leading logistics hot spots in Europe [Bonavero et al. 1999, Cappelin and Batey 1993, Brunet 1989, Derudder et al. 2007, Bonarich 2007).

The North-Sea Mediterranean Corridor connects UK and Ireland to the Continent. It is an extensive and complex corridor containing densely populated regions of long-standing economic importance and with a high degree of urbanization, along with more peripheral and less densely populated regions in the west and north. There are also contrasts in relation

to cultures for infrastructure investment within the Corridor. The continental Member States and Ireland tend to invest in transport infrastructure using public sector resources. It overlaps with the North Sea Baltic and Rhine-Alpine corridors in the Netherlands and Belgium, the Atlantic Corridor in Northern France and the Mediterranean Corridor in Southern France, and it is the only core network corridor reaching the UK and Ireland.

The Baltic-Adriatic Corridor involves six Member States, Poland, Czech Republic, Slovakia, Austria, Italy and Slovenia. The 1,800 km long Corridor allows for more possible itineraries between the Baltic and Adriatic Basins. The Baltic-Adriatic axis is one of the few corridors that do not include inland waterways. Excluding inland waterways at present, the backbone of the Corridor is therefore based on its railway and road routes, its urban nodes and ports, airports and rail-road terminals being interconnected only by rail and road infrastructure. The Corridor encompasses a total of 13 urban nodes and airports, 10 ports and nearly 30 rail-road terminals. The BA Corridor railway network corresponds mostly to the Baltic-Adriatic Rail Freight Corridor [Bugayevskiy and Snyder 1995, Derudder 2006, Burrough and McDonnel 1998, Cohen et al., 2002]. The length of Orient / East-Med Corridor infrastructure sums up to approximately 5.900 km (rail), 5.600 km (road) and 1.600 km. The number of core urban nodes along the Orient/East Med corridor is 15, with the majority located in Germany and Greece, as well as one per other Member State. The same number applies for core airports, from which 6 are dedicated airports to be connected with high-ranking rail and road connections until 2050. Furthermore, 10 Inland ports and 12 Maritime ports are assigned to the corridor, as well as 25 Road-Rail terminals. Several segments of the Orient/East Med Core Network Corridor are coinciding with other of the 9 Core network corridors, such as the Rhine-Danube Corridor and on shorter sections, the North Sea/Baltic corridor, the Scandinavian-Mediterranean corridor and the Baltic Adriatic corridor [Crevoisier and Camagni 2000, Cohen-Blankshtain and Nijkamp 2004, Castells 2001, Choi et al. 2006, Castells 1989].

The Rhine-Alpine Corridor stretches from the northern seaports in The Netherlands and Belgium to the Mediterranean basin in Genoa right through most of the important and economically strong urban regions of Europe. Countries directly involved are Netherlands, Belgium, Germany, Switzerland, Northern Italy and the eastern part of France, namely the Strasbourg area and Luxembourg. Altogether, more than 70 million people are living, working and consuming in the catchment area of the Rhine-Alpine Corridor. Lading manufacturing and trading companies are located along the corridor with production plants and distribution centres. Important industries are the steel industry, chemical and petroleum industry, car producers as well as power plants. The river Rhine is an important route for the containers and the transport of bulk commodities especially between the North Sea ports and Germany, France and Switzerland [Derudder and Taylor 2005, Gastner and Newman 2005, Doyle et al. 2005, Friedmann 1986]. Atlantic Corridor links the Iberian Peninsula ports of Algeciras, Sines, Lisboa, Leixões (Porto) and Bilbao through western France to Paris and Normandy and further east to Strasbourg and Mannheim. With a priority attention given to high speed rail lines and parallel conventional ones, the Corridor will provide for the continuity of the rail network between the Portugal, Spain, France and Germany. The Atlantic Corridor has a relevant maritime dimension since it is linked to the crossroad of global maritime routes notably toward North and South America, Neighbourhood countries and Africa.

The Rhine-Danube Corridor is the main east-west link between continental European countries connecting France and Germany, Austria, Slovakia, Hungary, Croatia, Romania and Bulgaria all along the Main and Danube rivers to the Black Sea by improving rail and inland waterway interconnections. The parts in the Czech Republic and Slovakia are also

covered by the Rail Freight corridor. The Member States Bulgaria and Croatia are only included in the Inland Waterways corridor. This concerns ports and inland waterways of the rivers Danube and Sava [Derudder et al. 2003, Gorman and Kulkarni 2004, Derudder and Witlox 2008, George 1968]. The Mediterranean Corridor will link ports in the south-western Mediterranean region to the Ukrainian border with Hungary, following the coastlines of Spain, France, and crossing the Alps towards the east. Given its nature, the Mediterranean corridor is expected to become a major European corridor, linking South-Western and Eastern EU countries. In particular, it represents a key access gateway to Ukraine and therefore it has a high potential in diverting part of the Western Europe-Asia traffic flows, which presently are ensured by the road mode. Therefore the traffic development along this corridor has to be interpreted also in terms of significant potential increase in the rail market share and the consequent reduction of environmental externalities in terms of reduction of gas emissions and roads and highways congestion [Derudder and Witlox 2005, Gillen and Morrison 2005, Gottmann 1983].

FIRMS STRATEGIES

As a center of intersection of several Corridors, Hungary can become a global hub. This connection has a potential to develop a partnership between the two convenient intermodal freight hub, the airport and seaport, for the inter-modality of transport of goods. In fact, the two intermodal freight hubs are reciprocally connected for both the inter-modality and partly because the goods that arrive at the port of Trieste can be routed on the intermodal freight hub of Budapest where they can be processed and distributed later. The rail corridors for the interconnection between the EU Countries and Easters Countries will give Budapest the role of bridge between the old and the new Europe. Another element of high strategic value is represented by the existing connection between Budapest and the port of Trieste [Grubesic and O'Kelly 2002, Hendricks et al. 1995]. Long-distance flights could arrive in Budapest where the discharged goods could be sent to final destinations through regional flights or trains or other conveyances. At this aim Cargo Airports will be able to fully meet the needs of many airlines and many logistics operators because, not having to share the space with services for passengers, there is more availability of free slots for the storage of the goods, and the surrounding transport infrastructure such as rail or roads, they are fully dedicated to the support of logistics activities [Malecki and Wei 2009, Townsend 2001, Salvatori 1987].

Another important element of high strategic value is Cargo City. It's a great strategic infrastructure for managing and handling of new freight traffic volumes expected in an area of strong growth as Budapest. It is an innovative structural, logistic, security and technology project [Graham 1998, Grubesic and Murray 2006, Hepworth 1989, Cantwell and Iammarino 1998, Chon 2004]. Another relevant element is Distripark and European Distribution Center. The Distripark has to be an advanced logistic platform that can also be a link between industry and services. Inside the Distripark there must be warehouses, management services, information technology and telecommunications services, but also sheds where manufacturing activities can be carried out to transform semis, international or national backgrounds, into finished products to enter foreign markets [Haggett 1965, Peet and Thrift 1989, Keeling 1995, Williams and Bala 2009]. The last elements are Free Trade Zone aimed at promoting import/export, trade and the opening of the national economy to the outside world. The free trade zone serves to encourage trade and foreign investment [Salvatori 1994, Malecki 2002a, Salvatori 1991, Li et al. 2005, Tranos and Gillespie 2009, Shy 2001]. It must provide business well-endowed of comfort, services and communications infrastructure needed to open a business and meet the needs of investors, in addition to the exemption from taxes and customs duties and no duties on exports and imports. The main objective of free trade zones is to attract foreign direct

investments by facilitating market entry for foreign investors [Beckmann 1968, George 1964, Dobruszkes 2006, Faloutsos et al., 1999].

As Budapest will become the center of a new route, there will be a host of opportunities for logistics service providers of all European countries. The creation of the intermodal freight hub Budapest and its regional production and logistics platform can really change the face of logistics, generating great investment opportunities for all companies wishing to settle and participate in this project [Lee 2009, Wheeler and O'Kelly 1999, Zook and Brunn 2006]. Through this the intermodal freight hub products and goods arrived from many areas of the world may be processed, re-exported and distributed, in the markets of Central and Eastern Europe, with considerable savings on duties and customs procedures [Patuelli et al., 2007, Rutherford et al., 2004, Malecki 2002]. Companies have to adapt to the local markets where they wish to expand. Logistics service providers have to take a targeted approach, which will require taking an active part in the design process of new transport corridors, developing adequate structures and pricing systems and initiating and building logistics clusters. Logistics service providers should adapt their firm to changes driven form TEN-T [Rimmer 1998, O'Kelly and Grubesic 2002, Malecki 2004]. However, not every firm will be able to increase its range of value-added service offerings, due to financial restrictions or lack of capabilities. Multinationals will accelerate the increase in professionalism of the logistics industry. Through cooperation, joint ventures or by following the lead of competitors who have established such practices, even small and medium size firms can increase their level of automation and implement a broader range of value-added services.

CONCLUSIONS AND DISCUSSION

The Trans-European transport network provides the basis for the balanced development of all transport modes in order to exploit their respective advantages, thereby maximizing the network's value added for Europe. One of the key components of the TEN-T is the concept of comprehensive network and core network. The first one aims to ensure full coverage of the EU and accessibility of all regions, while the second one aims to prioritize the most important links and nodes of the TEN-T. Both of them include road, rail, air, inland waterways and maritime transport, as well as intermodal platforms. They will affect 83 main European seaports, by rail and road links, 37 airports by rail links to major cities, 15000 km of rail lines converted to high speed and 35 large cross-border projects to reduce bottlenecks.

Core network corridors should be intermodal and cross at least three Member States, and if possible, they should establish a connection with a maritime port. The Core network corridors should help to develop the structure of the core network in such a way as to address bottlenecks, enhance cross border connections and improve efficiency and sustainability. They should also address wider transport policy objectives and facilitate interoperability, modal integration and multimodal operations. As Hungary becomes the center of a new route, there will be a host of opportunities for logistics service providers of all European countries. Companies must be willing to adapt to the local markets where they wish to expand. Logistics service providers will need to take a targeted approach, which will require taking an active part in the design process of new transport corridors, developing adequate structures and pricing systems and initiating and building logistics clusters. The creation of the intermodal freight hub Budapest and its regional production and logistics platform can really change the face of logistics, generating great investment opportunities for all companies wishing to settle and participate in this project. ■

REFERENCES

1. Abraham F. and Roumpuy van P. (1995), Economic Disparity under Condicions of Integrations. A Lon term View of the European Case, in Regional Science Journal, 74 (2), pp. 125–142.
2. Alderighi M., Cento A., Nijkamp P., Rietveld P. (2007), Assessment of new hub-and-spoke and point-to-point airline network configurations Transport Reviews 27, 529–549.
3. Allen J. (1999). Cities of power and influence: settled formations', in Unsettling Cities Eds J. Allen, D. Massey, M. Pryke (Routledge, London), pp. 186–237. Eds J. Allen, D. Massey, M. Pryke (Routledge, London), pp 7–48.
4. Antonelli C. (1995), The Economics of Localized Technological Change and Industrial Dynamics, Boston, Academic Publishers.
5. Ashworth G., Voogd H. (1995), Selling the city: marketing approaches in public sector urban planning, Chichester England, John Wiley & Sons Ltd.
6. Associazione Italiana Geomarketing (2005), Definizioni, www.valuelab.it.
7. Aydalot P. (1986); Milieux innovateurs en Europe – Innovative environments in Europe, Paris, GREMI.
8. Bakis H. (1981), Elements for a geography of the telecommunication Geographic Research Forum 4, 31–45.
9. Barker T. and Kohler J. (Eds.) (1998), International Competitiveness and Environmental Policies, Cheltenham, Edward Elgar.
10. Bathelt H. and Glukler J. (2003), Toward a relational economic geography, in Journal of Economic Geography 3(2), pp. 117–144.
11. Batowski M., Pastuszak Z. (2008), Sources of the success of Scandinavian knowledge economies International Journal of Innovation and Learning 5, 109–118.
12. Batten D.F. (1995), Network Cities: Creative Urban Agglomerations for the 21st Century, Urban Studies, 32 (2), pp. 313–327.
13. Beaverstock J.V. (2002), Transnational elites in global cities: British expatriates in Singapore's financial district Geoforum 33, 525–538.
14. Beckmann M. and Thisse C. (1986), The Location of Production Activities, in NIJKAMP P. (ed.), Handbook of Regional and Urban Economics, Vol. I, pp. 21–33.
15. Beckmann M. (1968), Location Theory, New York, Random House.
16. Benner M. (2003), The Scandinavian challenge: the future of advanced welfare states in the knowledge economy Acta Sociologica 46, 132–149.
17. Berry B.J.L. (1961), City Size Distributions and Economic Development, Economic Development and Cultural Change, 9, pp. 573–587.
18. Berry B.J.L. (1976), Urbanization and Controurbanization, Sage, London.

19. Berry B.J.L., Conkling C., Ray M. (1993), The Global Economy: Resource Use, Locational Choice, and International Trade, Englewood Cliffs - NJ, Prentice Hall College.

20. Bonarich P. (2007), Some unique properties of eigenvector centrality Social Networks 29, 555–564.

21. Bonavero P., Sforzi F., Dematteis G. (1999), The Italian urban system: towards European integration, Hampshire, Ashgate.

22. Bramanti A., Ratti R. (1997); The multi-faced dimensions of local development, in RATTI R., BRAMANTI A., GORDON R. (eds.), The dynamics of innovative regions: The GREMI Approach, Ashgate, Aldershot, pp. 3–44.

23. Brunet R. (1989), Les Villes Europeennes, Paris, DATAR-RECLUS, La Documentation Fransaise.

24. Bugayevskiy L.M. and Snyder J.P. (1995), Map Projections: A Reference Manual, London, Taylor & Francis.

25. Burrough P., McDonnel A. (1998), Principles of Geographical Information Systems, Oxford, Oxford University Press.

26. Camagni R. (1997), European Cities and Global Competition: the economic challenge, in EUROPEAN TERRITORIAL MINISTERS (ed.), European Spatial Planning, Roma, Poligrafico dello Stato.

27. Cantwell J., Iammarino S. (1998), MNCs, Technological Innovation and Regional Systems in the EU: Some Evidence in the Italian Case, in International Journal of the Economics of Business, 5(3), pp. 383–408.

28. Capello R. (2004), Economia regionale, Bologna, Il Mulino.

29. Cappelin R. et Batey P.W. (1993), Regional Networks, Border Regions, and European Integration, Pion, Letchworth.

30. Castells M. (2001) The Internet Galaxy (Oxford University Press, Oxford).

31. Castells M. (1989), The informational City: Information Technology, Economic.

32. Choi J.H., Barnett G.A., Chon B.-S. (2006), Comparing world city networks: a network analysis of Internet backbone and air transport intercity linkages Global Networks 6, 81–99.

33. Chon B.-S. (2004), The dual structure of global networks in the entertainment industry: interorganizational linkage and geographical dispersion The International Journal on Media Management 6, 194–206.

34. Claval P. (1976), Eléments de géographie économique, Paris, Litec.

35. Cohen G., Salomon I., Nijkamp P. (2002), Information-communications technologies (ICT) and transport: does knowledge underpin policy? Telecommunication Policy 26, 31–52.

36. Cohen-Blankshtain G, Nijkamp P, (2004), The appreciative system of urban ICT policies: an analysis of perceptions of urban policy makers Growth and Change 35, 166–197.

37. Crevoisier O., Camagni R. (éds) (2000) Les milieux urbains : innovation, systèmes de production et ancrage, Paris, Enquête.

38. Derudder B. (2006), On conceptual confusion in empirical analyses of a transnational urban network Urban Studies 43, 2027–2046.

39. Derudder B., Devriendt L., Witlox F. (2007), Flying where you don't walk to go: an empirical analysis of hubs in the global airline network Tijdschrift voor Economische en Sociale Geografie 98, 307–324.

40. Derudder B., Taylor P. (2005), The cliquishness of world cities Global Networks 5(1) 71–91.

41. Derudder B., Taylor P., Witlox F., Catalano G. (2003), Hierarchical tendencies and regional patterns in the world city network: a global urban analysis of 234 cities Regional Studies 37, 875–886.

42. Derudder B., Witlox F. (2005), An appraisal of the use of airline data in assessing the world city network: a research note on data Urban Studies 42, 2371–2388.

43. Derudder B., Witlox F. (2008) Mapping world city networks through airline flows: context, relevance, and problems Journal of Transport Geography 16, 305–312.

44. Dobruszkes F. (2006), An analysis of European low-cost airlines and their networks Journal of Transport Geography 14, 249–264.

45. Doyle J.C., Alderson D.L., Li L., Low S., Roughan M., Shalunov S., Tanaka R., Willinger W. (2005), The `robust yet fragile' nature of the Internet Proceedings of the National Academy of Science of the United States of America 102, 14497–14502.

46. Faloutsos M., Faloutsos P., Faloutsos C., (1999), On power-law relationships of the Internet topology Computer Communication Review 29, 251–262.

47. Freeman C. (1978 – 79), Centrality in social networks conceptual clarification Social Networks 1(3), 215–239.

48. Friedmann J. (1986), The world city hypothesis Development and Change 17, 69–84.

49. Gastner M.T., Newman M.E.J. (2005), The spatial structure of networks The European Physical Journal B: Condensed Matter and Complex Systems 49. 247–252.

50. George P. (1964), La Géographie active, Parigi, PUF.

51. George P. (1968), L'Action Humaine, Parigi, PUF.

52. Gillen D., Morrison W.G. (2005), Regulation, competition and network evolution in aviation Journal of Air Transport Management 11, 161–174.

53. Gorman S.P., Kulkarni R. (2004), Spatial small worlds: new geographic patterns for an information economy Environment and Planning B: Planning and Design 31, 273–296.

54. Gottmann J. (1983), The expanding City, J. Patten, Londra.

55. Graham B. (1998), Liberalization, regional economic development and the geography of demand for air transport in the European Union Journal of Transport Geography 6, 87–104.

56. Grubesic T.H., Murray A.T. (2006), Vital nodes, interconnected infrastructures, and the geographies of network survivability Annals of the Association of American Geographers 96, 64–83.

57. Grubesic T.H., O'Kelly M.E. (2002), Using points of presence to measure accessibility to the commercial Internet The Professional Geographer 54, 259–278.

58. Haggett P. (1965), Locational analysis in human geography, London, Edward Arnold.

59. Hendricks K., Piccione M., Tan G. (1995), The economics of hubs: the case of monopoly The Review of Economic Studies 62, 83–99.

60. Hepworth M. (1989) Geography of the Information Economy (Belhaven Press, London).

61. Keeling D.J. (1995), Transport and the world city paradigm, in World Cities in a World System Eds P.L. Knox, P.J. Taylor (Cambridge University Press, Cambridge), pp. 115–131.

62. Lee H.-S. (2009), The networkability of cities in the international air passenger flows 1992–2004 Journal of Transport Geography 17, 165–177.

63. Li L., Alderson D., Tanaka R., Doyle J.C., Willinger W. (2005), Towards a theory of scale-free graphs: definition, properties, and implications (extended version) Internet Mathematics 2, 431–523.

64. Malecki E.J. (2002a), The economic geography of the Internet's infrastructure Economic Geography 78 399–424.

65. Malecki E.J. (2002b), Hard and soft networks for urban competitiveness Urban Studies 39, 929–945.

66. Malecki E.J. (2004), Fibre tracks: explaining investment in fibre optic backbones Entrepreneurship and Regional Development 16, 21–39.

67. Malecki E.J., Wei H. (2009), A wired world: the evolving geography of submarine cables and the shift to Asia Annals of the Association of American Geographers 99, 360–382.

68. O'Kelly M.E., Grubesic T.H. (2002), Backbone topology, access, and the commercial Internet, 1997–2000 Environment and Planning B: Planning and Design 29, 533–552.

69. Patuelli R., Reggiani A., Gorman S.P., Nijkamp P., Bade F.-J. (2007), Network analysis of commuting flows: a comparative static approach to German data Networks and Spatial Economics 7, 315–331.

70. Rimmer P.J. (1998), Transport and telecommunications among world cities, in Globalization and the World of Large Cities Eds F.-C. Lo, Y.-M. Yeung (United Nations University Press, Tokyo), pp. 433–470.

71. Peet R. and Thrift N. (1989) (Eds), New models in Geography, voll I-II, London, Unwin Hyman.

72. Rutherford J., Gillespie A., Richardson R., (2004), The territoriality of pan-European telecommunications backbone networks Journal of Urban Technology 11, 1–34.

73. Salvatori F. (1987), Le industrie a tecnologia avanzata, in CORNA PELLEGRINI G. (a cura di), Aspetti e problemi della Geografia, Milano, Marzorati, pp. 283–307.

74. Salvatori F. (1994), Sviluppo locale e crescita economica nella Marsica, in Bollettino della Società Geografica Italiana, serie XI, XI (3–4), pp. 455–470.

75. Salvatori F. (1991), Impresa e territorio. Note sull'individuazione degli indicatori dello sviluppo economico locale, in Bollettino della Società Geografica Italiana, VIII (10–12), pp. 687–700.

76. Shy O. (2001) The Economics of Network Industries (Cambridge University Press, Cambridge).

77. Smith D., Timberlake M. (2002) Hierarchies of dominance among world cities: a network approach, in Global Networks: Linked Cities Ed. S. Sassen (Routledge, New York), pp. 117–141.

78. Townsend A.M. (2001b), The Internet and the rise of the new network cities, 1969–1999 Environment and Planning B: Planning and Design 28, 39–58.

79. Tranos E., Gillespie A. (2009), The spatial distribution of Internet backbone networks in Europe: a metropolitan knowledge economy perspective Journal of European Urban and Regional Studies 44, 423–437.

80. Wheeler D.C., O'Kelly M.E. (1999), Network topology and city accessibility of the commercial Internet The Professional Geographer 51, 327–339

81. Williams A.M., Bala V. (2009), Low-cost carriers, economies of flows and regional externalities Regional Studies 43, 677–691.

82. Zook M.A., Brunn S.D. (2006), From podes to antipodes: positionalities and global airline geographies Annals of the Association of American Geographers 96, 471–490.

Graziella Ferrara is Professor at Suor Orsola Benincasa of Naples. She was visiting researcher at Salem State College (USA). Her research interests concern geography, internationalization and corporate strategy. She published many articles on geography, internationalization and corporate strategy and she is in the editorial board of many relevant journals.

Vyacheslav N. Konishchev
Department of Cryolithology and Glaciology, Faculty of Geography, Lomonosov Moscow State University (Moscow); vkonish@mail.ru

THE ROLE OF CRYOGENIC PROCESSES IN THE FORMATION OF LOESS DEPOSITS

ABSTRACT. The paper describes a new approach to the analysis of the genetic nature of mineral substances in loess deposits. In permafrost under the influence of multiple alternate freezing and thawing in dispersed deposits, quartz particles accumulate the 0.05–0.01 mm fraction, while feldspars are crushed to a coarse fraction of 0.1–0.05 mm. In dispersed sediments formed in temperate and warm climatic zones, the granulometric spectrum of quartz and feldspar has the opposite pattern. The proposed methodology is based on a differential analysis of the distribution of these minerals by the granulometric spectrum. We have proposed two criteria – the coefficient of cryogenic contrast (CCC) and the coefficient of distribution of heavy minerals, which allow determination of the degree of participation of cryogenic processes in the formation of loess sediments and processes of aeolian or water sedimentation.

KEY WORDS: loess deposits; granulometric distribution, mineral composition; cryogenesis; cryolithozone; periglacial zone; historical and genetic approach

INTRODUCTION

Among researchers who have studied the problem of loess, there are virtually no large disagreements in the definition of their basic properties [Krieger 1965]. The properties include homogeneity of the size distribution, vertically and horizontally, within the vast expanses. Usually the silt content of the primary particles is in the range of 30–55 %, at the total porosity of 40–45 %; it contans lime and microaggregates and has a relatively high content of soluble salts; it is laminated, with the ability to maintain the vertical wall in the outcrops; it subsides when wet and often forms mantles and contains buried soils.

The situation is quite different in the genetic interpretation of the above characteristics and properties of loess, favored by a number of researchers. There are opposite points of view which show lack of understanding of the problem and lack of sufficiently certain genetic criteria for the interpretation of a particular characteristic or characteristics of loess. The most revealing in this respect is the size-distribution of these deposits.

Many researchers believe that the loess cover was formed in the cold Pleistocene era and is a product of the deposition of atmospheric dust. During glaciation maximums and coolings and accordingly, arid climate, there was an intensification of the atmospheric circulation. This caused the saturation of the atmosphere with dust; its content was 30 times higher than the dust content in the interglacial atmosphere [Broecker, 2000].

Even colder intervals of the Antarctic and Greenland ice cores are enriched with dust [Kotlyakov, Lorius, 2000]. In warm periods of Neopleistocene, the accumulation of dust either stopped or significantly slowed down and soils were forming on the surface of the deposits. Thus loess-soil sequences appeared which are considered very important nature sites in terms of completeness of paleoclimatic information.

The formation of loess horizons of the loess-soil sequences coincides with the cold stages of the oxygen isotope scale, while the formation of buried soils coincides with the warm phases [Bassinot et al, 1991]. According to many researchers, the aeolian nature of loess is most simply revealed [Zeuner, 1965] by comparing the size distribution of modern aeolian sediments on snowfields, glaciers, and other surfaces after dust storms in many modern parts of the world [Chapman, 1934 and al.; Page, 1934; Russel, 1936]. The leading role in the composition of these deposits is played by a large primary particles of aleurolite (0.05–0.001 mm), i.e., more than 40–50 %.

The work of many researchers has shown that transfer of disperse mineral matter is accompanied by differentiation of the particles by size and mineralogical composition [Rukhin, 1961; Sidorenko, 1956]. Quartz, feldspar, and other light minerals dominate; there are small quantities of heavy minerals.

Atmospheric dust carried over considerable distances contains varied sizes of particles and minerals, including heavy, i.e. is polymineral l and polydisperse, but with predominance of the primary particles, 0.05–0.01 mm in size.

It is important to emphasize that the bulk of heavy minerals concentrate within the fraction 0.05–0.01 mm, while quartz, i.e., the most stable mineral, tends to have larger particles.

Fig. 1 shows the particle-size and mineralogical composition of clusters of aeolian dust collected on the right branch of the glacier Shokalski (Trans-Ili Alatau, Tien Shan); altitude 3950 m; the rock framing is located at a distance of 800–900 m from the sampling site. Even at such a short distance, there is a noticeable particle size sorting accompanied by mineralogical sorting expressed in the distribution of heavy minerals (specific density of the granulometric specturm is greater than 2.9). The maximum weight of heavy minerals is associated with the fraction 0.05–0.01 mm. This sedimentary distribution of the heavy

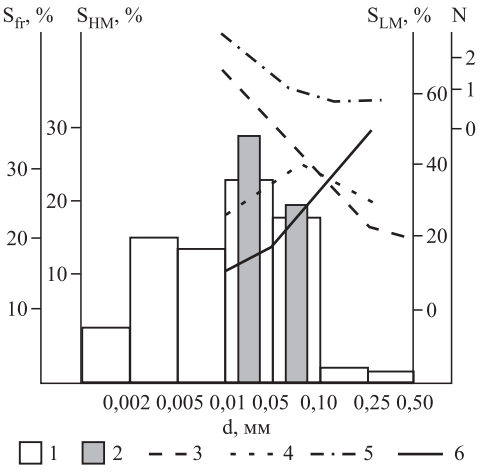

Fig. 1. The particle-size and mineralogical composition of aeolian fine earth on the right branch of the glacier Shokalski (Trans-Ili Alatau, Tien Shan, altitude 3950 m, rock framing is 800–900 m from the sampling site).

1 – size distribution S_{fr}; 2 – content of the heavy fraction S_{HM}; 3 – distribution of the quartz content by size-fractions (S_{LM}, %); 4 – distribution of feldspar content by size-fractions (S_{LM}, %); 5 – distribution of quartz/feldspar (N) ratio by size-fractions; 6 – distribution of rock fragments by size-fractions (%).

fraction by the granulometric spectrum is a general law for the truly aeolian deposits. In the aqueous environment, a similar granulometric and mineralogical sorting occurs, but in a somewhat less pronounced form, since the maximum effective sorting of mineral matter occurs in air.

Unfortunately, despite the huge amount of grain-size, microaggregate, and mineralogical analyses of loess and loess deposits, the data on the distribution of the mineral content of both light and heavy granulometric fractions are virtually absent in the literature. And, most importantly, the authors do not consider these parameters to have any significance for detection of genetic nature of the mineral matter of loess.

The same applies to the atmospheric dust studied under the framework of international projects. The proceedings of international conferences contain data on particle-size distribution of dust carried in the atmosphere

and the general content of minerals, including heavy, but recent data on the distribution by the granulometric spectrum are not available.

The particle size of atmospheric dust captured by special dust collectors is often an order of magnitude smaller than the large particles of dust dominant in loess deposits (0.6–3.0 microns). The ice cores in Greenland and Antarctica have increased contents of microparticles in the Late Pleistocene ice; it corresponds to the maximum decrease in temperature, which caused a decrease in rainfall, leading to a relative increase in the content of the microparticles. At the same time, we cannot, of course, completely deny the increased activity of the atmospheric circulation.

Evidence of permafrost processes, such as permafrost patterns and textures (pseudomorphs of ice wedges, cryoturbation and involution, post-schlieren texture, etc.) represent the proofs of cold climatic conditions. Long-term studies of paleopermafrost loesses, their classification, and mapping were carried out by A.A. Velichko and his followers [2004]. At the same time, these researchers adhere to the aeolian concept of loess formation. Despite the exhaustive classification of paleopermaforst phenomena, including microstructural features of mineral matrix of loess typical of loess-soil series within the East European Plain and Western Europe, the researchers have clearly underestimated the actual lithological aspect of repeated cycles of freezing and thawing, accompanied by accumulation of mineral mass of loess.

Many researchers wrote on the role of frost weathering processes in the formation of the loess fraction (0.05–0.01 mm). N.I. Krieger [1965] published a very good historical overview of this problem. Later, the problem was studied mainly by permafrost scientists. Numerous experiments have shown that under the influence of multiple cyclic freezing – thawing in various rocks, both monolithic (granite, sandstone, etc.) and dispersed (sands, sandy loams, loams), the loess fraction was accumulating due to both disintegration of larger particles (quartz, feldspar, etc.) and aggregation of clay particles.

Yet this did not mean that a criterion for differentiating between products of wind cryogenic separation and cryogenic transformation of mineral substances has been found.

RESEARCH METHODS

An earlier method of experimental research on cryogenic weathering based on testing of polymineral and polydispersed samples has led to conclusions about the accumulation of loess fraction in soils, but no analysis of any specific product of cryogenic mineral destruction has been performed. Therefore, uncertainty remained regarding genetic interpretation of the particle-size distribution of loess and loess deposits.

Particular characteristics of cryogenic weathering were identified only in the study of cryogenic stability and monomineral and monodisperse fractions. For the first time this approach to experimental research of cryogenic stability was carried out by [Konishchev, Rogov, Schurina, 1976]. They have determined that quartz grains break down to a fraction of 0.05–0.01 mm, while feldspar grains, not altered by earlier processes of pelitization, crush to a size of 0.1–0.05 mm. The limits of cryogenic destruction of other minerals have been established; however, it did not matter much because their content in the original deposits is usually small, i.e., no more than a few percent, whereas quartz and feldspar comprise the bulk of the deposits and their content is generally greater than 90–95 %

These findings were confirmed by the results of the experiments of A.V. Minervin [1982]. This experiment also studied cryogenic resistance of monomineral and monofractional samples, but the number of cycles of freezing-thawing was 1000, and the experiment lasted for more than 3 years, i.e., both were substantially greater than in our experiment (Table. 1).

Table 1. Results of modeling of large-silt loess fraction formation under different conditions based on [Minervin, 1982]

№ of experiment	Experimental conditions		Mineral	% content of fractions, diameter of particles in mm					
				0.25–0.1	0.1–0.05	0.05–0.01	0.01–0.005	0.005–0.001	<0.001
1	Before experiment		quartz	100	–	–	–	–	–
			microcline	100	–	–	–	–	–
			calcite	100	–	–	–	–	–
			biotite	100	–	–	–	–	–
2	Freezing (–10°) – Thawing (+15°–+20°)	water saturated	quartz	11	20	68	1	–	–
			microcline	7	44	48	1	29	–
			calcite	6	15	20	30	–	–
			biotite	98	1	1	–	–	–
3	Freezing (–10°) – Heating (+50°)	air-dry	quartz	98.5	1	0.5	–	–	–
			microcline	98.5	1.5	1	–	–	–
			calcite	93.5	5	–	–0.5	–	–
			biotite	100	–	–	–	–	–
4	Wetting-drying (in laboratory; +18°–+ 20°)		quartz	100	–	–	–	–	–
			microcline	100	–	–	–	–	–
			calcite	100	–	–	–	–	–
			biotite	100	–	–	–	–	–

However, the result, as follows from the table, was the same, but manifested more clearly – quartz disintegrated into smaller particles (up to 0.05–0.01 mm) compared to feldspar (microcline) – up to 0.1–0.5 mm. Unfortunately the author did not consider this result important, he simply did not notice it.

In fact, this conclusion is of fundamental importance. Firstly, it is clear why there is an absolute predominance of particles 0.05–0.01 mm in cryogenic-weathering products; this is determined by the dominant role of silica in the composition of sedimentary rocks (moraine, alluvial, marine, and other), which were the source parent rocks, subsequently altered by cryogenic weathering.

Secondly, there are special requirements to the procedure of analyzing the composition of disperse deposits in order to determine the role of cryogenesis in their formation. It is necessary to determine the mineralogical composition not in the bulk deposists, but individualy for separate granulometric fractions and primarily in fractions 0.05–0.01 mm and 0.1–0.5 mm that typically make up the large, and the largest in loess, part of the mineral mass.

A large number of studies are devoted to determination of relationships between granulometric and mineralogical composition of disperse sedimentary depostis [Ananiev, 1966; Lazarenko, 1964; Rukhin, 1961; Ryasina, 1961; Sergeev, 1954; Sidorenko, 1956; Strakhov, 1962; Fadeev. 1968 et al.; Tsekhomskiy, 1956].

In his major work, N.M. Strakhov [1962] summarized the vast amount of material and introduced the concept of distribution of minerals by the particle-size spectrum of different facies types formed in humid conditions, predominantly outside the cryolithogenic zone (Fig. 2). There is a region of maximum mineralogical diversity, limited by 0.25 0.01 mm particles. The granulometric spectrum maximums inside this area do not

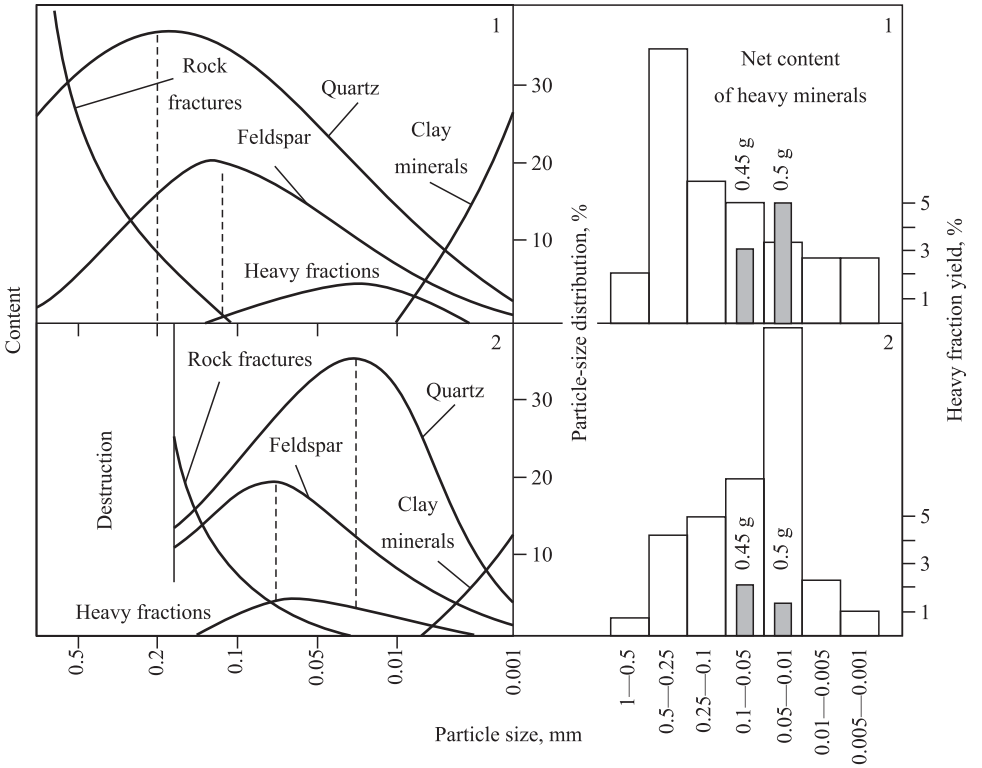

Fig. 2. Redistribution of the main mineralogical properties by particle-size during cryogenesis [Konishchev, 1981].

A – qualitative diagram: 1 – distribution of the content of the main mineral components by particle-size of the original rock, 2 – distribution of the main mineral components in products of cryogenesis.

B – quantitative diagram of redistribution relative to the bulk content of heavy minerals by particle-size at a constant absolute content: 1 – the original rock with the sedimentary-type distribution of the heavy fraction; 2 – supergene type of the heavy fraction content in products of cryogenesis.

coincide and are arranged consecutively in a series from the larger to finer particles: quartz → feldspar → heavy mineral fractions.

The nature of the upper limit of clastic minerals is inheritied and is the function of their regular size in the original massive-crystalline deposits.

The lower limit of the particle-size spectrum of the predominantly clastic minerals (0.001 mm) is due to a sharp increase of the instability of mineral grains in relation to the factors of chemical weathering in the course of their size-degradation. The crucial factor in localization of heavy minerals is specific weight and degree of sediment sorting. In the sorted sediments, the total maximum content of heavy minerals is mainly associated with the fraction 0.05–0.01 mm.

Numerous studies on the analysis of particle-size distribution and mineralogical composition of the typical loess practically do not apply this differentiated approach; a high degree of particle-size sorting has been considered the sufficient criterion for conclusions about genetic facial conditions of formation of these deposits.

At the same time, our studies on the composition of loess deposists in the modern cryolithozone, where typical carbonate loess formations are absent, showed that only a differentiated approach to the study of the composition allows one to judge more

objectively both the cryo-climatic and facial-genetic conditions of accumulation of mineral matter in these deposits.

Therefore, we propose a special coefficient as a characteristic of the degree of participation of cryogenic weathering in the formation of deposits; more specifically, it considers the limit fraction sizes within which these minerals accumulate during cryogenesis.

$$CCC = \frac{Q_1}{F_1} : \frac{Q_2}{F_2}.$$

It was named the *Coefficient of Cryogenic Contrast*, where Q_1 – quartz content in the fraction 0.05–0.01 mm; F_1 – feldspar content in the fraction 0.05–0.01 mm; Q_2 – quartz content in the fraction 0.1–0.5 mm; F_2 – feldspar content in the fraction 0.1–0.5 mm.

The deposits formed in the cryolithozone zone must have a CCC value greater than 1. Whereas the deposits formed outside the zone, i.e., in temperate and warm climates, have the values of CCC based on N.M. Strakhov's scheme [Strakhov, 1962], i.e., lower than 1.

Generalization of a large volume of data on the composition of deposits formed within and outside the zone of cryogenesis, has fully justified the proposed parameter [Konishchev, 1981].

ANALYSIS OF THE OBJECTS UNDER STUDY

Particular characteristics of the composition of products of cryogenic transformation have been most clearly revealed in the analysis of the composition of mantle loess-like formations of the Bolshaya Zemlya tundra. A comprehensive description of these deposits is given in [Konishchev 1981]; therefore, we will focus on the features of their differentiated granulocmetric and mineralogical composition. We should only note that mantle loess loams of the Bolshaya Zemlya tundra covers entirely tundra watersheds and are absent on the first terrace and in the river valleys; their thickness is 1.5–1.8 m and varies from 0.2–0.5 m to 3–3.5 m within interblock depressions of the polygonal relief. Mantle loams occur with a gradual contact on rubbly loams and, less often, on sands, which is reflected in their composition; they conjoin the polygonal system of frozen ground veins.

Differentiated mineralogical analysis (for individual granulometric fractions) showed that the maximum content of silica is observed in the most representative fraction of very fine sand – 0.05–0.01 mm (Fig. 3).

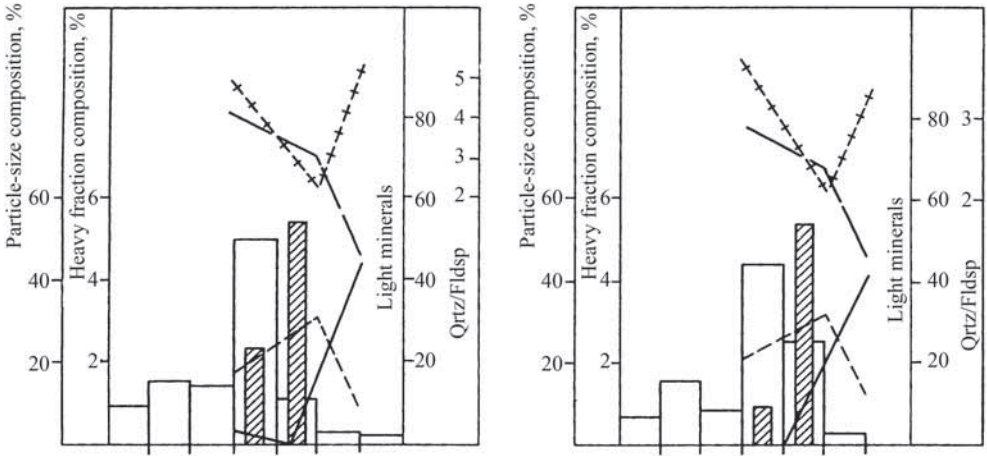

Fig. 3. Distribution of mineralogical parameters by granulometric range of mantle loess-like formations of the Bolshaya Zemlya tundra (for legend, see Fig. 1).

The amount of quartz in this fraction ranges from 74 to 85 %; it is markedly reduced in larger-size fractions (in 0.1–0.05 mm, 59–70 %; in 0.1–0.25 mm, up to 46–58 %) and in smaller-size fractions. The character of the particle-size spectrum of the feldspars content in all cases is the same and is characterized by a maximum of 30–42 % in the fraction 0.1–0.05 mm. In finer fractions, the content of feldspars is reduced (up to 15–26 % in the fraction 0.05–0.01 mm and up to 9–18 % in a larger fraction 0.1–0.25 mm).

As one can see, the ratio of distribution of the main rock-forming minerals (quartz and feldspar) by particle size of mantle loess-like formations of the Bolshaya Zemlya tundra is exactly opposite of the behavior of these minerals in the deposits formed in warm climatic conditions.

In the literature, there is a widespread point of view that loess and loess-like deposits are characterized by very insignificant weathering [Ryabchenkov, 1955; Khalcheva, 1975], which made it possible to deny the significant effects of weathering processes in their formation. This judgment is fraud with an obvious logical inconsistency. The essence of the weathering coefficient, defined as the ratio of stable minerals to the sum of unstable minerals in the total mass of deposits, without separation of granulometric fractions is the ratio (!) of physical processes (fragmentation of minerals) to chemical processes (their decomposition, transformation) of weathering. Low values of weathering coefficient mean low intensity of chemical weathering, not weathering in general, and high intensity of physical desintegration of minerals without alteration of their mineralogical composition.

The association of high quartz content with the most typical size fraction (0.005–0.001 mm) of mantle loess formations of the northern part of European Russia and the maximum content of feldspars in a larger fraction (0.01–0.05 mm) reveal the main mineralogical essence of the process of formation of these deposits, i.e., cryogenic fragmentation of minerals of the original deposits (rubbly loams, sands) to the characteristic of these minerals limits – 0.05–0.01 mm and 0.1–0.05 mm for quartz and feldspar, respectively, which is in accordance with the experimental and theoretical conclusions on the cryogenic stability of minerals.

The most important consequence of this process is the distribution of the overall total content of heavy minerals by particle-size (weight percentages of heavy minerals in certain size-fractions). In all analyzed samples of mantle loess-like loams, the maximum relative weight content of heavy minerals is observed in the fraction 0.1–0.05 mm and not in a finer fraction 0.05–0.01 mm (the shift of the maximum content of heavy minerals towards a larger fraction is a direct consequence of the cryogenic fragmentation of basic rock-forming minerals – quartz and feldspar (see. Fig. 2, A2).

From this, a fundamentally important conclusion follows: if the considered mantle loess-like formations had sedimentary origin and their high degree of particle size sorting were associated with the properties of sediment accumulation in water or air environment, one would expect that the distribution of the relative weight of heavy minerals by particle-size corresponds to the sedimentagenous distribution, as is the case in true aeolian deposits (see. Fig. 1).

The principle rock-forming position of quartz in the original deposits, the high degree of cryogenic crushability of quartz particles compared to other minerals, and stability of quartz particles 0.05–0.01 mm lead to the fact that during cryogenic transformation of the complex, in respect to the complex-composition mineral mass, the maximum content of quartz particles in the fraction 0.05–0.01 mm is reached; this fraction is the limit of the cryogenic fragmentation of this mineral. The process inevitably distorts the original distribution of heavy minerals by granulometric spectrum reducing their content in the fraction 0.05–0.01 mm, where

they are "substituted" with quartz grains and, thus, the maximum of the relative weight content of heavy minerals is shifted towards larger size fractions (see. Fig. 2, B2).

The established specific (non-sedimentagenous) nature of the distribution of the relative total weight of heavy minerals by the granulometric spectrum of mantle loess formations of the Bolshaya Zemlya tundra is one of the basic characteristics of the cryogenic eluvium (with a corresponding value of CCC) and proves that its high degree of particle-size sorting has cryogenic origin and is not associated with aeolian sedimentation, as stated in some publications [Astakhov, 2011].

Other features of the mantle loess-like loams of the Bolshaya Zemlya tundra are their close association with permafrost ground structures [Popov, 1958, 1962]; the micropolygonal mircrostructure of the mineral mass [Konishchev 1981] is even more convincing of the cryogenic eluvial nature of these formations. Primary, i.e., not redeposited, mantle loams have low thickness (up to 1.5–18 m), which generally corresponds to the thickness of the layer of seasonal thawing. The increased thickness (up to 3.5 m) is characteristic of inner depressions of the polygonal-block relief. However, there are no sedimentagenous features in the mineral composition, although the bands of peat and bog soils are sometimes present.

Under such conditions, mantle loams are the product of the nearest redeposition of cryogenic eluvium.

Mantle loams of the Bolshaya Zemlya tundra can be seen as a model for identifying the degree of participation of cryogenic factors in the formation of any of the types of loess material in different regions.

Along with the CCC parameter (see above), which specifically allows assessing cryogenic nature of mineral substances of the studied deposits, there is a need to introduce one more index that can be called the index of heavy fractions.

It is the ratio of the weight content of heavy minerals in the fraction 0.05–0.01 mm to the weight content of heavy minerals in the fraction 0.1–0.05 mm; it characterizes the degree of sorting impact of aqueous or air environment on the formation of deposits or its absence, which means the principle influence of cryogenic fragmentation of light-fraction minerals, primarily of quartz, on the formation of loess deposits.

Application of the above-mentioned coefficients to the analysis of genetic nature of the "ice complex" of Northern and Central Yakutia, much of which is represented by loess deposits, has allowed us to establish the leading role of cryogenic fragmentation in the formation of mineral matter of these deposits.

We have isolated various facial-genetic types of loess-like deposits of the "ice complex" and, first of all, the products of the nearest redeposition of cryogenic eluvium, with certain values of the suggested indices, and deposits that are the products of redeposition of cryogenic silt in various dynamic conditions of the aqueous environment [Konishchev, 1981, 2013].

Mantle loams of the northern part of East European Plain represent the most northern part of the expanse of non-carbonate loess-like formations [Chizhikov, 1982]. To the south, they transition to low-carbonate loess loams that occur from the southern margins of the sod-podzolic zone. Further south there is a zone of carbonate loess loam and carbonate loess [Chizhikov, 1982].)

Such a natural geographic association of different types of loess sediments is a good reason to consider them genetically related, which has been repeatedly expressed by many researchers, although they have put a different meaning in the genetic relatedness of these deposits.

N.I. Krieger in his fundamental study "Loess, its properties, and the connection with the geographical environment" [Krieger, 1965] quite rightly concluded that "since the area of distribution of loess is related only to the peripheral part of the territory of distribution of permafrost phenomena, ... one can reach the most probable conclusion that loess is confined to the margins of the periglacial (subarctic) zone and mainly to the temperate climate zone. Loess-like deposits are confined to the areas with more pronounced cryogenic phenomena associated with continuous permafrost" [Krieger, 1965, p. 24].

Somewhat generalizing the above formulation, it can be said that the area of distribution of loess, the whole range from the typical loess to non-carbonate mantle loess-like loam, almost coincides with the area of the Late Pleistocene cyrolithozone. This pattern is most pronounced in Europe, North America, and Asia (Fig. 4).

Nevertheless N.I. Krieger [1965] is of the view that the typical loess is a subaerial formation, mainly of aeolian origin. This point of view is shared by many researchers and currently by [Velichko, 1965; Zykina, Zykin, 2012].

Within the East European Plain, thickness of loess formations increases from north to south; at the same time, their structure is becoming more complicated. As was mentioned above, in the far north, in the Bolshaya Zemlya tundra, the primary not re-deposited mantle loams have thickness of 1.5–1.8 m and have a single-tier structure, i.e., without layers of buried soils. Their thickness increases to the south, reaching 5-8 m, and even further, reaching 10 m and more. The loess structure becomes multi-tiered. Along with the increase in thickness of the loess layer, the complexity of its structure increases too; there is an increasing number of buried soils with soil complexes, which allowed the isolation of the loess-soil formation or the loess-soil sequence. Since alternating

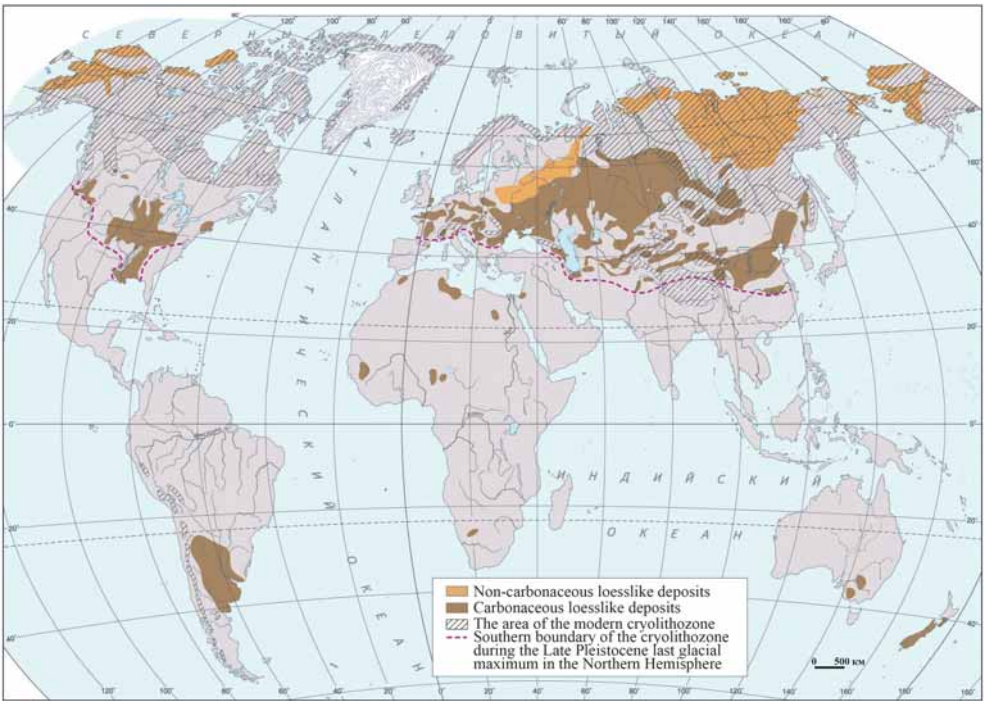

Fig. 4. Distribution of loess, loess-like sediments and the modern Late Pleistocene Cryolithozone (compiled by V.N. Konishchev and N.A. Koroleva).

loess and buried soils horizons are further complicated by horizons of cryogenic structures (pseudomorphs of ice vein and initially-ground wedges), some researchers call these deposits the loess-soil-cryogenic formation [Velichko, 1965, 2004; Makeev, 2012]. The reason for the development of the latter is the paleogeographic predetermination of the off-glacier area of the East European Plain. This resulted in the alternation in the area of periods of loess accumulation, the formation of permafrost structures during cold phases, and the formation of soils during warm phases of paleogeographic development.

Thus the idea that loess is a component of the glacial (more precisely, cold) epochs became widespread; this loess formed as a result of synchronous processes of accumulation, mainly by air, of the predominantly aleurolitic mineral mass and of its transformation under the complex impact of the arid synlithogenic soil forming process and cryogenic weathering [Makeev, 2012; Zykina et al., 2012]. However, uncertainty remains: what is the decisive factor in the formation of the mineral matter of loess silt – aeolian accumulation or cryogenic weathering, and how they relate to the stadial lithogenenic sequence.

Of fundamental importance is the fact that the spatial consistency of the loess-soil series in watersheds and their significant thickness (up to several dozens of meters), should leave no doubt, according to some researchers, that the leading factor of accumulation of rather homogeneous silty loess horizons was aeolian accumulation.

However, there is evidence in the literature, casting doubt on the objectivity of the above picture of the conditions of occurrence of loess-soil series. Analysis of information on the conditions of occurrence of loess-soil series contained in large generalizations [Zykina, et al., 2012; Loess Deposits…, 1966; Makeev, 2012] leads to the conclusion that the most general law is that in the watershed areas of the East European Plain, as well as in the south of the West Siberian Plain, the loess thickness varies from 1.5–2.0 m to 80 m and more; the thicker loess deposits occur mainly in depressions of the pre-loess relief.

This pattern is typical of the territory of Belarus, where large areas of loess deposits have thickness of 0.5–1 m. Within the Azov Upland watershed areas and the Bug-Dniester watershed, loess has thickness of 1–5 m [Loess Deposits…, 1966].

The most complete sections of loess in the Dnepropetrovsk region are in somewhat low areas of the faulted plateau. In Transcarpathia, in the areas of inclined piedmont plains, there is an increase in loess thickness in low parts to 15 m, sometimes up to 20 m [Loess Deposits…, 1966].

Most of the territory occupied by loess deposits includes gentle slopes and extensive river valleys and ravines. Loess deposits cover interfluves and line the micro- and meso-relief, down to the valleys of rivers and streams, where they are gradually replaced by water-glacial deposits of high terraces [Makeev, 2012].

In Western Siberia, most of the areas occupied by loess deposits are slopes [Zykina et al., 2012].

Thickness of loess deposits usually increases from the central portions of interfluves to the slopes of the main valleys.

In the descriptions of the specific sections of the loess-soil series, the authors [Zykina et al., 2012] have repeatedly pointed to the admixture of sand, gravel, and fine gravel both in the soil horizons and in the loess deposits.

Some authors [Zykina et al., 2012] show that in the layers of buried soils, hydromorphic soils formed under excess of moisture are often found as related genetic types.

All these features, in our opinion, indicate that loess-soil series were forming in depressions that were filling with aleuritic fine-grained soil,

often with an admixture of detrital material (gravel, crushed stone, pebble), coming from the nearest slopes. Recently, some researchers have directly written about paleo-incisions (buried forms of meso-relief) where thickness of the Late Pleistocene deposits (soil-loess series) reaches 10 and more meters in contrast to the upland sections [Sycheva, 2011].

However, in some places of the uplands, gentle hills are composed entirely of loess, which gives an impression of its mantle cover. Such cases are explained by the inversion of the relief in the period of its development after the accumulation of loess strata. Loess, having increased structural strength due to its carbonate content, in cases of catastrophically fast washing-out, when its long-term occurrence and subsidence are ruled out, is somewhat more stable compared, for example, with sandy strata. Thus massifs of loess can be isolated by fast erosion from the surrounding massifs composed of other loose sediment deposits and they can represent secondary (inversion) uplands.

HISTORICAL-GEOLOGICAL (FORMATIONAL) APPROACH TO THE ANALYSIS OF THE GENESIS OF LOESS DEPOSITS

The data presented above can be interpreted not only from the point of view that in the era of aridity and activation of the atmospheric circulation, the atmosphere was saturated with dust which was deposited and formed loess horizons that divided the buried soils.

It is logical to assume that this complex covering complex was formed as explained by the classical lithogenetic scheme set out in the fundamental work of N.M. Strakhov [1962].

With regard to the theoretical scheme of sedimentation staging by N.M. Strakhov [1962], specific formational stages of loess, as a result of permafrost lithogenesis, look like the following: cryogenic weathering of the original source rocks (moraines, fluvioglacial, alluvial) in the layer of seasonal thawing and the formation of primary not redeposited mantle loess loasm, up to 2–2.5 m in thickness; transfer of cryogenic aleuritic fine-grained material along slopes and its partial depositiion even during transport into local depressions; and, finally, flow of cryogenic aleuritic fine-grained material into large depressions of relief (paleo-incisions, lacustrine basins) and footslopes. This is also evidenced by the dependence of the $CaCO_3$ content in loess and loess-like deposits on the terrain [Krieger et al., 1965, see below].

Cryogenic processes (cryogenic weathering, solifluction, cryogenic creep, frost cracking that causes primary ground veins, repeated ice wedges that later melt down during warm phases and turn into pseudomorphs) play the leading role at all stages of the formation of loess deposits During Pleistocene, cryochrons and the corresponding stages of cryolithogenesis alternate with thermochrons that correspond to the stages of soil formation, which ultimately leads to the formation of loess-soil series.

The leading role of cryogenic processes in the formation of loess deposits of the cryolithozone, including, the unique strata of the ice complex in North and Central Yakutia, which is essentially a cryogenic version of the loess-soil series, has been demonstrated in several studies [Gravis, 1969; Zubakov, 1966; Konishchev, 1981]. Two lithological criteria for assessment of the degree of involvement of cryogenic processes in the formation of not only loess-like strata of the modern cryolithozone, but also for analysis of the mineral substances of loess strata in general, have been suggested to prove the cryogenic nature of mineral matter of these deposits.

INVESTIGATION OF THE COMPOSITION OF LOESS DEPOSITS WITHIN THE PLEISTOCENE PERIGLACIAL ZONE

To date, studies that use the technique described above within the Pleistocene periglacial zones have not been carried out. The exception, perhaps, is a special study of

paleocryogenic structures (pseudomorphs, ground veins) and the microstructure of the mineral mass [Velichko, 1965; Zykina, 2012], which, however, the authors do not connect specifically with the genesis of the aleuritic mass of loess deposits.

Nevertheless, there is some evidence pointing to the prospect of the use of specifically cryolithological analysis of mineral substances of loess deposits within Pleistocene cryolithozones.

Even today, the data by S.S. Morozov [1949] on the chemical and mineralogical composition and properties of different-size fractions of loess in the Dnieper region and genetically close deposits, remain unique. Table 2 shows some parameters of the composition of loess and other types of cover deposits from five locations of the East European Plain. Unfortunately, four samples were taken from the surface, 2.5 m deep, layer and only one (Mstislavsky loess) was taken from a depth of 3 m. Therefore, the interpretation of the composition has to consider the influence of the Holocene and modern soil processes that lead to "loess removal" and the destruction of cryogenic evidence [Golovanov, Verba, 1998]. Four samples from the mantle formations exhibit non-sedimentogenic distribution of the heavy fraction weight. This property, typical of cryoeluvial formations, is also associated with the interformational Paleogene crust of weathering of sedimentary deposits. It can be assumed that the anomalous, in terms of sedimentogenesis, distribution of the heavy fraction is associated with the eluvium of sedimentary deposits in general. Taking into account the environment of occurrence of the samples analyzed by S.S. Morozov, this parameter may reflect the general manifestation of the supergenesis factors. And only in a sample of the Mstislavsky loess, one can specifically link the anomalous distribution of the heavy fraction with the Pleistocene cryogenesis because it lies at the depth of 3 m, which apparently excludes, in these conditions, a significant influence of the modern soil processes.

Mineralogical analysis showed enrichment of the fraction 0.05–0.01 mm with quartz compared with larger grains in the samples of the Mstislavsky and Tula loess loams, i.e., in the most northern points of the investigated area. When interpreting the values of the quartz-feldspar ratio in various-size fractions, one also needs to consider the possibility of the influence of the supergenesis processes imposed later, which could have changed this ratio. In the sample of the Mstislavsky loess (depth of 3 m), the distribution of quartz and feldspar in two size-fractions corresponds to that of the cryogenic. In other samples, this parameter characterizes a non-cryogenic type of supergenesis, which can be explained by the influence of the modern soil-forming processes.

More definite results were obtained in the study of the composition of loess-like loams and underlying sediments from the city of Roslavl area, 100 km to the east of the area where S.S. Morozov collected the Mstislavsky loess. A.A. Velichko [1961, 1965] and T.P. Kuznetsova [1976] described there thick wedge- and related mantle formations of the Late Pleistocene cryogenic epoch, similar to polygonal structures of other regions of the paleocryogenic area and various locations of the modern permafrost tundra of Bolshaya Zemlya, Central Yakutia, and other regions. [Popov, 1958a, 1962].

According to T.P. Kuznetsova [1976], in the quarries of a brick factory located within the extensive depressions of relief near the city of Roslavl, the super-moraine layer of sediments is clearly divided into two parts: the lower one is subaqueous, composed of blue-gray loam with plant residues; the upper one is subaerial, composed of light gray and light brown homogeneous loess loam. In subaerial-subaqueous layer, there are thick wedgeshaped structures of a two-tier type. The lower and narrower ends of the veins are manifested very distinctly; they are wedge-shaped and are located in the subaquatic horizon. The upper broad structures that open at the surface "dissolve" in the layer of loess-

Table 2. Selected parameters of composition (%) of different fractions (mm) of loess on the Russian Plain

Deposits, Region	Depth, m	Granulometric composition (without removal of carbonates)						SiO_2 content in carbonate-free samples		Yield of heavy minerals		Ration of quart to feldspar contents	
		1–0.25	0.25–0.05	0.05–0.01	0.01–0.005	0.005-0.001	<0.001	0.05–0.01	deposit in general	0.25–0.05	0.05-0.01	0.25–0.05	0.05-0.01
Penza cover clay reddish-pale, rich with carbonates; N 52°50′	1.44–1.54	0.40	2.35	17.12	29.86	4.49	45.09	**83.40**	**66.01**	**0.17**	**0.08**	3.319	3.284
Tula loess loam, pale, with reddish shade; N 53°30′	2.0	0.06	2.76	42.78	26.06	4.80	23.18	**86.47**	**73.64**	traces	0.13	**3.424**	**3.595**
Priluky loess, pale, porous; N 50°30′	1.8–1.9	0.05	5.42	57.44	21.28	1.44	13.67	**89.11**	**83.23**	**0.62**	**0.08**	4.503	4.319
Mstislavsky loess, pale; N 54°30′	3.0	1.97	11.47	49.00	22.91	3.91	10.43	**85.53**	**79.17**	**0.21**	**0.02**	**2.144**	**3.51**
Trubachev loess, pale, porous; N 52°30′	2.5	0.23	9.38	67.47	11.98	2.01	8.52	**88.28**	**85.06**	**0.13**	**0.08**	6.129	4.030

Note: Bold font is for the values that, in the author's opinion, indicated cryogenic nature of the mineral matter of the studied loess samples.

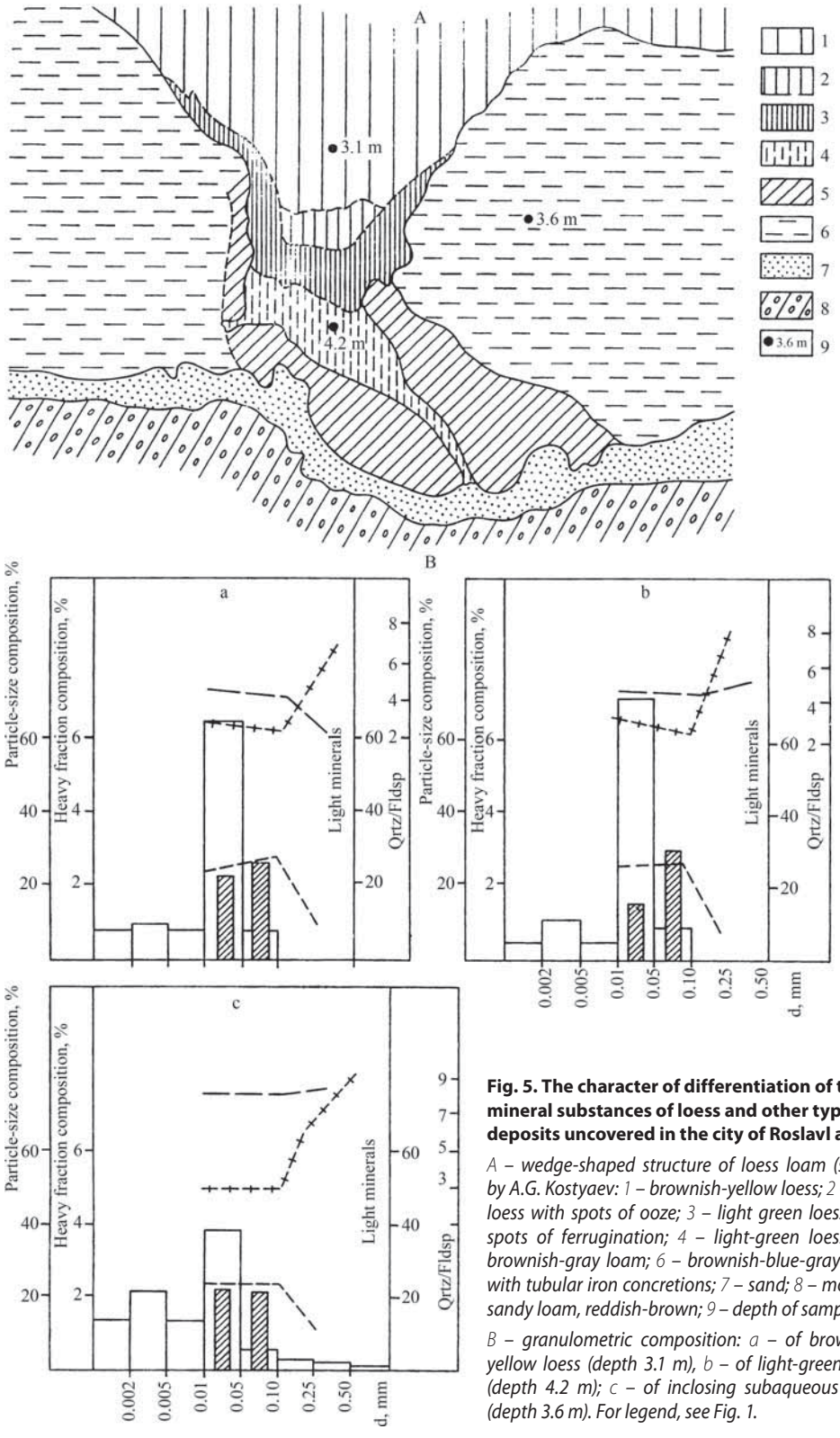

Fig. 5. The character of differentiation of the mineral substances of loess and other types of deposits uncovered in the city of Roslavl area:

A – wedge-shaped structure of loess loam (sketch by A.G. Kostyaev: 1 – brownish-yellow loess; 2 – pale loess with spots of ooze; 3 – light green loess with spots of ferrugination; 4 – light-green loess; 5 – brownish-gray loam; 6 – brownish-blue-gray loam with tubular iron concretions; 7 – sand; 8 – moraine sandy loam, reddish-brown; 9 – depth of sampling.

B – granulometric composition: a – of brownish-yellow loess (depth 3.1 m), b – of light-green loess (depth 4.2 m); c – of inclosing subaqueous loam (depth 3.6 m). For legend, see Fig. 1.

like sandy loams that fill the whole structure and change the color to gray or pale green at the bottom of the wedgeshaped part The two-tier type of the structures, according to T.P. Kuznetsova [1976], can be attributed to their original ground type and reflects the contact of the two horizons of cryolithogenesis, i.e., permafrost and the layer of seasonal thawing.

Fig. 5 presents a sketch of a typical structure in one of the quarries of the city of Roslavl. A.G. Kostyaev kindly provided us with some samples of the main types of deposits of this cross-section.

The lower, subaqueous horizon of the mantle layer (3.6 m) has clearly sedimentary features, i.e., the yield of the heavy fraction is maximum in the finest grains of the sandy-aleuritic range (Fig. 5). The values of quartz, feldspars, and the quartz-feldspar coefficient in the fractions of 0.05–00.01 and 0.05–0.1 mm indicate the cryogenic type. CCC here is 1.2, while $K_{h.f.} = 1.1$.

Loess-like deposits in the upper and lower parts of the relict cryogenic structure are more uniform in terms of mechanical composition, especially due to the decreased content of the finely dispersed (< 0.005 mm) particles; the content of the large-aleuritic fraction increases by 25–30 % compared with the subaqueous loam. Despite greater uniformity and particle-size sorting of the loess-like sandy loams, the distribution of the heavy fraction by the granulometric spectrum is reversed, i.e., it is clearly non-sedimentary. $K_{h.f.} = 0.6$ и 0.4. There is a clear trend in the distribution of the main deposit-forming mineral components (quartz, feldspars). In the pale-yellow loess-like sandy loam (depth 3.1 m), the quartz content consistently increases from the fraction 0.25–0.1 mm to the fraction 0.05–0.01 mm, as well as in the upper horizon of the most homogeneous loess-like formations of the Bolshaya Zemlya tundra.

However, it should be noted that in general contrast of the contents of the minerals listed above in the comparable-size fractions is slightly lower compared with the loess-like formations of the modern permafrost.

The reason is the large initial degree of weathering of feldspars in the source deposits in the city of Roslavl area (the taiga zone) compared with the parent rocks of the mantle loess-like formations of the Bolshaya Zemlya tundra.

More specific results, indicating a decisive influence of cryogenic weathering on the composition of loess-soil series, were obtained from the Nikitino and Suvorotino sections (Fig. 6). Loess and buried soils alternate in the sections. Cryolithogenitic analysis of the sediments in the Nikitino section showed the following (Fig. 7). In the modern soil, CCC is 0.51. In the underlying loess horizon (loess II + III according to Velichko [1961]), CCC reaches 1.4 in the upper part of the horizon, decreasing to 1.08 at the bottom. In the underlying buried soil, presumably Bryansk [Velichko, 1961], at a depth of 370 cm, CCC is smaller than 1 (0.59). Further down the section of loess I, CCC is greater than 1 (1.31). In the underlying lacustrine sediments, CCC is 1.08 in the middle part of the layer; at a depth of 610 cm, CCC is 1.06.

Fig. 6. Location of the Nikitino and Suvorotino sections.

In the Suvorotino section, there is the upper layer of modern soils with two horizons of loess and two horizons of buried soil below – the Bryansk and the complex Mezensky soil body [Velichko, 1961, 1965].

In the modern soil, CCC ranges within 0.59–0.63. In the underlying loess II + III at the

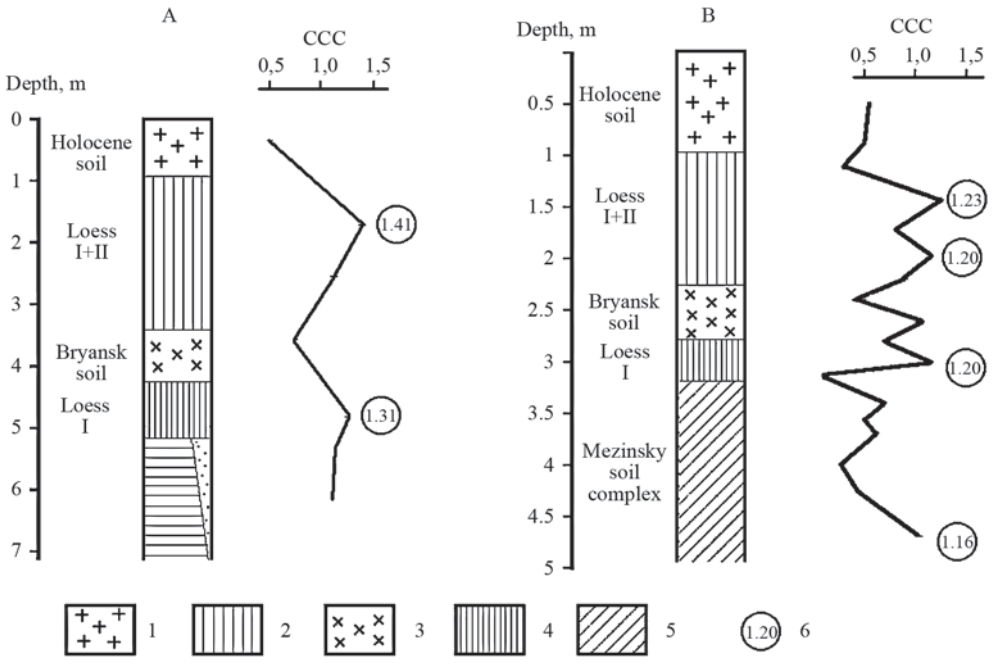

Fig. 7. CCC values of deposits of the loess-soil series in the Nikitino (A) and Suvorotino (B) sections. The explanation is in the text.

1 – modern soils; 2 – loess-like loam (loess II + III); 3 – buried soil; 4 – loess-like loam (loess I); 5 – silty sand with lenses of gravel; 6 – CCC values.

very top of the horizon and directly below the modern soil, CCC is 0.38; further down, at a depth of 140 cm, CCC reaches 1.23. In the Bryansk soil, CCC in the upper part is 0.44, while in its lower part at the contact with loess I, CCC is 1.12. In the underlying horizon of loess in its middle part at a depth of 300 cm, CCC is 1.2. In the Mezensky buried soil body, CCC decreases sharply to 0.35 in the upper part. However, in the very bottom part of the Mezensky soil body, probably at the boundary with the underlying loess that was not revealed in the section, CCC increases to 1.45.

These data show that the CCC parameter rather clearly reflects the role of cryogeneisis in the formation of loess horizons and its absence in the phases of formation of buried soils. These data agree well with the conclusions of paleogeographers on the course of the natural process during formation of loess-soil series in the center of the East European Plain. Unfortunately, in the examined sections, determination of the coefficients of distribution of the heavy mineral fraction was not conducted as it has been done for the section in the Rostov region (see above). This would have also allowed drawing definite conclusions about sedimentation environment of the loess horizons formation.

Analysis of individual samples of loess sediments of the periglacial areas of Central Germany (near the section in the Lengenboden region, to the south of Berlin) also showed promising prospects of cryolithological analysis of mineral matter in the territory of the periglacial zone of Western Europe [Konishchev, Rogov, Lebedeva-Verba, 2005].

Chinese permafrost scientists [Guoqing Qiu and Cheng Guodong, 1995] have successfully used the CCC method to determine the altitudinal limit of the cryolithozone in the Chinese Tien Shan during the late Pleistocene cryochron, by collecting samples of loess at different altitudinal

levels. The CCC values were greater than 1, starting from a height of 2100 meters, which is 1,000 meters lower than at present.

GENESIS OF THE CARBONATE CONTENT OF LOESS DEPOSITS

A characteristic feature of the typical loess is its high carbonate content, which defines a number of specific properties of these deposits, especially the ability to maintain the vertical wall in the outcrops and subsidence at wetting.

First of all, there is a question about the sources of carbonates in loess. There are a large number of views on this account in the literature, whose analysis is provided in the work of N.M. Krieger [1965]. In our opinion, the closest to the correct understanding of this problem, are the authors who believe that the source of carbonates in loess is the original rock, whose minerals provided the basis for the formation of the composition of loess. This is evidenced by the fact of a joint presence in loess of both primary clastic and secondary chemogenic carbonate. And these are not the exceptional cases, but practically a rule, which follows from the analysis of the fundamental generalizing works [Loess deposits…, 1966; Loess cover…, 2001].

The process of transformation of primary carbonates in the original source rocks (dissolution and migration of the hydrocarbon solution) and precipitation of secondary carbonates in the course of the modern loess forming process in the alpine steppes of inner Tien Shan was well described by A.G. Chernyakhovsky [1966].

Something similar was happening during the formation of the typical loess in the periglacial zone in the Pleistocene cryochrons.

Cryogenic process played also a certain role. Table 1 indicates that the process of multiple alternating freezing-thawing cycles leads, in moist conditions, to the almost complete disintegration of the original 0.25–0.1 mm carbonate grains into fine sandy and clay particles, 0.005–0.001 mm in size.

Under natural conditions, this process significantly increases the rate of dissolution of primary carbonate particles. A.G. Chernyakhovsky [1966] indicates that different areas of modern loess formations are in harsh climate – the winter temperature is –38 ÷ 40 °C and the summer temperature is rather high, up to + 30 °C. In summer, night frosts are frequent, when 15 cm thick ice forms on lake surfaces. In swampy areas, permafrost is developed. Naturally, the rest of the area has seasonal and short term freezing, which, we believe, contributes to the disintegration of the original bedrock, including destruction of carbonate grains in the latter rocks to a powdered state, which contributes to a more rapid dissolution.

The content of carbonates in loess of the East European Plain and the southern regions of Western Siberia ranges from the first fraction of a percent up to 15–20 %. Fluctuations of the carbonate content are observed not only over the vertical profile of loess, largely depending on the buried soils, but also horizontally, depending on the terrain.

B.B. Polynov [1952] has already emphasized geomorphological localization of loess carbonate as the accumulative (*underlined by the author, V.K.*) weathering crust. It lies on the cleaved surface area above the chloride-sulphate accumulative weathering crust and below the area of siallite weathering. This law has been established by B.B. Polynov [1952] for the mountain areas of the Kenteya and Khangai territories. The summarizing work of N.I. Krieger [1965] gives examples of the content of $CaCO_3$ depending on the relief not only for the mountain areas, but also for plains, although the data are limited and require further study of this problem.

Cryogenic processes have contributed not only to the disintegration of the primary carbonate to a fine state, and thus, their dissolution, but also to the formation of several generations of authigenic (secondary) carbonate minerals that precipitate out of solution in the process of freezing of loess sediments, as observed in the syncryogenic

Pleistocene sediments of Northern Yakutia [Kurchatov Rogov, 2013].

According to some researchers, the formation of the typical (carbonate) loess was occurring in the Pleistocene periglacial areas, in cold steppes [Krieger, 1965, Chernyakhovsky, 1966]. The hydrothermal conditions of the loess layer were largely determined by cryogenic processes (alternate freezing and thawing) and allowed the movement of calcium solution by ground and soil water and its precipitation in the form of new formations and secondary carbonate [Rozanov, 1952; Krieger, 1695]. In Holocene, the carbonate content of the typical loess has been preserved as the northern boundary of the typical loess is close to the northern boundary of steppe and forest-steppe, and the Pleistocene soils buried in loess of the semiarid zones are similar to the modern soils [Krueger, 1965; Zykina, 2012]. To the north of this boundary in more humid conditions of the periglacial zones, there are non-carbonate or low-carbonate loess deposits; in these regions, the processes of leaching were occurring more intensely.

CONCLUSIONS

1. The proposed lithological criteria (the coefficients of cryogenic contrast and of the heavy fraction) allow distinguishing the genetic nature of the particle-size distribution of loess deposits, whether it is a product of cryogenic weathering or aeolian sedimentation.

Thus, in hydromorphic conditions of relief depressions and on footslopes, there was accumulation of secondary carbonate during cold phases of the loess-soil series formation. During phases of relative warming, decrease in the input of cryogenic melkozem and retardation of soil formation, there was partial or complete leaching of $CaCO_3$ along with partial disturbance of the cryogenic distribution of quartz and feldspars by granulometric spectrum. To the north of this boundary in more humid conditions of the periglacial zones, non-carbonate or low-carbonate loess deposits are common; there, the processes of leaching were occurring more intensely.

2. Wide application of these criteria to the study of the genetic nature of loess non-carbonate deposits (mantle loam of the northern part of European Russia, Western Siberia, and the ice complex of East Siberia) of the current cryoloithozone, where evidence of the Pleistocene periglacial areas remained, made it possible to establish the cryogenic nature of mineral matter of these deposits.

3. Within the typical carbonate loess area, analysis of the genetic nature of their particle-size distribution using the proposed criteria have not yet received wide application. Nevertheless, the data provided in this paper on the composition of loess in different areas (center of the European part of Russia, Tien Shan) indicate its cryogenic nature. Certainly, further research with methodological positions proposed in this paper is necessary; it would reveal areas of loess of both the cryogenic nature of its mineral matter and sedimentary origin, including aeolian. ■

REFERENCES

1. Ananiev V.P. (1960) O svyazi granulometricheskogo sostava s mineralogicheskim v lessakh [On the relationship between particle-size and mineralogical distribution in loess]. Byul. Komis. po izucheniyu chetvertichnogo perioda AN SSSR, № 24, pp. 66–71 (In Russian).

2. Astakhov V.I., Swensen I. (2011) Pokrovnaya formatsiya finalnogo pleistotsena na krainem severo-vostoke Evropeiskoy Rossii [Mantle formation of the final Pleistocene in the extreme north-east of European Russia]. Regionalnaya geologiya i metallogeniya, № 47, pp. 12–27 (In Russian).

3. Bassinet F.C., Labeyrie L.D., Vincent E., Quidelleur X., Shackleton N.J., Lancelot Y. The astronomical theory of climate and the age of the Brunhes-Matuyama magnetic reversal // Earth and Planet. Sci. Lett. – 1994. – V. 126. – P. 91–108.

4. Broecker W.S. Abrupt climate change: causal constraints provided by the paleoclimate record // Earth Sci. Rev. – 2000. – V. 51. – P. 137–154.

5. Chernyakhovsky A.G. (1966) Sovremennoye lessoobrazovaniye v vysokogornykh stepyakh vnutrennego Tyan-Shanya [Modern loess formation in alpine steppes of Inner Tien Shan]. In: Sovremenny i chetvertichny kontinentalny litogenez. M., Izd-vo Nauka, pp. 17–35 (In Russian).

6. Chizhikov P.N. (1962) O rasprostranenii pokrovnylh lessovidnykh suglinkov na Russkoi ravnine [On the extent of mantle loess loam on the Russian Plain]. Byulleten komissii po izucheniyu chetvertichnogo perioda, № 27, pp. 28–33 (In Russian).

7. Golovanov D.L., Verba M.P. (1998) Sootnosheniye kriogennogo I pedogennogo vyvetrivaniya pervichnykh mineralov v pochvakh na pokrovnykh suglinkakh severnoy poloviny Russkoy ravniny [Relationship between cryogenic and pedogenic weathering of primary minerals in soils on mantle loams of the northern half of the Russian Plain]. Regionalnye problemy ekologii, geografii i kartografii pochv. Sbornik. – Moskva–Smolensk, Izd-vo SGU. pp. 189–197 (In Russian).

8. Gravis G.F. (1969) Sklonovye otlozheniya Yakutii. [Slope deposits of Yakutia]. M., Nauka. 128 p (In Russian).

9. Guoqing Qiu and Cheng Guodong. Permafrost in China: Past and Present. Permafrost and Periglacial Processes, Vol. 6: 3–14 (1995).

10. Hodaka Kawahata, Takanobu Okamoto, Eiji Matsumoto, Hiroshi Ujiie. Fluctuations of eolian flux and ocean productivity in the mid-latitude North Pacific during the last 200 kyr. Quaternary Science Reviews 19 (2000). 1279–1291.

11. Khalcheva T.A. (1975) Spetsifika izucheniya mineralogicheskogo sostava lessovoi tolshchi pleistotsena basseina Dnepra [Specificity of the study the mineralogical composition of the Pleistocene loess stratum in the Dnieper basin]. In: Problemy regionalnoi i obshchei paleogeografii lessovykh i periglyatsialnykh oblastei. M., Nauka, pp. 69–79 (In Russian).

12. Konishchev V.N. (1981) Formirovaniye sostava dispersnykh porod v kriolitosfere [Formation of dispersed rocks in cryolithosphere]. Novosibirsk, Izd. Nauka, Sibirskoye otdel., 195 p (In Russian).

13. Konishchev V.N. (2013) Priroda tsiklicheskogo stroyeniya ledovogo kompleksa Vostochnoy Sibiri [The nature of the cyclic structure of the ice complex of Eastern Siberia]. Kriosfera Zemli. T. XVII, № 1, pp. 3–16 (In Russian).

14. Konishchev V.N. Rogov V.V., Shurin G.N. (1974) Vliyaniye kriogennykh protsessov na glinistye mineraly [Influence of cryogenic processes on clay minerals]. – Vestn. Mosk. un-ta, Ser. geogr., № 4, pp. 40–46 (In Russian).

15. Konishchev V.N., Lebedeva-Verba M.P., Rogov, V.V., Stalina E.E. (2005) Kriogenez sovremennykh i pozdnepleistotsenovykh otlozheniy Altaya i periglyatsialnykh oblastei Evropy

[Cryogenesis of the modern and Late Pleistocene deposits of Altai and periglacial areas of Europe]. Moskva, Geos, 133 p (In Russian).

16. Kotlyakov V.M., Lorius C. (2000) Chetyre klimaticheskikh tsikla po dannym ledyanogo kerna iz glubokoi skvazhiny na stantsii Vostok v Antarktide [Four climatic cycles according to the ice core from a deep well at the Vostok station in Antarctica]. Izv. RAN. Ser. geogr. – № 1. – pp. 7–19 (In Russian).

17. Krieger N. (1965) Less, yego svoistva i svyaz s geograficheskoi sredoi [Loess, its properties, and the relation to the geographical environment]. Moskva, Izd-vo Nauka., 296 p (In Russian).

18. Kurchatova A.N., Rogov V.V. (2013) Autigennye karbonaty v otlozheniyakh ledovogo kompleksa primorskikh ravnin Vostochnoi Arktiki [Authigenic carbonates in the sediments of the ice complex of the coastal plains of Eastern Arctic]. Kriosfera Zemli. T. XVII, № 3, pp. 60–69 (In Russian).

19. Kuznetsova T.P. (1976) O klinovidnykh strukturakh tsentralnoi chasti Russkoi ravniny [On the wedge-shaped structures of the central part of the Russian Plain]. In: Problemy kriolitologii. Vyp. 5. M., Izd-vo Mosk. un-ta, pp. 160–167 (In Russian).

20. Lazarenko A.A. (1964) Litologiya allyuviya ravninnykh rek gumidnoi zony (na primere Dnepra, Desny i Oki) [Alluvial lithology of plain rivers of the humid zone (the Dnieper, Desna, and Oka, as examples)]. M., Nauka. 228 p (In Russian).

21. Lessovy pokrov Zemli i yego svoistva [Loess mantle of the Earth and its properties] (2001). Pod. red. V.T. Trofimova. Izd-vo Mosk. un-ta. 464 p (In Russian).

22. Lessovye porody SSSR [Loess deposits of the USSR] (1966). Moskva, Izd-vo Nauka. 256 p (In Russian).

23. Makeev A.O. (2012) Poverkhnostnye paleopochvy lessovykh vodorazdelov Russkoi ravniny [Surface paleosoils of loess watersheds of the Russian Plain]. M.: Molnet, 260 p. (In Russian).

24. Meng Li, Zhibao Dong, Zhengcai Zhang. Calculation of the aeolian sediment flux-density profile based on estimation of the kernel density. Aeolian Research. 16 (2015), p. 49–54.

25. Minervin A.V. (1982) Rol kriogennykh protsessov v formirovanii lessovykh porod [The role of cryogenic processes in the formation of loess deposits]. In: Problemy kriolitologii. Vyp. X. Izd-vo Mosk. un-ta. pp. 41–60 (In Russian).

26. Morozov S.S. (1949) Khimiko-mineralogichesky sostav i fiziko-khimicheskiye svoistva otdelnykh granulometricheskikh fraktsiy lessov Pridneproviya i genetiheski blizkikh im porod [Chemical and mineralogical composition and physico-chemical properties of the individual size-fractions of the Near Dnieper loess and genetically close deposits]. Uch. zap. Mosk. un-ta. Gruntovedeniye. Kn. 1, vyp. 133, pp. 12–38 (In Russian).

27. Page L.R., Charman R.W. The dustfall of December 15–16, 1933. –Amer. J. Sci., 1934, v. 28, № 1.

28. Polynov B.B. (1952) Geomorfologicheskiye usloviya raspredeleniya produktov vyvetrivaniya [Geomorphological conditions of the distribution of weathering products]. Geograficheskiye raboty. Geografgiz (In Russian).

29. Popov A.I (1958) Blochny relief na severe Zapadnoi Sibiri I v Bolshezemelskoi tundre [Block terrain of the north of Western Siberia and the Bolshaya Zemlya tundra]. – Voprosy fizicheskoi geografii polyarnykh stran. M., Izd-vo Mosk. un-ta, vyp. 1, pp. 146–154 (In Russian).

30. Popov A.I. (1962) Pokrovnye suglinki I poligonalny relief Bolshezemelskoi tundry [Mantle loams and polygonal terrain of the Bolshaya Zemlya tundra]. – In: Voprosy geograficheskogo merzlotovedeniya I periglyatsialnoi morfologii. M., Izd-vo Mosk. un-ta, pp. 109–130 (In Russian).

31. Rozanov A.N. (1952) Problema lessa i serozemoobrazovaniye [The problem of loess and serozems formation]. Pochvovedeniye, № 7 (In Russian).

32. Rukhin L.B. (1961) Osnovy litologii [Fundamentals of lithology]. Izd. 2-e. L., Gostontekhizdat. 770 p (In Russian).

33. Russel R.D. The mineral composition of atmospheric dust collected at Baton Rouge, Louisiana. – Amer. J. Sci., 1936b, v. 31, № 181.

34. Ryabchenkov A.S. (1955) K voprosu o proiskhozhdenii lessa Ukrainy v svete mineralogicheskikh dannykh [On the origin of loess in Ukraine in the light of mineralogical data]. – Byul. Komis. po izucheniyu chetvertichnogo perioda AN SSSR, № 2, pp. 45–59 (In Russian).

35. Ryasina V.E. (1961) O nekotorykh zakonomernostyakh raspredeleniya terrigennykh mineralov v razlichnykh fatsiyakh sovremennogo allyuviya r. Volgi [On some patterns of distribution of terrigenic minerals in different facies of the modern alluvium of the Volga River]. – Byul. MOIP. Otd. geol., T. 36, vyp. 1, pp. 106–114 (In Russian).

36. Sergeev E.M. (1954) Otnositelno vzaimosvyazi mezhdu mineralogicheskim I granulometricheskim sostavom gruntov [On the relationship between mineralogical and granulometric composition of soil]. – Vestn. Mosk. un-ta, № 2, pp. 41–50 (In Russian).

37. Sidorenko A.V. Eolovaya differentsiatsiya veshchestva v pustyne [Aeolian differentiation of substance in the desert]. – Izv. AN SSSR. Ser. geogr., № 3, pp. 3–22 (In Russian).

38. Strakhov N.M. (1962) Osnovy teorii litogeneza [Fundamentals of the lithogenesis theory]. T. 1, 2. M., Izd-vo AN SSSR. T. 1. 203 p. T. 2. 549 p (In Russian).

39. Sycheva S.A. (2011) Pozdnepleistotsenovye merzlotnye fenomeny v periglyatsialnoi oblasti Russkoi ravniny i ikh svyaz s paleopochvami [Late Pleistocene periglacial frost phenomena in the periglacial region of the Russian Plain and their relationship with paleosoils]. In: Problemy paleogeografii i stratigrafii pleistotsena. Vyp. 3. Materialy Vserossiyskoi nauchnoi konferentsii Markovskiye chteniya 2010. M. pp. 228–237 (In Russian).

40. Tsekhomskiy A.M. (1956) O nekotorykh osobennostyakh mineralnogo sostava kvartsevykh peskov [On some features of the mineral composition of quartz sands]. – Materialy po litologii. Nov. ser. M., VSEGEI, vyp. 1, pp. 31–45 (In Russian).

41. Vandenberghe J., Nugteren G. Rapid climatic changes recorded in loess successions. Global and Planetary Change 28 (2001), 1–9.

42. Velichko A.A. (1961) Geologichesky vozrast verkhnego paleolita tsentralnykh raionov Russkoy ravniny [The geological age of the Upper Paleolithic of the central regions of the Russian Plain]. M., Izd-vo AN SSSR. 296 p (In Russian).

43. Velichko A.A. (1965) Kriogenny relief pozdnepleistotsenovoy periglyatsialnoy zony (kriolitozony) Vostochnoy Evropy [Cryogenic relief of the Late Pleistocene periglacial zones (cryolithozone) of Eastern Europe]. In: Chetvertichny period i yego istoriya. M., Izd-vo AN SSSR, pp. 104–120 (In Russian).

44. Velichko A.A., Zelikson E.M., Borisova O.K., Gribchenko Yu.N., Morozova T.D., Nechaev V.P. (2004) Kolichestvennye rekonstruktsii klimata Vostochno-Evropeiskoy ravniny za poslednive 450 tysyach let [Quantitative reconstruction of climate of the East European Plain in the last 450 thousand years] Izv RAN Ser. geogr. – № 1. pp 7–25 (In Russian).

45. Zeuner F. (1963) Pleistotsen [Pleistocene]. M., Izd-vo inostr. lit. 502 p. (Trans. from English).

46. Zubakov V.A. (1966) Opyt geologicheskoy klassifikatsii kriogennykh yavleny [Practice of geological classification of cryogenic phenomena]. In: VIII Vsesoyuz. mezhduved. soveshch. po geokriologii (merzlotovedeniyu). Vyp. 2. Yakutsk, pp. 11–27 (In Russian).

47. Zykina V.S., Zykin V.S. (2012) Lessovo-pochvennaya posledovatelnost i evolutsiya prirodnoy sredy i klimata Zapadnoy Sibiri v pleistotsene [The loess-soil sequence and evolution of the environment and climate in Pleistocene in West Siberia]. Nauchn. red. M.I. Kuzmin; Ros. akad. nauk, Sib. Otd-niye, In-t geologii i mineralogii im. V.S. Soboleva. – Novosibirsk, Akademicheskoye izdatelstvo "GEO". 477 p (In Russian).

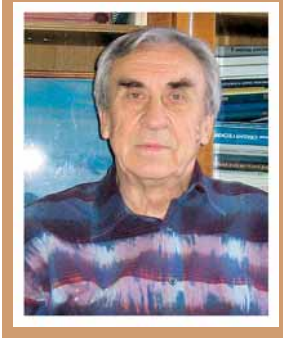

Vyacheslav N. Konischev graduated from the Department of Polar Countries (renamed in 1967 to the Department of Cryolithology and Glaciology) of the MSU Faculty of Geography. He received the D. Sc. degree in Geography in 1978 and became a full Professor in 1981. In 1999 he was awarded a title of the Honored Worker of Science of the Russian Federation. Professor V.N. Konischev has served as a Chair of the Department of Cryolithology and Glaciology since 1993. The areas of his scientific and teaching activities include permafrost science, cryolithology (composition and structure of cryolithic zone), and history and geo-ecology of the Earth's cryosphere. He has participated in scientific field expeditions in different regions of Northern Eurasia and North America; delivered lectures in the universities of Canada, Iceland, Poland, China and Japan. He is the author (co-author) of nine monographs and a textbook, and over 200 papers in peer-reviewed journals and conference proceedings.

Yurij K. Vasil'chuk[1*], Nadine A. Budantseva[2], Hanne H. Christiansen[3], Julia N. Chizhova[4], Alla C. Vasil'chuk[5], Alexandra M. Zemskova[6]
[1] Department of Landscape Geochemistry and Soil Geography, Lomonosov Moscow State University; e-mail. vasilch_geo@mail.ru
Corresponding author
[2] Department of Landscape Geochemistry and Soil Geography, Lomonosov Moscow State University; e-mail. nadin.budanceva@mail.ru
[3] Center for Permafrost (CENPERM), Department of Geosciences and Natural Resource Management, University of Copenhagen, Øster Voldgade 10, 1350 Copenhagen K, Denmark; e-mail. hanne.christiansen@unis.no
[4] Department of Landscape Geochemistry and Soil Geography, Lomonosov Moscow State University; e-mail. eacentr@yandex.ru
[5] Laboratory of Geoecology of the North, Lomonosov Moscow State University; e-mail. alla-vasilch@yandex.ru
[6] Department of Geography and Environmental Studies, Carleton University, 1125 Colonel By Drive, Ottawa, ON K1S 5B6, Canada; e-mail. alzemskova@gmail.com

OXYGEN STABLE ISOTOPE VARIATION IN LATE HOLOCENE ICE WEDGES IN YAMAL PENINSULA AND SVALBARD

ABSTRACT. The stable oxygen isotope composition of Late Holocene syngenetic ice wedges from the Erkutayakha River valley in the Yamal Peninsula and from the Adventdalen valley in Svalbard was studied. It was demonstrated that the studied ice wedges located 2000 km apart were formed during the last 2–3.5 ka and continue to grow at present. Variations of $\delta^{18}O$ values of the ice of both ice wedges do not exceed 2–3.5‰. Based on the oxygen isotope variations is has been calculated that mean winter air temperatures did not change by more than 3°C during the Late Holocene.

KEY WORDS: permafrost, oxygen isotopes, ^{14}C-dating, ice wedge, winter palaeotemperatures.

INTRODUCTION

The last two-three thousand years are of special interest for the palaeoclimatic reconstructions. There are detailed palaeoclimatic curves based on studies of lacustrine clay on Baffin Island [Thomas, Briner, 2009], tree rings in the Alps [Buntgen et al., 2005], and multi-disciplinary research on palaeoclimatic changes of the last twenty centuries in different regions of the Earth [Goosse et al., 2006; Jones and Mann, 2004; Lilleøren et al., 2012; Luterbacher et al., 2004; Mann et al., 1998; Maasch et al., 2005].

There are two key periods in the last 3 ka: the Medieval Warm Period (MWP) and the Little Ice Age (LIA). There are no universally accepted precise definitions for the duration of the LIA or the MWP. The MWP varied both spatially and temporally. The MWP is dated to about 800–1200 AD [Maach et al., 2005].

The span from 820 to 1050 AD was the warmest period with the average annual temperatures 0.6 °C higher than the modern temperatures, i.e. mean annual temperatures were only slightly higher than the modern ones in many parts of the world [Maach et al., 2005]. In Arctic Canada, the MWP is dated to 1375–1575 AD; it was 1.2 ± 0.6 °C cooler than today, and only slightly (0.1 ± 0.2 °C) warmer than the average for the last millennium in northeast Baffin Island [Thomas, Briner, 2009].

The transition from the MWP to the LIA was one of the most rapid global climatic events [Maach et al., 2005]. It occurred not only as a rapid temperature change, but also as changes in the atmospheric circulation and oceanic circulation. The culmination of the MWP is dated to approximately 1400 ± 40 AD, and its onset is dated to 1220 ± 40 AD [Moberg et al., 2005]. The LIA is characterized by a global decrease of 0.5–1.0 °C of the average air temperature and a lowering of the snowline by 100 m relative to its modern position [Maasch et al., 2005]. The LIA contains a coldest period called the Maunder minimum, the period of long-term decreasing solar spots [Eddy, 1976] from approximately 1645 to 1715 AD. Data from a varved proglacial lake sediments on northeast Baffin Island, Arctic Canada, [Thomas, Briner, 2009] show that the LIA (1575–1760 AD) was 1.5 ± 0.2 °C cooler than today and 0.2 ± ± 0.2°C cooler than the last millennium. January temperature reconstructions of both Northern and Southern Norway based on numerous studies in Scandinavia examining pollen and plant macrofossils in lake sediment cores, show that the LIA was the coldest period in the last 3 ka [Lilleøren et al., 2012].

Recent studies have shown that ice wedges in flood plains and peat bogs actively grew during the last 3–2 ka, e.g., within the floodplain near Fairbanks [Hamilton et al., 1983] and in the Da Hinggan Mountains, northeastern China [Yang, Jin, 2011]. This motivates us to consider in detail the palaeo-geocryological history of the Late Holocene based on a comparison of isotope data of ice wedges from the Yamal Peninsula and Svalbard, which have common morphological and genetic characteristics, but developed in rather different climatic conditions.

Ice wedges are the object to provide proxy-data for palaeoclimatic and palaeoenvironmental reconstructions. The origin of the ice infilling a crack can be attributed not only to unmodified winter snow, but also to hoarfrost accretion during winter and melting snow in spring, that subsequently refreezing in the crack. As a rule, wedge ice accumulates from

Table 1. $\delta^{18}O$ values for samples of recent syngenetic ice wedges and temperature parameters for Yamal Peninsula and adjacent regions and Russian Arctic Islands (from [Vasil'chuk, Kotlyakov 2000] with additions)

Ice wedge location	Latitude, Longitude	$\delta^{18}O$, ‰	FDD	$T_{m.w}$	$T_{m.J}$	$T_{gr.m.an}$
Yamal Peninsula						
Neromoyakha River	67°57′N, 66°20′E	–15.0	–3700	–15	–22	–10
Shchuch'ya River	66°57′N, 68°22′E	–18.2	–4000	–16	–24	–8
Seyakha settlement	71°10′N, 72°30′E	–18.0	–4173	–16	–23	–9
Vorkuta region						
Vorkuta	67°30′N, 62°02′E	–16	–2500	–12	–21	–6
Amderma	69°45′N, 61°40′E	–15.2	–3086	–13	–19	–7
Arctic Islands						
Henrietta Island	77°06′N, 156°30′E	–15.3	–5330	–17	–27	–12
Kotelny Island	75°27′N, 140°50′E	–18.1	–5400	–20	–29	–14
Novaja Sibir Island	75°03′N, 148°28′E	–18.0	–5500	–20	–30	–14
Chetyrehstolbovy Island	70°47′N, 161°36′E	–20.0	–5143	–19	–30	–13
Ayon Island	69°47′N, 168°39′E	–20.0	–5047	–20	–29	–12

FDD – cumulative freezing degree days; $T_{m.w}$ – mean winter air temperature (average temperature during period when mean days air temperature are lower than 0 °C), °C; $T_{m.J}$ – mean January air temperature, °C; $T_{gr.m.an}$ – mean annual ground surface temperature °C.

melting snow in spring. The isotope values of ice wedges correspond to the total winter isotope signal. Vasil'chuk [1993] established close relationship between oxygen isotope values ($\delta^{18}O$) in recent ice wedges and winter air temperatures (Table 1) that is described by the equations:

$$t_{mean\ winter} = \delta^{18}O_{ice\ vein}\ (\pm 2\ ^{\circ}C)$$

$$t_{mean\ January} = 1{,}5\ \delta^{18}O_{ice\ vein}\ (\pm 3\ ^{\circ}C).$$

Stable isotope study of ice wedges, both syngenetic and epigenetic, allows reconstructing the winter palaeotemperatures. However, syngenetic ice wedges are best for this purpose because it is possible to evaluate their age using ^{14}C dates of the host sediments. Sampling across the horizontal extent of ice wedges provides comprehensive information for reconstructions [Vasil'chuk, 2006, 2013; Yang and Jin, 2011].

Syngenetic ice wedges formed actively during the last 3 ka in various permafrost landforms: within floodplains and marshes, peatbogs, and in loess and slope sediments. Ice wedges are characterized by assumed symmetric isotope profiles that indicate symmetrical growth and frost cracking at relatively fixed intervals.

The aim of the paper is to study the oxygen-isotope composition of the Late Holocene ice wedges from the Erkutayakha River valley in the Southern Yamal Peninsula and from the Adventdalen valley in Svalbard and to reconstruct the winter palaeotemperatures for the last 3 thousand years.

STUDY AREAS

Erkutayakha River valley, Southern Yamal Peninsula

The Erkutayakha River valley is located in the Southern Yamal Peninsula (Fig. 1). This is the area of continuous permafrost with thickness of 100 m. The thickness of the active layer is about 95–100 cm [Trofimov et al., 1989]. The climate of the region is subarctic with long

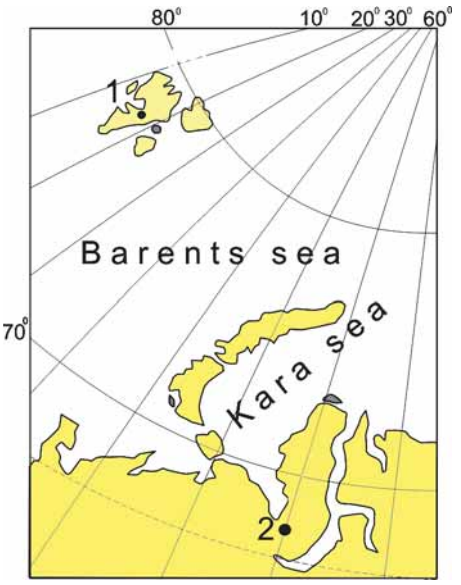

Fig. 1. Map showing the locations of the study sites: *1 – Svalbard, 2 – Yamal.*

severe winters and very short summers (no longer than 50–60 days). The warmest months are July and August with mean monthly temperature ranging from 5 to 7 °C, while the coldest months are January and February with mean air temperature ranging from –22 to –24 °C. Mean annual air temperature fluctuates between –8 and –10 °C, and the surface ground temperature is close to the same values: –8 to –10 °C [Vasil'chuk, 2006].

Most of the ice wedges on the Southern Yamal Peninsula occur within floodplains. The Holocene syngenetic floodplain with ice wedges was studied on the left bank of the Erkutayakha River. The height of the floodplain is about 2.5–3 m. The polygons with open frost cracks are more distinct in drier areas. In the cross-section of the floodplain, were revealed (Fig. 2, A):

0–0.2 m – unfrozen brown peat with stems, roots, and some peat layers 2–3 cm thick;

0.2–0.7 m – grey sand with massive cryostructure;

0.7–1.5 m – peaty and stratified sand with massive cryostructure and lenses of ice.

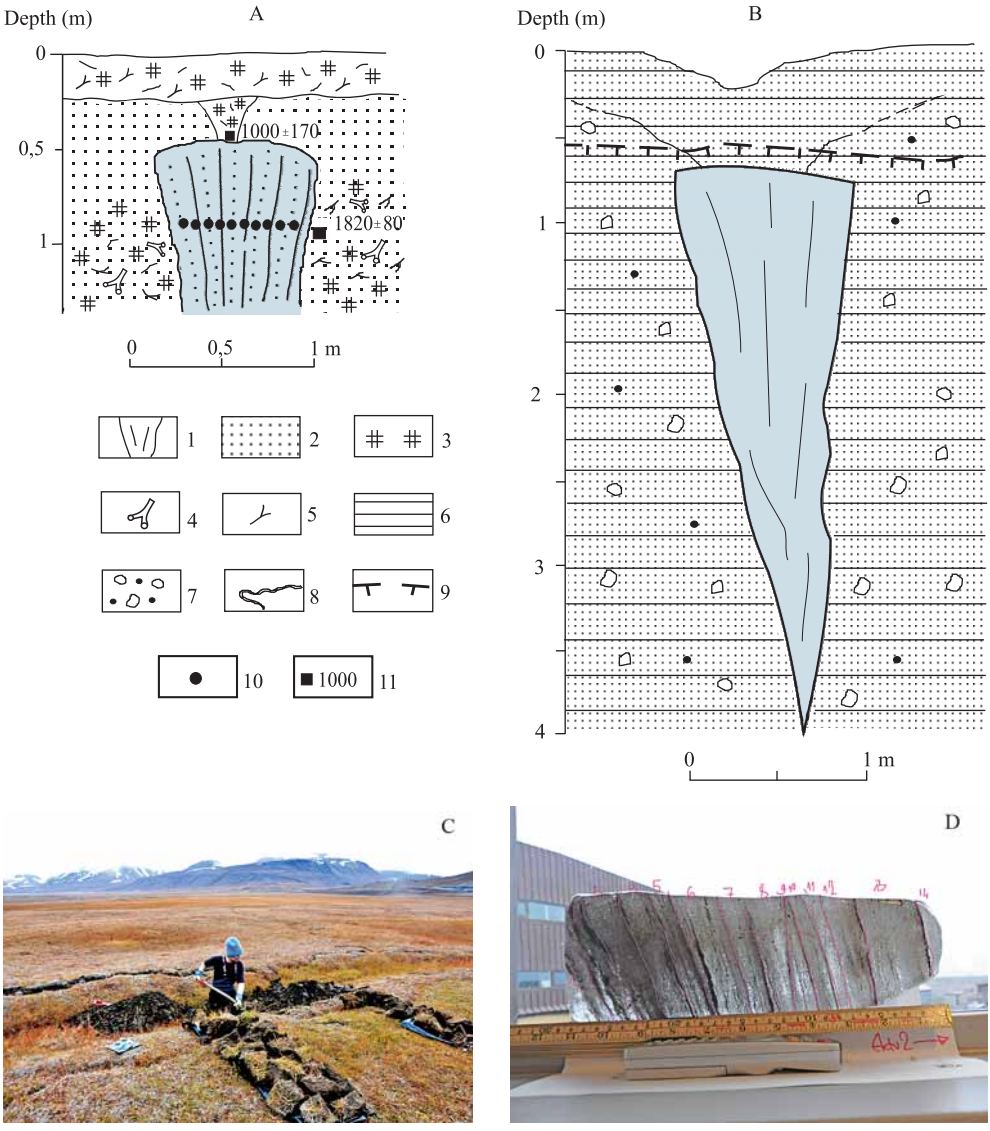

Fig. 2. Studied ice wedges:

A – Erkutayakha River floodplain, Yamal Peninsula, B – D – Adventdalen valley, Svalbard; B – sketch of a typical ice wedge in the Adventdalen valley (from [Matsuoka, Hirakawa, 1993]; C – the study site in the Adventdalen valley; D – internal structure of the ice wedge ice in the Adventdalen valley.

1 – ice wedge; 2 – sand; 3 – peat; 4 – twigs; 5 – roots; 6 – clay; 7 – gravel; 8 – clayey layers; 9 – base of active layer; 10 – sampling of ice wedge; 11 – ^{14}C dates.

At the depth of 0.4 m, an ice wedge was exposed. It consisted of about 160 individual ice veins. The ice was clear without admixtures. A ground peaty vein adjoined the top of the ice wedge (see Fig. 2, A).

Adventdalen valley, Svalbard

The Adventdalen valley is located in the central part of Svalbard and extends from east to west towards the fjord (see Fig. 1). It is a wide U-shaped valley, 3.5 km wide and 27

km long. The Adventdalen area is one of the driest parts of Svalbard; the average amount of precipitation is only about 190 mm.

The area is characterized by considerable temperature fluctuations during winter due to its maritime location. Mean air temperature of the coldest winter month is around –15 °C, mean air temperature of the warmest summer month is around 6 °C. Mean annual air temperature varies from –4 °C to –6 °C [Christiansen et al., 2013]. This is the area of continuous permafrost with thickness about 100 m thick. The thickness of the active layer is about 80–115 cm.

Ice wedges are widespread in Svalbard primarily in the lower parts of large valleys (e.g. Reindalen and Adventdalen valleys, Fig. 3) [Vtjurin, 1989; Matsuoka, Hirakawa 1993; Christiansen, 2005]. Thermal observations at the polygons in Adventdalen, where mean annual ground temperature at the bottom of the active layer was about –6 °C, showed that frost cracking was particularly active when mean daily air temperature dropped down to –20 °C and ground temperature at the bottom of the active layer decreased to –15 °C [Christiansen, 2005].

Ice wedges studied in the Adventdalen valley (78° 12´05´´ N, 15° 50´04´´ E) are located on the outer part of a large alluvial fan covered by aeolian deposits. The studied ice wedge, 2.5 m wide at the top, was exposed down to 3–3.5 m (see Fig. 2, B, C). About 345 elementary veins have been counted in the ice wedge.

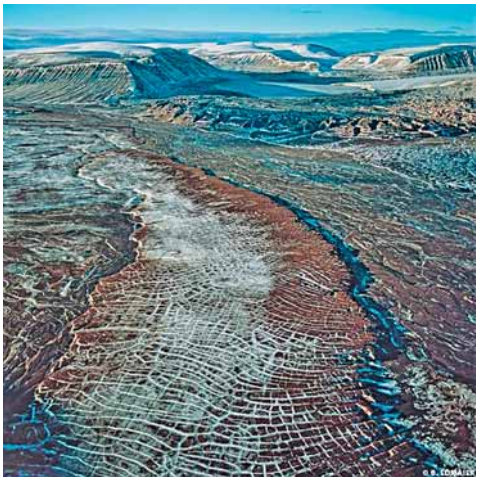

Fig. 3. Ice-wedge polygons in the central part of Svalbard.

According to Matsuoka and Hirakawa [1993], each ice vein cracks and acquires a new annual elementary vein every 6–7 years. Considering the amount of elementary veins, we may assume that the studied ice wedge has been growing during for the last 2500 years.

MATERIALS AND METHODS

11 samples of the ice wedge from the Erkutayakha site and 65 samples of the ice wedge from the Adventdalen site were sampled for isotope analysis. Both ice wedges were sampled horizontally in the top part using a chain saw to get large ice samples from across the entire ice wedges.

The ice samples were kept at a freezing temperature of –19.5 °C and then they were analyzed in the laboratory at –5 °C. The mineral admixtures were scrapped out. All ice samples were described on a light table, photographed in transmitted light, and further sawn up with a handsaw to obtain samples with widths from 0.7 to 2 cm (see Fig. 2, D). The ice samples were thawed at 7 °C and then poured into 50 ml plastic vials.

The oxygen stable isotope analysis was carried out in the Stable Isotope Laboratory of the Geography Department at Lomonosov Moscow State University, using a Delta-V mass spectrometer equipped with a standard gas bench. Oxygen isotope ratio was determined using equilibration techniques: samples for $\delta^{18}O$ analysis were equilibrated with CO_2 for 24 hours. For the measurements, international standards V-SMOW and international laboratory standards of the IAEA, as well as of the isotope laboratory of the Austrian Institute of Technology, were used. The precision of the measurements is 0.1‰.

The oxygen isotope composition of the ice wedge from the Erkutayakha site was determined by D. Rank and W. Papesch in the Arsenal Scientific Research Center in Vienna and by E. Soninnen in the Isotope Laboratory of the University of Helsinki, Finland. The organic matter from the floodplain was ^{14}C dated in the Geology Institute of RAS and in the radiocarbon laboratory of the University of Helsinki. ^{14}C AMS dates of ice wedges from the Adventdalen valley published by Jeppesen [2001] and Vittinghus et al. [2008] were used.

RESULTS

Oxygen stable isotope variations

The $\delta^{18}O$ values in the ice wedge from the *Erkutayakha River valley* varied from –18.0 to –20.63‰ (Table 2, Fig. 4). A segregated ice lens from the host sediment had higher $\delta^{18}O$ values – from –15 to –19.8‰.

The relatively narrow range of $\delta^{18}O$ (2.63‰) values indicates rather stable winter conditions during ice-wedge growth. The $\delta^{18}O$ value of a recent ice vein from floodplain sediments is –16.1‰ (see Table 2).

Table 2. $\delta^{18}O$ values in the ice wedge from the Erkutayakha River valley, Yamal Peninsula (site no 375–YuV)

Field no.	Depth, m	Distance from left contact zone, cm	$\delta^{18}O$, ‰
Holocene ice wedge in floodplain outcrop			
375-YuV/26*	1.0	0–7	–18.8
375-YuV/4*	1.0	10	–19.0
375-YuV/27*	1.0	10–14	–18.7
375-YuV/28*	1.0	14–28	–19.0
375-YuV/30*	1.0	28–40	–19.6
375-YuV/30**	1.0	28–40	–19.7
375-YuV/7*	1.0	40	–19.8
375-YuV/7**	1.0	40	–19.0
375-YuV/8*	1.0	40	–20.0
375-YuV/9*	1.0	40	–20.2
375-YuV/9**	1.0	40	–19.5
375-YuV/10*	1.0	40	–20.6
375-YuV/31*	1.0	40–50	–20.4
375-YuV/32*	1.0	50–54	–19.9
375-YuV/33*	1.0	54–64	–20.3
375-YuV/33**	1.0	54–64	–20.2
375-YuV/34**	1.0	64–70	–19.0
375-YuV/35*	1.0	70–80	–18.3
Recent ice vein in floodplain sediments			
375-YuV/36*	0.3	–	–16.1

* – isotope measurements made by D. Rank and W. Papesch in the Arsenal Scientific Research Center, Vienna,
** – isotope measurements made by E. Sonninen at the isotope laboratory of the University of Helsinki.

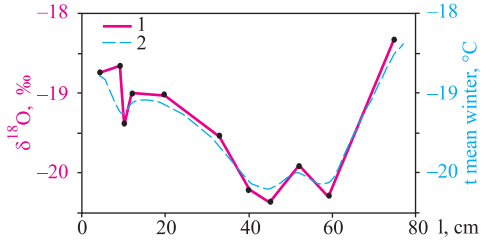

Fig. 4. $\delta^{18}O$ variations along the horizontal profile of the ice wedge, the Erkutayakha River valley, Yamal Peninsula, (1) and reconstructed mean winter air temperatures (2) based on Vasil'chuk's equations [1993]. *l* – distance from the left contact zone.

The $\delta^{18}O$ values in the presently growing parts of the ice wedge in the Southern Yamal Peninsula vary from –16 to –18‰ (see Table 2). These ice wedges occurred at the upper part of floodplain which formed 2–3 ka BP; thus, in the middle and early Holocene, the ice wedges in the Southern Yamal Peninsula were active also [Vasil'chuk et al., 2000]. In recent ice wedges on the islands of the Arctic Ocean, $\delta^{18}O$ values vary from –18 to –20‰ (see Table 1).

The $\delta^{18}O$ values in the ice wedge in the *Adventdalen valley* range from –12.2‰ to –15.4‰ (Table 3, Fig. 5) that correspond to the earlier obtained oxygen isotope data for ice wedges in the Adventdalen valley: $\delta^{18}O$ values vary from –11.5‰

Table 3. $\delta^{18}O$ values in the ice wedge from the Adventdalen valley, Svalbard

Distance from left contact zone, cm	$\delta^{18}O$, ‰	Distance from left contact zone, cm	$\delta^{18}O$.,‰	Distance from left contact zone, cm	$\delta^{18}O$, ‰
0.9	–12.3	59.2	–13.9	165	–14.1
1.8	–12.7	62	–14.1	169	–14.1
3.6	–14.1	77.4	–13.3	179	–12.3
5.4	–14.2	82.2	–14.7	185	–13.4
7.2	–14.1	87	–14.0	189	–12.2
9	–14.5	89	–13.2	193	–14.6
12	–15.4	91.8	–13.7	197	–14.1
14.4	–14.9	96.6	–14.3	211	–14.1
16.4	–15.0	99	–14.2	213	–14.1
19.8	–14.9	103	–13.0	219	–13.9
21	–14.7	110	–13.9	222	–13.4
23	–14.8	114	–14.1	225	–14.9
25	–14.5	118	–14.1	229	–14.7
27	–14.4	126	–12.9	234	–13.9
30	–13.8	128.5	–12.3	238	–14.2
32	–13.8	131	–13.5	245	–13.3
34	–14.2	134	–13.5	249	–13.4
36	–13.5	137	–13.5	252	–13.1
40	–13.7	147	–13.5	263	–13.5
43	–14.0	151	–13.9	264	–13.5
50.8	–14.8	155	–14.0	265	–13.6
56.4	–14.4	159	–12.5		

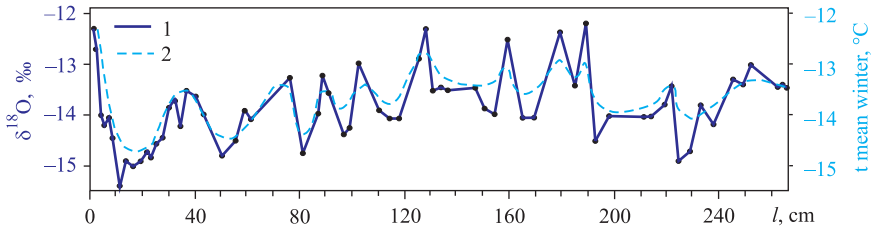

Fig. 5. $\delta^{18}O$ variations along the horizontal profile of the ice wedge, the Adventdalen valley, Svalbard (1) and reconstructed mean winter air temperatures (2) based on Vasil'chuk's equations [1993]. *l* – distance from the left contact zone.

Fig. 6. The Late Holocene ice wedge studied by Jeppesen [2001] in the Adventdalen valley.

to –15.5‰ [Jeppesen, 2001] and from –10.5‰ to –14.8‰ [Vittinghus et al., 2008] (Fig. 6, 7). The oxygen isotope composition of modern precipitation collected in Longyearbyen is characterized by $\delta^{18}O$ values from –5‰ to –30‰ [Ole Humlum, pers.comm].

These dates were obtained in the Geology Institute of RAS. ^{14}C age of the roots often is younger than in host sediment, due to the development of the root system only after sedimentation. However, the roots in permafrost may be quite reliable material for ^{14}C dating of syngenetic sediments with ice wedges [Vasil'chuk et al., 2001] due to excellent preservation and the barrier function of permafrost blocking root growth below the active layer. ^{14}C age of 1820 ± 100 yr BP (Hel-4492) (cal. 1747 ± 119) for moss sampled at a depth of 1.0 m was obtained in the Radiocarbon Laboratory of Helsinki University, that confirms the validity of the dates obtained.

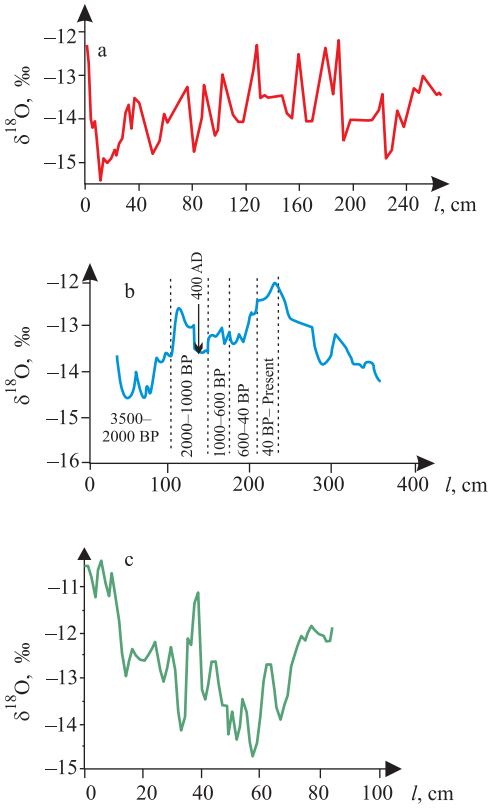

Fig. 7. Comparison of variations of $\delta^{18}O$ values across the Late Holocene ice wedges from the Adventdalen valley with the distance from the left contact:

a) This study, b) From Jeppesen [2001], c) From Vittinghus et al. [2008].

Table 4. ^{14}C AMS ages of organic matter from the ice wedges and host sediments from the Adventdalen valley, Svalbard

Depth, m	Dated material	cal.^{14}C age, BP*	Author
1.5	Peat	1618	[Jeppesen, 2001]
1.5	Peat	1766	
1.9	Peat	2018	
1.9	Peat	2166	
2.6	Peat	2710	
2.6	Peat	3680	
0.5	Organic material (Salix leaves) from outer part of the ice wedge	2900	
1.0	Organic matter from the ice wedge	2150	[Christiansen, 2005]
1.0	Organic matter from the ice wedge	1980	

^{14}C DATING AND AGE OF ICE WEDGES

The radiocarbon dating revealed a relatively young age of the floodplain sediments in the Erkutayakha River valley (see Fig. 2, A). The ^{14}C age of the peat from the ground vein above the ice wedge at a depth of 0.3 m is 1000 ± 170 yr BP (GIN-10632) (cal. 916 ± 167), while roots at a depth of 1.0 m were dated to 1820 ± 80 yr BP (GIN-10986) (cal. 1748 ± 97).

We suggest that roots are the "in situ" position because of the ages of the roots and the moss remains are close. We assume that about 1000 yr BP, the Erkutayakha River floodplain transitioned to subaerial regime of accumulation and ice wedges started to grow (so we think that the lower part of the studied ice wedge is actually epigenetic as it would not have been able to form when the site was flooded.

Radiocarbon dating of ice wedges in the *Adventdalen valley* has shown their Late Holocene age. The leaves of *Salix* found "in situ" in the outer part of ice wedge 160 cm wide at the top were ^{14}C AMS dated to 1980–2150 cal yr BP [Vittinghus et al., 2008].

^{14}C AMS dating of plant remains found directly in another ice wedge and in ice-wedge polygon sediments indicate that the oldest ice wedges grew syngenetically from app. 3.7 cal ka BP [Jeppesen, 2001]. Most of the AMS ^{14}C dates of peat or organic material from the ice-wedge host sediment ranges from 3.5 to 2 ka BP (Table 4).

AMS ^{14}C ages of plant fragments in the ice-wedge polygon sediments in the Adventdalen indicate that floodplain accumulation started from 3.3–3.9 cal ka BP [Oliva et al., 2014], supporting the assumption that ice wedges were formed since then, as these AMS ^{14}C dates provide direct maximum ages for syngenetic ice wedges.

The ^{14}C dated oxygen isotope diagram of the Holocene ice wedge from the Lena River Delta in the Siberian Arctic published by Meyer et al. [2015] became a good reference point for chronological binding of the oxygen isotope diagram of the Adventdalen ice wedge. ^{14}C AMS dates of 40 samples of ice provided a reliable dating of the isotope curve for the last 7 ka.

Comparison of the fragment of the isotope curve for the last 2–3 ka for the ice wedge from the Lena River Delta with the isotope curve for the Adventdalen ice wedge has shown satisfactory correlation of the isotope maxima and minima (Fig. 8).

It should be noted that the similarity of the isotope value ranges for the last 2–3 ka: in the ice wedge from the Lena River Delta, δ^{18}O

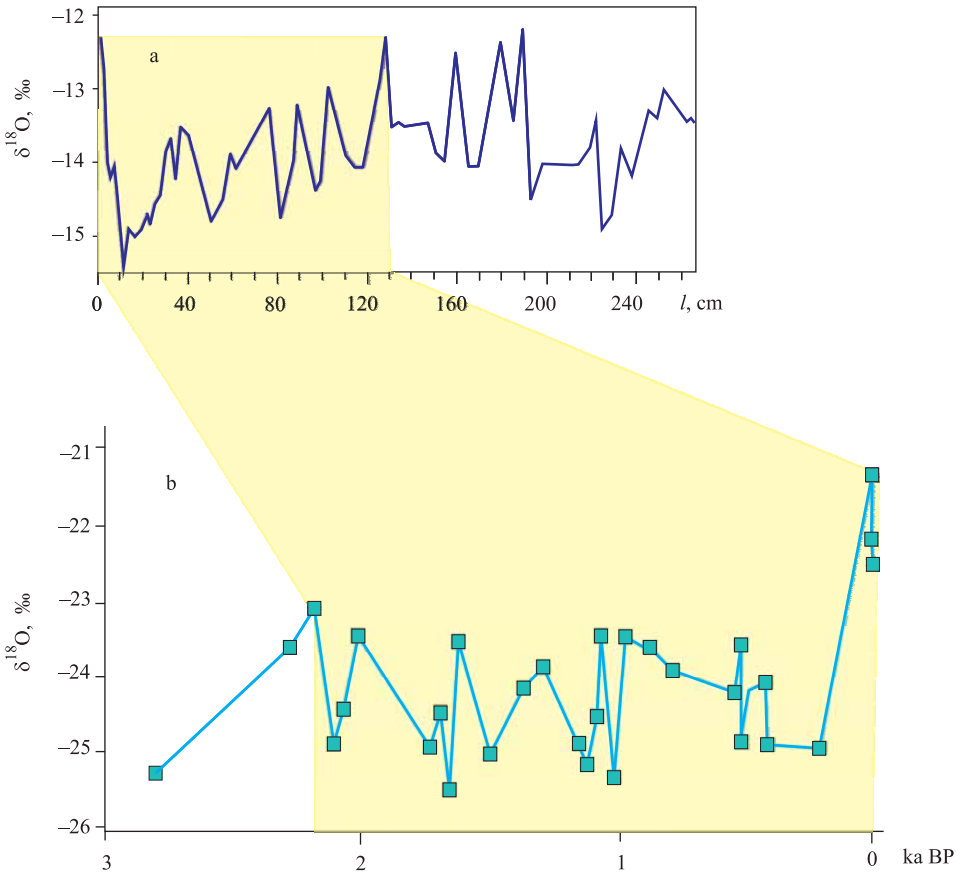

Fig. 8. Comparison of the oxygen isotope curve of the ice wedge from the Adventdalen valley, Svalbard, indirectly dated to the last 3 ka (a), with the ^{14}C dated fragment of the oxygen isotope curve of the ice wedge from the Lena River Delta, Siberian Arctic (b, from [Meyer et al., 2015]). Yellow area marks the fragments of the isotope curves that we assume have an approximately similar age.

values vary from –25.7 to –21.4‰, with 6 minima and 8 maxima; in the Adventdalen ice wedge, $\delta^{18}O$ values vary from –12.2 to –15.4‰, with 5 minima and 7 maxima.

DISCUSSION

Oxygen isotope composition of ice wedges and palaeotemperature reconstructions

^{14}C dating of ice wedges and host sediments as well as the amount of elementary veins in the ice wedge from Adventdalen allows us to consider that both studied ice wedges grew in the Late Holocene during the last 3–3.5 ka.

The difference of the oxygen isotope composition of the two ice wedges reflects the fact that winter conditions on Svalbard during the Late Holocene were less severe but more variable due to the marine environment, compared with continental climatic conditions of the Southern Yamal Peninsula, where winter temperatures were consistently lower.

Comparison of both ice-wedge isotope curves may be carried out by matching the most evident extreme peaks. These are the MWP dated from 1000 up to 700 years BP, and the Maunder minimum dated about 200 years BP [Isaksson et al., 2003]. We have selected the

part from the Adventdalen ice wedge isotope curves, which is most similar to that of the ice wedges in the Erkutayakha valley. We suppose that fragment 0–20 cm of the isotope curve of the ice wedge from the Erkutayakha River (Fig. 9) corresponds to the end of the MWP. The interval 20–80 cm corresponds to the subsequent transition period to the LIA and as this interval is characterized by two minima divided by a low positive peak and possibly the subsequent maximum of modern warming at the Yamal Peninsula curve at the interval 20–80 cm (see Fig. 9). Obviously, in this period, the ice wedges grew more intensely due to a more intensive frost cracking.

On the isotope curve for the Adventdalen ice wedge, the MWP interval is more expressive and possibly corresponds to the interval between 180 and 200 cm from the left contact zone (see Fig. 9). A subsequent transition period and the LIA show the same contrast as in the Yamal Peninsula.

Based on the oxygen isotope records of the ice wedges it is possible to reconstruct mean winter temperatures for the last 3 ka using the equations of Vasil'chuk [1993]. In the Southern Yamal Peninsula, mean winter air temperatures varied from –18 to –21 °C; in Svalbard, they varied from –12 to –15 °C.

Thus, the range of the mean winter temperatures values does not exceed 3 °C

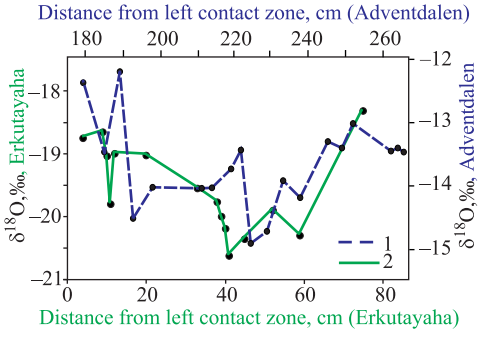

Fig. 9. Relation between the $\delta^{18}O$ curve fragments and the distance from the left contact zone from the ice wedges in the Adventdalen valley (1) and Erkutayakha valley (2).

for both sites. However, there is a difference between extremely maritime Svalbard and the much more continental Yamal Peninsula with more contrasting winter temperature oscillations during the MWP in Svalbard.

Oxygen isotope composition of Late Holocene ice wedges in the Northern Hemisphere

Comparison of the isotope data of the ice wedges from the Yamal Peninsula and Svalbard with published isotope data for ice wedges in the Northern Hemisphere formed during the last 3 ka, shows that the variations of the isotope values are rather moderate, but nevertheless noticeable. The Maunder minimum of the LIA (200 years BP) is characterized by relatively low isotope values, whereas the MWP (from 1000 to 700 years BP) is characterized by relatively high isotopic values.

Hamilton et al. [1983] have dated ice wedges in the floodplain near Fairbanks, Alaska, and concluded that the ice wedges actively formed during last 2–3 ka. They actively grew in the last 300–400 years despite a rather high mean annual air temperature (about –3.5 °C), and an even high ground temperature (mean annual values are up to –0.5, –1 °C higher than modern values). The ice wedge studied near the Vault Creek Tunnel, Fairbanks area, [Meyer et al., 2008] directly dated to 3.6 ka ^{14}C BP, shows a mean $\delta^{18}O$ value of –21.8‰. This is a typical isotope signature for Holocene ice wedges.

In the Da Hinggan Mountains, northeastern China, Yang and Jin [2011] studied ice wedges and found that they were formed from 1.6 to 3.3 ka BP. The isotope curve based on 16 samples collected along a horizontal profile at a depth of 1.3–1.4 m shows the range of $\delta^{18}O$ values from –20.9 to –17.8‰. There are three short cold periods in the isotope curve: 2.8, 2.3, and 1.9 ka BP, corresponding to a decrease of the mean air temperature of 2.1, 1.1, and 1.3 °C, respectively. The scale of the temperature variations in the Da Hinggan Mountains is similar to the Yamal Peninsula and Svalbard.

Late Holocene Northern Hemisphere palaeotemperatures from proxy data and their correlation with the studied ice-wedge isotopic data

Analysis of the Late Holocene palaeoclimatic reconstructions for the Northern Hemisphere shows relatively good correspondence of the regional and local scale and chronology of the major palaeoclimatic fluctuations with global changes during the last 2 ka.

Reconstruction of summer temperatures for Baffin Bay by varves from Big Round Lake (the thickness of varves correlates with average air temperature from July to September) demonstrated that mean summer air temperature during the LIA (1575–1760 years AD) was approximately 1.5 °C below the modern values (average temperature for 1995–2005 AD) and 0.2 °C below the average temperature for the last 1000 years [Thomas, Briner, 2009].

Ljungqvist et al. [2011] analyzed spatio-temporal patterns of centennial temperature variability over the Northern Hemisphere land areas for the last twelve centuries based on 120 proxy records (ice-cores, pollen, marine sediments, lake sediments, tree rings, speleothems, and historical documentary data). These data include the Lomonosovfonna ice core from Svalbard and tree rings from the Southern Yamal Peninsula and nearby Polar Ural mountains. The temperatures from 800 to 1100 AD were generally above the long-term mean, gradually cooling to below the mean during 1500–1800 AD, with maximum cooling at 1600–1700 AD. The warming of 1900–2000 AD raised the centennial mean back to a level comparable to that of 800–1100 AD. The resulting maps showing gridded, weighted, centennial proxy anomalies derived from 120 proxy records reveal remarkable large-scale spatial coherency of warm and cold conditions over the Northern Hemisphere land areas for the past twelve centuries [Ljungqvist et al., 2011].

An evident cool period in Southern Yamal Peninsula and Svalbard is dated to 1500–1800 AD. The temperatures of this period, according to Ljungqvist et al. [2011], were 0.5–1 °C below the long-term mean, and during the coldest part of the LIA – 1.5 °C below the long-term mean (Fig. 10, D). The reconstructed palaeotemperature based on the ice-wedge isotope values from Adventdalen valley dated to this period is characterized by low mean winter values (–14.2 °C, –14.5‰). Possibly the lowest values of mean winter temperature (–20.3 °C) reconstructed from the ice wedge from Erkutayakha valley are also dated to the coldest time of the LIA (Fig. 10, F, G).

According to Ljungqvist et al. [2011], warm anomalies in the Northern Hemisphere occurred from 800–1200 AD in the Medieval warming and about 1400 AD, when temperatures were from 0.5 to 2 °C above the long-term mean (see Fig. 10, D). These warm peaks correspond to higher mean winter temperatures, based on $\delta^{18}O$ values from contact zones of ice wedges (see Fig. 10, E, F): –19.5 °C (Erkutayakha River valley) and –12.3 °C (Adventdalen valley). A warm anomaly of the 20th century is noted in many regions of the Northern Hemisphere including the Yamal Peninsula and Polar Ural [Ljungqvist et al., 2011].

This warming is matched with the palaeotemperature curves of the ice wedge from the Adventdalen valley by mean winter temperatures close to Medieval warm values. The 20th century warming is not identified on the palaeotemperatures curve of the ice wedge from the Erkutayakha valley, most probably due to the relatively coarse sampling space of this ice wedge. However, the isotope value ($\delta^{18}O$ = –16.1‰) of modern ice veins in the study site corresponds to a mean winter temperature value of –16 °C, allowing us to assume that the present mean winter temperatures are almost 2 °C above those of the Medieval warm period.

There is a clear correspondence in the range of mean annual air temperature variations of 2–2.5 °C over the Northern Hemisphere

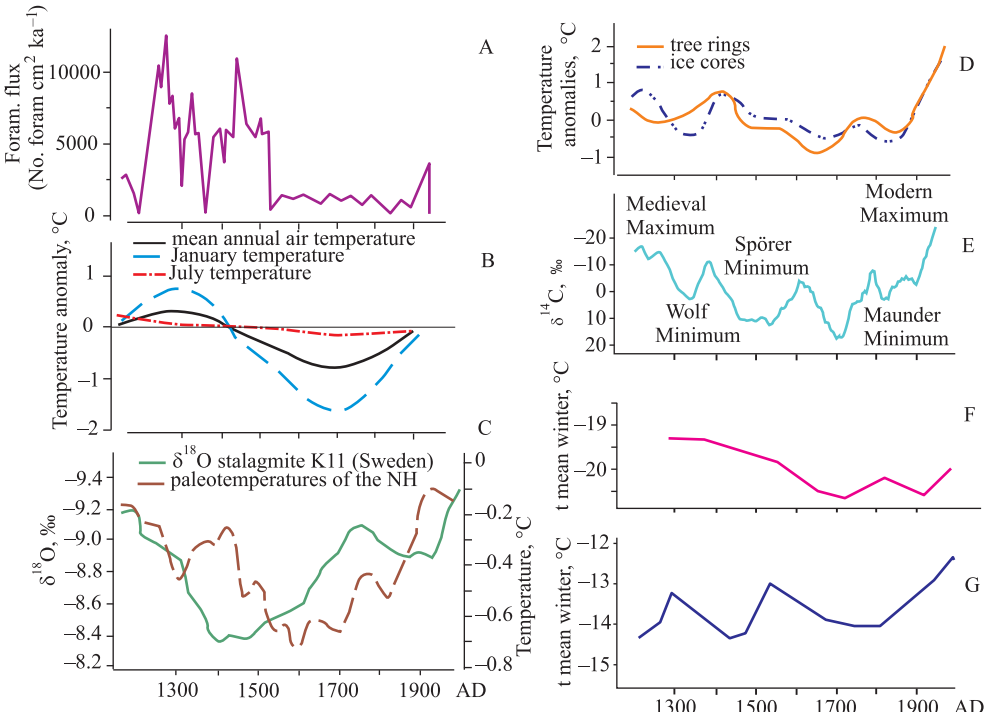

Fig. 10. Comparison of the Late Holocene Northern Hemisphere air temperature proxy records with the reconstructed palaeotemperature proxy from the ice wedges from the Yamal Peninsula and Svalbard:

(A) Benthic foraminiferal specimen flux in Hinlopen Trough (northern Svalbard), after Jernas et al. [2013].

(B) Anomalies of mean annual air temperature, January and July temperatures relative to present temperatures for northern Norway, after Lilleoren et al. (2012).

(C) Comparison between the $\delta^{18}O$ record of stalagmite K11 (northwestern Sweden) and the low-frequency component (480 yr scales) of the NH air temperature reconstruction by Moberg et al. [2005] after Sundqvist et al. [2010].

(D) Mean time-series of centennial temperature proxy anomalies reconstructed from tree rings and ice cores after Ljungqvist et al. [2011].

(E) Solar activity events recorded in the sunspot record for the last 1100 years; minima in $\Delta^{14}C$ correspond to maxima in sunspot number and maxima in $\Delta^{14}C$ lead minima in sunspot number. The radiocarbon signal in the Earth's atmosphere is response to changes in solar activity. The cycles in sunspot minima ($\Delta^{14}C$ maxima) with periodicities of about 200 years are referred to as Suess Cycles.

(F) Mean winter temperature reconstruction for the Erkutayakha River valley, Yamal Peninsula. This curve is not precisely dated; dating is made only by comparison of ^{14}C dates from the surrounding sediments.

(G) Mean winter temperature reconstruction for the Adventdalen valley, Svalbard. This curve is not precisely dated; dating is made only by AMS-dating of the adjacent ice wedges.

land areas during the past 1200 years, presented by Ljungqvist et al. [2011] and the reconstructed air temperature variations based on the isotope data from ice wedges in Svalbard and the Yamal Peninsula, where the range of mean winter air temperatures is also 2.5–3 °C. To understand the correlation of the temperature trends, we compared the isotope curves of a 4000-year-old stalagmite K11 with ice wedges of Svalbard and the Yamal Peninsula.

Two main temperature anomalies during the past 2000 years were noted by Sundqvist et al. [2010]. They studied the isotope composition of a 4000-year-old stalagmite, K11 from Korallgrottan in northwestern Sweden, and hypothesized that the interval of high $\delta^{18}O$

values (–8.5‰) in the stalagmite at 1300–1700 AD was driven by cooler and drier conditions, while the depleted isotopic values ($\delta^{18}O$ around –9.5‰) in 800–1000 AD were driven by warmer conditions. This suggests a negative relationship between calcite $\delta^{18}O$ and air temperature.

The K11 stalagmite $\delta^{18}O$ record shows an overall rather similar evolution of low-frequency (Fig. 10, C) temperature changes to that in the Northern Hemisphere temperature reconstruction by Moberg et al. [2005]. The main difference is that the observed warm peak in Medieval times and the LIA maximum cooling in K11 precede that in the hemispheric temperature record by 100–150 years. However, this apparent time-lag may, at least to some extent, be explained by uncertainties in the stalagmite age model, which is sensitive to the detrital correction at young ages [Sundqvist et al., 2010]. This MWP peak chronologically coincides with the warm peaks of the reconstructed palaeotemperature curves from the ice wedges from Svalbard and the Yamal Peninsula. The cooling peak on the stalagmite isotope curve ($\delta^{18}O$ around –8.5‰) was dated to about 1400 AD. This is, on average, 50–150 years earlier, than on the palaeotemperature curves of these ice wedges (see Fig. 10, C, E, F).

The LIA maximum cooling, identified in the studied ice wedges, practically coincides in scale and chronology with the cooling peak noted by Lilleøren et al. [2012]. They studied the regional distribution of mountain permafrost in Norway during the Holocene based on modelling of ground temperatures and long-term observations of modern ground temperatures in boreholes.

It was found that in all the boreholes, the coldest simulated permafrost occurred during the LIA, and the largest areal distribution of Holocene permafrost in Norway was in the LIA (see Fig 10, B).

During this period, the mean annual air temperatures were 0.8 °C below the present, while mean winter temperatures were 1.2–1.8 °C below the present. The MWP on the palaeotemperature curve is dated to 1000–1100 AD, and mean annual air temperatures were 0.5 °C above the present [Lilleøren et al., 2012], which also chronologically corresponds to the warm peaks on the reconstructed palaeotemperature curves of the ice wedges from Svalbard and Yamal Peninsula.

Palaeoenvironmental conditions on the northern and western continental shelves of Svalbard during the past 2000 years were studied by Jernas et al. [2013], who analyzed two marine sediment cores from the Kongsfjorden Trough (western Svalbard) and Hinlopen Trough (northern Svalbard) with respect to benthic foraminifera and lithology. Superimposed on the long-term trend, five centennial-scale main intervals were isolated at both sites, reflecting variations in the advection of Atlantic water onto the Svalbard shelf, and resulting in variations of climatic conditions in Svalbard. From AD 300 to 700, a diminished inflow of Atlantic water and, most probably, an enhanced inflow of cold and fresher Arctic water took place, followed by a renewed seasonal inflow of chilled, more saline waters of Atlantic origin and an overall diminished influence of Arctic water from AD 700 to 1200. Enhanced inflow of Atlantic water to the Hinlopen Trough from AD 1200 to 1500 led to maxima in foraminiferal fluxes (see Fig. 10, A) and the development of oceanic fronts. In this period, increases in ice rafting reflect either growth or surges of glaciers on Svalbard [Jernas et al., 2013] caused by an increase of humidity due to the influence of Atlantic water. The period AD 1200–1500 may be considered as the maximum influence of Atlantic water, which could be represented by positive peaks in the reconstructed palaeotemperature curves from the ice wedges from Svalbard and the Yamal Peninsula (see Fig. 10, E, F). From AD 1500 to 1900, particularly harsh conditions prevailed in the Hinlopen area owing to larger sea-ice cover and reduced inflow of Atlantic water, which led to minima in the foraminiferal fluxes (see Fig. 10, A).

This cold period of the LIA chronologically coincides with the cool peaks marked on the reconstructed palaeotemperature curves from the ice wedges from Svalbard and the Yamal Peninsula.

Comparison of the reconstructed palaeotemperatures from the Svalbard and Yamal Peninsula ice wedges with the results of the palaeoclimatic review shows that the most evident events are the MWP (800–1200 AD) and the LIA (1600–1800 AD).

CONCLUSIONS

1. Thick syngenetic ice wedges in the upper profile of the high floodplains in the Erkutayakha River valley in the Southern Yamal Peninsula and in the Adventdalen valley in Svalbard, separated by a distance of 2000 km, have been compared with respect to isotope values. These ice wedges developed during the last 2–3 ka and are continuing to grow at present.

2. Ice wedges that have been studied in different permafrost regions (i.e. Alaska, Siberia, Northern China, Yakutia and Chukotka) dated about 2–3 ka BP that implies an active ice-wedge growth during the Late Holocene.

3. For ice wedges formed during 2–3 ka in the subarctic Northern Hemisphere permafrost zone, variations of $\delta^{18}O$ values do not exceed 2–3.5‰ even for ice wedges located in significantly different climatic and geocryological conditions. In the ice wedge from Erkutayakha River valley in Southern Yamal Peninsula, the $\delta^{18}O$ values vary by 2.6‰ (from –18.0 to –20.6‰), and in the ice wedge from Adventdalen valley, the $\delta^{18}O$ values vary by 3.2‰ (from –12.2 ‰ to –15.4‰).

4. During the last 2–3 ka in the subarctic permafrost, changes of mean winter air temperatures did not exceed 3 °C; these changes have been also confirmed by comparison with proxy data (dendrochronological, palynological, and microfaunistic) in different regions of the Northern Hemisphere.

ACKNOWLEDGEMENTS

The authors are grateful to A. Sinitsin and P. Valthard for field sampling assistance in Svalbard. The University Centre in Svalbard, UNIS, supported the Svalbard part of the fieldwork by Alexandra Zemskova, when she was a UNIS student.

FINANCIAL SUPPORT

This research is based upon work supported by the Russian Science Foundation Grant #14-27-00083. Work of H. Christiansen and A. Zemskova is supported by the University Centre in Svalbard, UNIS. ■

REFERENCES

1. Buntgen U., Esper A.J., Frank D.C., Nicolussi K., Schmidhalter M. (2005). A 1052-year tree ring proxy for Alpine summer temperatures // Climate Dynamics. N 25. pp. 141–153.

2. Christiansen H.H. (2005). Thermal regime of ice-wedge cracking in Adventdalen, Svalbard // Permafrost and Periglacial Processes. N 16. pp. 87–98.

3. Christiansen H.H., Humlum O., Eckerstorfer M. (2013). Central Svalbard 2000–2011 Meteorological Dynamics and Periglacial Landscape Response // Arctic, Antarctic and Alpine Research. N 45. pp. 6–18.

4. Eddy J.A. (1976). The Maunder Minimum // Science. Iss. 192. pp. 1189–1202.

5. Goosse H., Renssen H., Timmermann A., Bradley R.S., Mann M.E. (2006). Using paleo-

climate proxy-data to select optimal realizations in an ensemble of simulations of the climate of the past millennium // Climate Dynamics. N 27. pp. 165–184. doi: 10.1007/s00382-006-0128-6.

6. Hamilton T.D., Ager T.A., Robinson S.W. (1983). Late Holocene ice wedges near Fairbanks, Alaska, U.S.A.: environmental setting and history of growth // Arctic and Alpine Research. N 15. pp. 157–168.

7. Isaksson E., Hermanson M., Hicks S., Igarashi M., Kamiyama K., Moore J., Motoyama H., Muir D., Pohjola V., Vaikmäe R., van de Wal R.S.W., Watanabe O. (2003). Ice cores from Svalbard–useful archives of past climate and pollution history // Physics and Chemistry of the Earth, Parts A/B/C. N 28. pp. 1217–1228.

8. Jeppesen J.W. (2001). Palaeoklimatiske indikatorer for central Spitsbergen, Svalbard. Eksemplificeret ved studier af iskiler og deres vaertssediment. Master's thesis, University of Copenhagen. UNIS. Svalbard. 35 pp.

9. Jernas P., Kristensen D.K., Husum K., Wilson L., Koç N. (2013) Palaeoenvironmental changes of the last two millennia on the western and northern Svalbard shelf // Boreas. Vol. 42. pp. 236–255. doi: 10.1111/j.1502-3885.2012.00293.x.

10. Jones P.D., Mann M.E. (2004). Climate over past millennia // Reviews of Geophysics. Vol. 42. RG2002. doi:10.1029/2003RG000143.

11. Ljungqvist F.C., Krusic P.J., Brattström G., Sundqvist H.S. (2011). Northern Hemisphere temperature patterns in the last 12 centuries // Climate of the Past Discussions. N 7. pp. 3349–3397. doi:10.5194/cpd-7-3349-2011.

12. Lilleøren K.S., Etzelmüller B., Schuler T.V., Gisnås K., Humlum O. (2012). The relative age of mountain permafrost–estimation of Holocene permafrost limits in Norway // Global and Planetary Change. Iss. 92–93. pp. 209–223.

13. Luterbacher J., Dietrich D., Xoplaki E., Grosjean M., Wanner H. (2004) European seasonal and annual temperature variability, trends and extremes since 1500 AD // Science. Iss. 303. pp. 1499–1503.

14. Maasch K.A., Mayewski P.A., Rohling E.J., Stager J.C., Karlén W., Meeker L.D., Meyerson E.A. (2005). A 2000-year context for modern climate change // Geografiska Annaler. N 87A. pp. 7–15.

15. Mann M.E., Bradley R.S., Hughes M.K. (1998). Global-scale temperature patterns and climate forcing over the past six centuries // Nature. Vol. 392. pp. 779–787.

16. Matsuoka N., Hirakawa K. (1993). Critical polygon size for ice-wedge formation in Svalbard and Antarctica // Proceedings of the Sixth International Conference on Permafrost. Beijing, China. South China University of Technology Press, Wushan, Guangzhou. N 1. pp. 449–454.

17. Meyer H., Yoshikawa K., Schirrmeister L., Andreev A. (2008). The Vault Creek Tunnel (Fairbanks Region, Alaska): A Late Quaternary Palaeoenvironmental Permafrost Record // Pro-

ceedings of the Ninth International Conference on Permafrost. Kane DL, Hinkel KM (eds). Institute of Northern Engineering, University of Alaska Fairbanks. N 2. pp. 1191–1196.

18. Meyer H., Opel T., Laepple T., Dereviagin A.Yu., Hoffmann K., Werner M. (2015). Long-term winter warming trend in the Siberian Arctic during the mid- to late Holocene // Nature Geoscience. Letters. Published online: DOI: 10.1038/NGEO2349.

19. Moberg A., Sonechkin D.M., Holmgren K., Datsenko N.M., Karlen W. (2005). Highly variable Northern Hemisphere temperatures reconstructed from low- and high resolution proxy data // Nature. Vol. 433. pp. 613–617.

20. Oliva M., Vieira G., Pina P., Pereira P., Neves M., Freitas M.C. (2014). Sedimentological characteristics of ice-wedge polygon terrain in Adventdalen (Svalbard). Environmental and climatic implications for the Late Holocene // Solid Earth Discussions. N 6. pp. 1191–1225.

21. Sundqvist H.S., Holmgren K., Moberg A., Spötl C., Mangini A. (2010). Stable isotopes in a stalagmite from NW Sweden document environmental changes over the past 4000 years // Boreas. N 39. pp. 77–86. doi: 10.1111/j.1502-3885. 2009.00099.x.

22. Thomas E.K., Briner J.P. (2009). Climate of the past millennium inferred from varved proglacial lake sediments on northeast Baffin Island, Arctic Canada // Journal of Paleolimnology. N 41. pp. 209–224.

23. Trofimov V.T., Baulin V.V., Vasil'chuk Y.K., Grechishchev S.E. (1989) Geokriologija SSSR. Zapadnaja Sibir. (Geocryology of Russia. Western Siberia) Izd-vo Nedra. Moskva. 454 s (In Russian).

24. Vasil'chuk Y.K. (1993). Northern Asia cryolithozone evolution in Late Quaternary // Proceedings of the Sixth International Conference on Permafrost. Beijing, China. South China University of Technology Press, Wushan, Guangzhou. Vol. 1. pp. 945–950.

25. Vasil'chuk Y.K. (2006). Povtorno-zhil'nye l'dy: geterociklichnost', geterogennost', geterohronnost'. (Ice wedge: heterocyclity, heterogeneity, heterochroneity). Izd-vo MGU. 404 s (In Russian).

26. Vasil'chuk Y.K. (2013). Syngenetic ice wedges: cyclical formation, radiocarbon age and stable-isotope records // Permafrost and Periglacial Processes. N 24. pp. 82–93.

27. Vasil'chuk Y.K., Kotljakov V.M. (2000). Osnovy izotopnoj gljaciologii i geokriologii. (Principles of isotope geocryology and glaciology) Uchebnik. Izd-vo MGU. 616 s (In Russian).

28. Vasil'chuk Y.K., Vasil'chuk A.C., Rank D., Kutschera W., Kim J.-C. (2001). Radiocarbon dating of $\delta^{18}O$-δD plots in Late Pleistocene ice-wedges of the Duvanny Yar (Lower Kolyma River, northern Yakutia) // Radiocarbon. N 43. pp. 541–553.

29. Vasil'chuk Y.K., van der Plicht J., Jungner H., Vasil'chuk A.C. (2000). AMS-dating of Late Pleistocene and Holocene syngenetic ice-wedges // Nuclear Instruments and Methods in Physics Research. Section B: Beam Interactions with Materials and Atoms. Vol. 172. pp. 637–641.

30. Vittinghus H., Christiansen H.H., Meyer H., Elberling B. (2008). Hydrogen and oxygen isotope studies from an ice wedge in Svalbard // Extended Abstracts of the Permafrost Ninth International Conference. University of Alaska. Fairbanks, USA. pp. 333–334.

31. Vtjurin B.I. (1989). Podzemnye l'dy Shpitsbergena (Underground ice of Svalbard) // Materialy gljaciologicheskih issledovanij. Vyp. 65. s. 69–85 (In Russian).

32. Yang S., Jin H. (2011). $\delta^{18}O$ and δD records of inactive ice wedge in Yitulihe, Northeastern China and their paleoclimatic implications // Science China. Earth Sciences. N 54. pp. 119–126.

Yurij K. Vasil'chuk is Professor of the Department Landscape Geochemistry and Soil Geography of Lomonosov Moscow State University. He obtained his PhD from Moscow State University in 1982, under the supervision of Professor Trofimov, and his Doctor of Science degree from the Permafrost Institute of RAS in 1991. He has held professor positions at the Cryolithology and Glaciology Department of Moscow State University since 1996, and was appointed Full Professor at the Department of Landscape Geochemistry and Soil Geography in 2009. His research interests relate to the use of stable and radioactive isotopes in ice wedge, massive ice, palsa, lithalsa, pingo, and glaciers, as well as in soils and landscapes. He was elected a member of the Russian Academy of Natural Sciences in 2004. He is the author of three university textbooks and 14 monographs.

Nadine A. Budantseva is Senior Research Scientist of the Department Landscape Geochemistry and Soil Geography of Lomonosov Moscow State University. She obtained her PhD from Moscow State University in 2003, under the supervision of Professor Vasil'chuk. In 2007, she joined the mass-spectrometry laboratory of Moscow State University. Her research interests are in the area of the use of stable isotopes in ice wedge, pingo, lithalsa, and massive ice. She is the author of a research monograph and a textbook "Stable isotope geochemistry of atmosphere and hydrosphere" published in 2013 in the series "Isotope Ratios in the Environment."

Hanne H. Christiansen is Professor and Head of the UNIS Arctic Geology Department. Her main research topic is periglacial geomorphology with focus on permafrost and its climatic controls. She is the coordinator of the "Permafrost Observatory Project: A Contribution to the Thermal State of Permafrost in Norway and Svalbard" (TSP Norway) IPY research project and the "Climate change effects on high arctic mountain slope processes and their impact on traffic in Svalbard" (Cryoslope Svalbard) Norklima research project. In 2008, she was elected Vice President for the International Permafrost Association (IPA).

Julia N. Chizhova is Senior Research Scientist of the Department of Landscape Geochemistry and Soil Geography of Lomonosov Moscow State University. She obtained her PhD from Moscow State University in 2006, under the supervision of Professor Vasil'chuk. In 2007, she joined the mass-spectrometry laboratory of Moscow State University. Her research interests relate to the use of stable isotopes in glacier ice, snow, and ice wedges. She is the author of a research monograph and a textbook "Stable isotope geochemistry of atmosphere and hydrosphere" published in 2013 in the series "Isotope Ratios in the Environment."

Alla C. Vasil'chuk is Senior Research Scientist of the Laboratory of Geoecology of the North of Lomonosov Moscow State University. She obtained her PhD from Moscow State University in 1987, under the supervision of Prof. Lazukov and Dr. Vasil'chuk, and her Doctor of Science degree from the RAS Geography Institute in 2009. In 2004, she began working on pollen ratios in the massive ice and ice wedge and palsa at Moscow State University. More recently, he has developed method to identify massive-ice origin, with confidence, by pollen. She is the author of 4 research monographs and two text books: "Stable isotope geochemistry of natural ice" and "Stable isotope geochemistry of atmosphere and hydrosphere" published in 2011 and 2013 in the series "Isotope Ratios in the Environment."

Alexandra M. Zemskova is Teaching Assistant of the Carleton University, Geography and Environmental Studies. She is the author of two tutorials on physical geography for the first-year students and teaches different geographical laboratory courses including field methods. Her Master's thesis, under supervision of Professor C. Burn, was devoted to quantitative estimation and comparison of near-surface ground ice (permafrost) properties in different geomorphological settings at Herschel Island, Yukon territories. Her Bachelor's Thesis of Science (B.Sc.) at Lomonosov Moscow State University, Cryolithology and Glaciology Department, was devoted to permafrost conditions at Western coast of Taymyr Peninsula.

Eniola D. Ashaolu
Department of Geography and Environmental Management, Faculty of Social Sciences, University of Ilorin, P.M.B 1515, Ilorin, Nigeria; Tel: + 2348036070929, e-mail: damash007@yahoo.com.

GROUNDWATER RESPONSE TO WEATHER VARIABILITY IN A POOR AQUIFER UNIT: AN EXAMPLE FROM TROPICAL BASEMENT COMPLEX ROCK OF NIGERIA

ABSTRACT. More than 50 % of Nigeria is underlain by basement complex rock which is a poor aquifer unit and evidences abound that the climate of Nigeria is changing. The posing question is how this poor aquifer will respond to the vagaries of climate variability and change. However, understanding the response of groundwater to climate variability and change in Nigeria will be hampered by dearth of data, because the nature of change in groundwater is not monitored. On this basis, the study tried to understand how groundwater responds to weather variability in a poor aquifer unit of Ilara-mokin and its environs in the tropical area of Nigeria. Rainfall and temperature data for forty years (1973–2012) were collected from NIMET and groundwater level were monitored in the area for two years (2012–2014).The general trends in rainfall and temperature received in the last forty years were examined using regression analysis and moving average. The dry and wet episodes were also examined using Standard Rainfall Anomalies Index (SAI). Also, the percentage changes in the rainfall and temperature received were determined using reduction pattern analysis. The response of groundwater to weather variability was however established using Pearson Moment Correlation and multiple regression analysis. The results of the analyses revealed an average of six years dry episode every decade in the last 40 years. The temperature of the study area is increasing in the last 20 years. Groundwater responded negatively to temperature but positively to rainfall in the area. Rainfall and temperature accounted for 67 % of variability in monthly groundwater level. This study is a good starting point in understanding groundwater response to climate in poor aquifer units of Nigeria despite the dearth of data.

KEY WORDS: groundwater, climate, weather, variability, management, poor aquifer, trend.

INTRODUCTION

Groundwater is an important natural resource which serves as a primary source of water for domestic, agriculture and industry in many countries of the world. According to Taylor et al. [2009], the current assessments of the effects of historical and projected climate variability and change on water resources commonly omit groundwater. However, there should be a great concern for this omission in the continent of Africa, where current usage and future adaptation to response of climate change and rapid population growth, place considerable reliance upon groundwater to meet domestic, agricultural and industrial demands [Taylor et al., 2009]. The effects of climate on surface water resources is directly through changes in the major long-term climate variables such as air temperature, precipitation, and evapotranspiration, however, the relationship between the changing climate variables and groundwater is more complicated and poorly understood [Jyrkama and Sykes, 2010; Singh and Kumar, 2010].

The relationship between climatic variables and groundwater is considered to be more complicated than surface water [Holman, 2006; IPCC, 2007] cited in Green et al. [2011]. This is because groundwater residence time can range from days to tens of thousands of years, which may delay and diffuse the effect of climate change on groundwater and may not be detected immediately [Chen et al., 2004] cited in Green et al., [2011]. This was why Sekhar et al., [1994] and Nyagwambo [2006] stressed that climate variability, being a relatively short term compared to climate change will have greater impact on crystalline basement aquifer systems. This study was based on their submissions to understand the relationship between groundwater and monthly weather variability in Ilara-mokin and its environs.

The implications of a changing climate on water resources of the world and Africa in particular especially on groundwater resources cannot be overemphasized. This was why UNESCO International Hydrological Programme (IHP) and its Groundwater Resources Assessment under the Pressure of Humanity and Climate change (GRAPHIC), in its attempt to raise the global attention on the interaction of climate and groundwater, supported the compilation of a book edited by Triedel et al. [2012] titled "Climate Change Effects on Groundwater – A Global Synthesis of Findings and Recommendations". They made a compilation of about 20 case studies on climate and groundwater resources from more than 30 different countries. The studies in the book addressed groundwater resources in different hydrological settings ranging from mountainous to coastal aquifer systems, including unconfined, semi-confined and confined aquifers to unconsolidated to fractured-rock material and different climatic settings/scenarios. However, the studies of groundwater under the influence of climate have not received enough consideration in developing countries especially Africa and Nigeria in particular. Very few studies have been carried out in this part of the world solely because of the dynamic nature of groundwater resources and the dearth of hydrological data and expertise.

More than 50 % of Nigeria is underlain by basement complex rock which is a poor aquifer unit. Basement rock aquifers are very poor aquifer because of their very low level of porosity and permeability which resulted into poor groundwater yield and recharge in areas located on this type of aquifer. Although, there are places on a basement complex rock with very thick overburden produced by weathering which have sizeable amount of extractable groundwater. Sekhar et al., [1994] and Nyagwambo [2006] reported that in a basement complex rock aquifer, groundwater is characterized by the presence of shallow water table and recharge is primarily from rainfall. The presence of shallow water table and recharge primarily from rainfall is an indication that groundwater in a basement complex aquifer will respond more to the vagaries of climate variability than the long term climate change.

However, this study is trying to understand how groundwater respond to monthly weather variability in a shallow overburden aquifer, an example from Ilara-mokin and its environs which is underlain by basement complex rock in tropical area of Nigeria. This reason why the study is based on groundwater response to monthly weather variability was because the available groundwater data is not enough to determine the influence of climate variability on groundwater in the area. The population of this area depends mainly on groundwater resources for their domestic needs and is faced with the challenges of inadequate water supply as the population is increasing [Oladapo et al., 2009].Two major studies have been carried out in this area to understand structural configuration of the basement rocks, groundwater potential [Oladapo et al., 2009] and groundwater yield and flow pattern [Ashaolu and Adebayo, 2014] to have an insights if the available groundwater will keep up with the increasing population. None of these studies in their quest to understand the groundwater resources of this area

have tried to see the influence of climate or weather variables on groundwater of the area in this era of pronounced climate variability and change. Therefore there is a need to understand how groundwater in this area responds to monthly weather variability for sustainable groundwater supply.

STUDY AREA AND DATA

Study area description

Ilara-mokin and its environs (Ipogun, Ikota, Ero and Ibule) are in Ifedore LGA of Ondo state, south-western Nigeria. The town and its surrounding villages are located between latitude 07°21′16″and 07°22′20″N and longitude 005°05′58″ and 005°07′12″ E (Fig. 1). The climate of Ilara-mokin and its' environ can be described as the Lowland Tropical Rain Forest type, with marked wet (April to October) and dry (November to March) seasons. The dry season is marked with little or no rainfall. The total annual rainfall in this area is about 1800 millimeters. The mean monthly temperature is between 27 °C to 30 °C. The geology of Ilara-mokin and its environs is Precambrian Basement Complex rocks and which is mainly of the medium grained gneisses. These are strongly foliated rocks frequently occurring as outcrops. According to Oladapo et al. [2009] the lithological units include variably migmatized biotite-hornblende-gneiss with intercalated amphibolite. They further stressed that the greater part of the study area is underlain by marginally thick overburden which constitute a shallow aquifer units. Its estimated population is about 45,000 people and most of the local residents practiced fish and poultry farming.

Data Sources

The secondary data for this study are rainfall and temperature data which were obtained from the Nigeria Meteorological Agency (NIMET). The data spanned from 1973–2012 (40 years), it is believed that these length of years will be enough to ascertained variability in the climatic data set obtained. This is because World Meteorological Organization in 1956 suggested thirty to thirty five years as the minimum period for averaging climatic variables before variability can be detected [WMO, 2009, 2007]. The groundwater level data were obtained directly from field observation that spanned for two (2012–2014). It is important to note that there are no observation wells in the study area which is a peculiar characteristic of most of the developing countries of the tropics. Forty wells with peculiar characteristics (hand-dug,

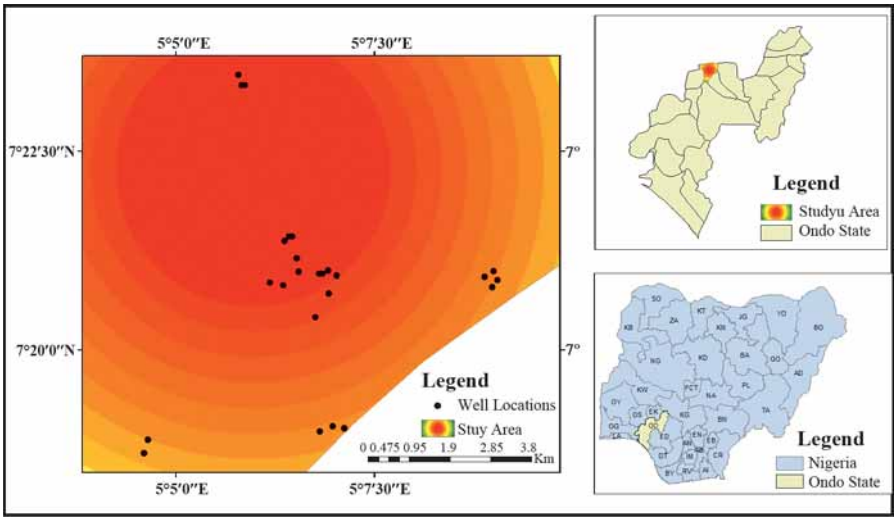

Fig. 1. Map showing Nigeria, Ondo state, the study area and locations of monitored wells.

installed with circular ring, fetching period is between 7am and 6pm daily) were however selected in the whole of the study area which were monitored consecutively for two years.

METHODS

This section discussed the method employed for the well monitoring and the methods of data analysis.

Well Monitoring

A total of 40 wells were monitored consecutively for two years (2012–2014) in the study area. A total of 24 wells were selected in Ilara-mokin and 4 wells each from the four surrounding villages (Ipogun, Ikota, Ero and Ibule). The surface elevation, latitude and longitude of each well location were taken using Global Positioning System (Garmin GPS Channel 76 model). Well estimator was used to measure the depth to water early in the morning around 6:00am on an average of three times per week for two years. Most especially after individual rainfall incidence in the previous day, this is to determine how the well responds to rainfall occurrence. This was based on the observation of Sekhar et al. [1994] and Nyagwambo [2006] that recharge in a basement complex aquifer is solely from rainfall. Although the wells were also monitored during the dry season when there are little or no rainfall in the study area. Groundwater level of the research area was computed by deducting depth to water from the surface elevation. This is written as shown in equation 1:

$$S_{wl} = E - D_{wt}, \tag{1}$$

where S_{wl} = Static water level; E = Surface elevation; D_{wt} = Depth to water table

Methods of data analysis

The trend, anomalies and percentage changes in the climate condition of the area were first established. Then the relationship between the two major climatic drivers (rainfall and temperature) and groundwater level were examined to determine the response of groundwater to these climatic variables on monthly basis.

Trend analysis

The Kolmogorov–Smirnov test was carried out on the climatic variables to determine that they were normally distributed. Two methods (simple regression analysis and moving average) were adopted in determining the trend in the climatic variables used. Scatter plot was carried out on the data set and the assumption of linearity was fulfilled. This is to validate the result of the trend analysis using regression. The formula is as written in equation 2:

$$Y = aX + b, \tag{2}$$

where X is the time (year), a is the slope coefficient and b is the least square estimates of the intercept. a and b were obtained from equations 3 and 4 respectively.

$$a = \frac{n\sum(xy) = \sum x \sum y}{n\sum\left(x^2\right) - \left(\sum x\right)^2}; \tag{3}$$

$$b = \frac{\sum y - b\sum x}{n}. \tag{4}$$

Standard Rainfall Anomalies Index (SAI)

This is used to determine the departure of rainfall from the normal climatic condition established for the forty years period under consideration. According to Olaniran [2002], any departure above or below the established normal climatic condition are referred to as anomalies. According to him, a persistent departure from the normal condition constitutes a climatic fluctuation. SAI is used in this study to determine the number of dry and wet episodes experienced in the study area during the period under consideration. The equation is as shown in equation 5:

$$SAI = \frac{x_1 - \overline{x}}{SD}, \; SAI = \frac{x_1 - \overline{x}}{SD}, \tag{5}$$

where x_1 is the annual rainfall total; x is the mean rainfall for the period of study and SD is the standard deviation from the mean rainfall for the period of study.

Reduction pattern analysis

This method is used to determine the percentage changes in the climatic variables on a decadal scale. Reduction analysis has been used by researchers to determine the fluctuation and percentage change in hydro-climatic variables [Salami et al., 2010; Makanjuola et al., 2010; Ifabiyi and Ashaolu, 2013]. To get the percentage changes in the climatic variables, the record years of climatic variables were divided into groups of 10 years interval. The average (annual) variable (X_i) for the 10 years was calculated. The corresponding deviations from the average (X_m) for the groups and the corresponding percentage changes are obtained. The percentage changes in the climatic variables were obtained from equation 6:

$$\frac{X_i - X_m}{X_m} \cdot 100 \ \%. \tag{6}$$

Pearson Moment Correlation

This method was employed to determine the response of groundwater to the monthly weather variables. This was carried out on monthly basis because of the limited number of years of record for the groundwater level. Also, monthly analysis is considered to be the best since the focus is on management and sustainability of groundwater in a shallow aquifer of a basement complex rock which is a poor aquifer unit [Ashaolu and Adebayo, 2014] and where recharge is solely from rainfall [Sekhar et al., 1994; Nyagwambo, 2006]. The relationship was established from equation 7:

$$r = \frac{\sum(x-\overline{x})(y-\overline{y})}{\sqrt{\sum(x-\overline{x})^2 \sum(y-\overline{y})^2}}, \tag{7}$$

where r is the Product Moment Correlation, y is the groundwater level and x is the weather variables.

Multiple Regression Analysis

This analysis was carried out to further ascertain the response of groundwater to weather variability and determine the percentage of variability in groundwater level that can be attributed to weather variability. The analysis was first carried out by ordinary multiple regression and later subjected to stepwise multiple regression analysis. This result was derived from equation 8.

$$y = a + b_1x_1 + b_2x_2 + e, \tag{8}$$

where y is groundwater level, a is the intercept on y-axis, b_1–b_n is partial regression coefficient of the independent variables, x_1 = rainfall and x_2 is air temperature.

RESULTS

Before the groundwater response to weather variability was determined, the general trend, anomalies and percentage changes in climatic variables in the study area was first determined. Hence, the relationship between groundwater and weather (rainfall and temperature) variability was established.

Trend analysis

Two methods were adopted in determining the trend in the climatic variables. These are simple regression analysis and moving average. The trend in the climatic variables in relation to time was first determined by regression analysis. The result of the regression analysis is displayed in Table 1. The p-value for the rainfall slope is 0.69 which is greater than 0.05, thus, there is no statistically significant relationship between rainfall and year at 95 % confidence level. The R-squared statistic shows that the model, as fitted, explains 0.40 % of the variability in rainfall. The correlation coefficient of 0.06 reveals a very weak relationship between the rainfall and time (year). The p-value for the air temperature slope is 0.01 which is less than 0.05, thus, there is a statistically significant relationship between

Table 1. Climatic trend derived from regression analysis

Variables	Regression equation	P-value	Statistically Significant	Sample correlation	R^2
Rainfall	Y = 1586.98 + 1.79X	0.69	No	0.06	0.40 %
Air Temperature	Y = 30.38 + 0.021X	0.01	Yes	0.40	16.10 %

air temperature and year at 95 % confidence level. The R-squared statistic reveals that the model, as fitted, explains 16.10 % of the variability in air temperature. The correlation coefficient of 0.40 indicates a mild relationship between air temperature and time (year).

Figure 2 shows the annual rainfall and five year moving average curve for Ilara-mokin and its' environ, from 1973–2012. The five year moving average curve shows an increasing trend from 1987 to 1998 but revealed a declining trend from 1999 to

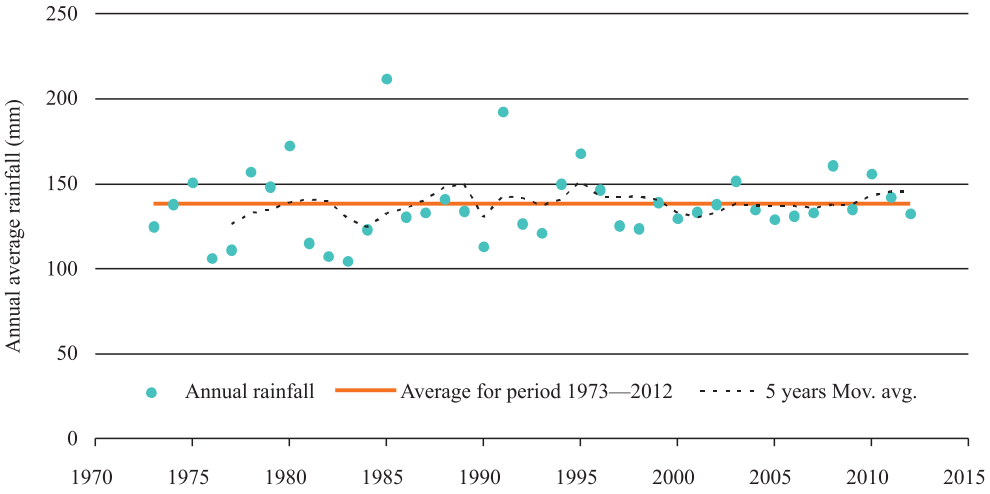

Fig. 2. Annual rainfall at Ilara-mokin and its' environs for period 1973–2012.

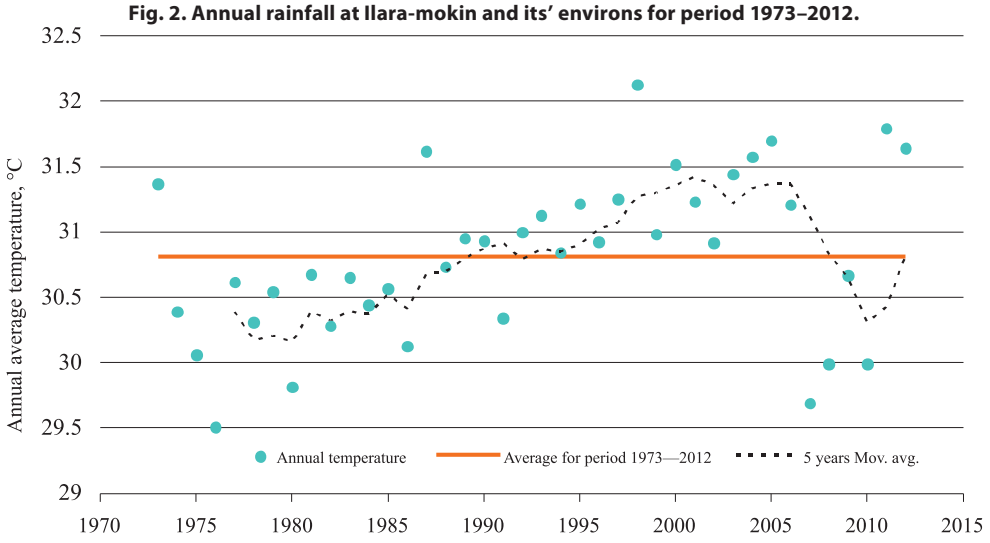

Fig. 3. Annual temperature at Ilara-mokin and its environs for period 1973–2012.

2009, however the curve start increasing again from 2010. Figure 3 shows the annual temperature and five year moving average curve for Ilara-mokin and its environ from 1973–2012. The five year moving average curve shows an increasing trend from 1988 to 2008 but dropped for four years and peaked again in 2012.

Rainfall anomalies, percentage changes in rainfall and temperature

Rainfall anomalies are the departure above or below the long term established normal (rainfall) climatic condition [Olaniran, 2002]. According to him, a persistent departure from the normal condition constitutes a climatic fluctuation. SAI is used to establish the dry and wet episodes in the study area under the period of consideration and the results are presented in Table 2. The forty years under consideration were divided into four periods of ten years (decade) and the number of dry and wet episodes (years) within these ten years period were identified. Table 2 shows an average of six dry episodes in every ten years in the last four decades in the study area.

The record years of rainfall and temperature are divided into groups of 10 years intervals for decadal analysis. This was used to get the percentage change in rainfall and temperature over time in Ilara-mokin and its' environ. The results of percentage changes in rainfall for the forty years period are presented in Table 3. From the rainfall record of 1973–2012 in Ilara-mokin and its' environ, the average rainfall was 138.12 mm. From 1973–1982 rainfall decreased slightly to 133.18 mm, showing a percentage change of –3.58 %. From 1983–1992, rainfall increased to 141.11 mm, showing a positive change and a percentage increase of 2.16 %. From 1993–2002, rainfall decreased to 137.52 mm, showing a negative change with a percentage difference of –0.43 %. Rainfall rose again to 140.66 mm from 2003–2012 with a positive change of 1.84 %.

The results of percentage changes in air temperature for the forty years period are presented in Table 4. From the air temperature record of 1973–2012 in Ilara-mokin and its' environ, the average air temperature was 30.82 °C. From 1973–1982 and 1983–1992, air temperature decreased slightly to 30.66°Cand 30.74 °C respectively. These show a negative

Table 2. Dry and Wet Episodes in the Study Area in the last Four Decades (1973–2012)

Periods	Dry years	Wet years
1973–1982	1973 (*–0.60*), 1974 (*–0.00*), 1976 (*–1.45*), 1977 (*–1.21*), 1981 (*–1.04*), 1982 (*–1.38*)	1975 (*0.57*), 1978 (*0.85*), 1979 (*0.45*), 1980 (*1.56*)
1983–1992	1983 (*–1.51*), 1984 (*–0.67*), 1986 (*–0.34*), 1987 (*–0.22*), 1989 (*–0.18*), 1990 (*–1.13*), 1992 (*–0.52*)	1985 (*3.35*), 1988 (*0.14*), 1991 (*2.47*)
1993–2002	1993 (*–0.77*), 1997 (*–0.57*), 1998 (*–0.65*), 2000 (*–0.38*), 2001 (*–0.21*), 2002 (*–0.01*)	1994 (*0.53*), 1995 (*1.35*), 1996 (*0.38*), 1999(*0.05*)
2003–2012	2004 (*–0.15*), 2005 (*–0.40*), 2006 (*–0.31*), 2007 (*–0.22*), 2009 (*–0.13*), 2012 (*–0.25*)	2003 (*0.61*), 2008 (*1.03*), 2010 (*0.81*), 2011 (*0.18*)

**Standard Rainfall Anomalies Index are italics in parentheses.

Table 3. Percentage Changes in Rainfall over Ilara-mokin and its Environs 1973–2012

Period	Decadal Averages (mm)	Average for the period of study (mm)	Deviation from long term average	% Change
1973–1982	133.18	138.12	–4.94	–3.58
1983–1992	141.11	138.12	2.99	2.16
1993–2002	137.52	138.12	–0.6	–0.43
2003–2012	140.66	138.12	2.54	1.84

Table 4. Percentage Changes in Temperature over Ilara-mokin and its Environ 1973–2012

Period	Decadal Averages (°C)	Average for the period of study (°C)	Deviation from long term average	% Change
1973–1982	30.36	30.82	–0.46	–1.49
1983–1992	30.74	30.82	–0.08	–0.26
1993–2002	31.21	30.82	0.39	1.27
2003–2012	30.97	30.82	0.15	0.49

change and a percentage reduction of –1.49 % and –0.26 %. However, from 1993–2002 and 2003–2012, air temperature at Ilara-mokin and its' environ increased to 31.21 °C and 30.97 °C, with a percentage difference of 1.27 % and 0.49 % respectively.

Groundwater response to weather (rainfall and temperature) variability

To determine how groundwater responds to weather variability, the relationship between groundwater, rainfall and air temperature were determined using multiple correlation analysis. Also, the response of groundwater to climatic variable was estimated with multiple regression analysis. The results of the multiple correlations were presented in Table 5. The result revealed a very strong negative relationship between air temperature and rainfall (r = –.807**) at 99 % confidence level. Also, there existed a very strong negative relationship between air temperature and groundwater (r = –.716**) at 99 % confidence level. While a very strong positive relationship was revealed between rainfall and groundwater (r = .815**) at 99 % confidence level. Figures 4 and 5 show the graphical representation of the relationship between rainfall and groundwater, air temperature and groundwater respectively.

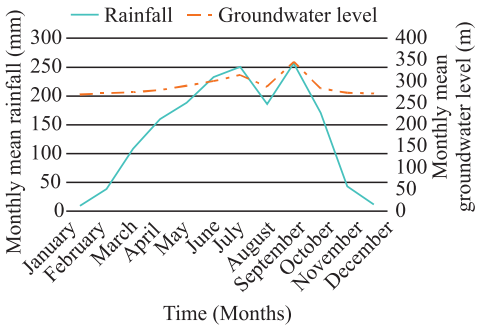

Fig. 4. Relationship between rainfall and groundwater level.

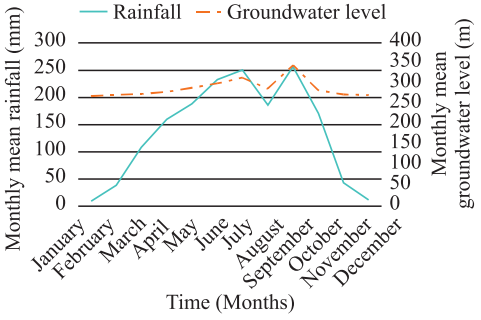

Fig. 5. Relationship between air temperature and groundwater level.

Table 5. Relationship between Rainfall, Air temperature and Groundwater level

Variables	Rainfall	Air temperature
Rainfall		
Air temperature	–.807**	
Groundwater level	.815**	–.716**

**. Correlation is significant at the 0.01 level (2-tailed).

Table 6 shows the results of the multiple regression analysis between groundwater (dependent), rainfall and temperature (independents). The model using enter method has an R^2 of .673, standard error of 14.01 and p-value of 0.006 which indicates that the model is statistically significant at 95 % confidence level. Also, the stepwise method has an R^2 of .663, standard error of 13.38 and p-value of 0.001 which indicates

Table 6. Groundwater response to climatic variables

Methods	R	R^2	Adjusted R^2	Std. Error of the estimate	Sig.
Enter	.821	.673	.601	14.01	0.006
Stepwise	.815	.664	.630	13.38	0.001

that the model is statistically significant at 95 % confidence level.

The estimated models from the regression analysis using enter and stepwise methods are presented in equations 9 and 10 respectively.

$$GroundwaterLevel = = 316.88 + 0.163_{ra\ \mathrm{inf}\ all} - 1.632_{temperature}; \quad (9)$$

$$GroundwaterLevel = = 262.160 + 0.195_{ra\ \mathrm{inf}\ all}. \quad (10)$$

DISCUSSION

Rainfall and air temperature revealed a positive trend in the area. Rainfall has a positive trend line and an R^2 value of 0.004, which indicates that there is a very weak relationship between rainfall and year. Also, from the regression equation Y = 1586.98 + 1.79X, it is observed that there is a positive correlation between time (year) and rainfall for Ilara-mokin and its environs. This indicates that there will be increment of 1.79 mm in rainfall relative to time but this trend is not statistically significant because p-value is 0.69. This may be attributed to high rate of year to year variability in the amount of rainfall received in the area. Further, the five year moving average curve shows an increasing trend from 1987 to 1998 but revealed a declining trend from 1999 to 2009, however the curve start increasing again from 2010. This indicates there is variability in rainfall from decade to decade in the area. It is however, not clear if this may represent the part of a longer climatic cycle or climate change in the area.

On the other hand, air temperature has an R^2 value of 0.1610, indicating a weak relationship between air temperature and time. The regression equation of air temperature Y = 30.38 + 0.021X shows that there is a positive correlation between temperature and time (year), meaning that air temperature of Ilara-mokin and its environs will increase in relation to time, but at a very low rate. Though air temperature will increase at a very slow rate, the increment is however statistically significant with p-value of 0.01. Also, the five year moving average curve shows an increasing trend from 1988 to 2008 (20 years) but dropped for four years and peaked again in 2012. This cycle clearly indicate that the air temperature of this area is gradually increasing which may be tagged to the general increase in the world surface temperature as reported by IPCC [2007].

Olaniran [2002] described rainfall anomalies has the departure above or below the long term established normal (rainfall) climatic condition of an area. According to him, a persistent departure from the normal condition constitutes a climatic fluctuation. The forty years under consideration were divided into four periods of ten years (decade) and the number of dry and wet episodes (years) within these ten years period were identified using Standardized Rainfall Anomalies Index (SAI). The results of SAI in Table 2 show an average of six dry episodes in every ten years in the last four decades in the area. This shows that this area is always experiencing dry spell for nothing less than six years in every decade. Since recharge in a basement complex aquifer is solely from rainfall, this will seriously affect recharge and groundwater in this area. The people in this environment will always experience water stress during this dry spells since they depend mainly on shallow groundwater.

From the rainfall record of 1973–2012 in Ilara-mokin and its' environ, the average rainfall was

138 mm. The result of percentage changes in rainfall for the forty years period in Table 3, shows that from 1973–1982 rainfall decreased slightly to 133.18 mm, showing a percentage change of –3.58 %. From 1983–1992, rainfall increased to 141.11mm, showing a positive change and a percentage increase of 2.16 %. From 1993–2002, rainfall decreased to 137.52 mm, showing a negative change with a percentage difference of –0.43 %. Rainfall rose again to 140.66 mm from 2003–2012 with a positive change of 1.84 %. Sandstorm [1995] reported that a 15 % reduction in rainfall results to 40–50 % reduction in recharge, which means that small changes in rainfall can lead large change in recharge and groundwater response. These result also indicated that the rainfall received in this area is fluctuating from decade to decade and there is every possibility that this scenarios will continue into the future, greatly affecting groundwater resources of this area.

From the air temperature record of 1973–2012 in Ilara-mokin and its' environ, the average air temperature was 30.82 °C. The result of percentage changes in air temperature for the forty years period presented in Table 4 shows that from 1973–1982 and 1983–1992, air temperature decreased slightly to 30.66°Cand 30.74 °C respectively. These show a negative change and percentage reduction of –1.49 % and –0.26 % respectively. However, from 1993–2002 and 2003–2012, air temperature at Ilara-mokin and its' environ increased to 31.21 °C and 30.97 °C, with a percentage difference of 1.27 % and 0.49 % respectively. This is an indication that the temperature of this area is increasing in the last 20 years and also confirmed the results of the trend analysis which is statistically significance. The increasing temperature observed may also be as a result of increase in urbanization at the state capital (Akure) where the weather station is located and which is very close to the research area, population growth and the associated changes in land use type also in the area. A study by Olanrewaju [2009] attributed the steady rise in air temperature of Ilorin city to the population growth rate of Ilorin.

The results of the multiple correlation in Table 5 revealed a very strong negative relationship between air temperature and rainfall ($r = –.807^{**}$) at 99 % confidence level. This is an indication that any month when there is high temperature, there will be low rainfall and vice versa. It can be concluded that monthly rainfall and monthly air temperature are inversely related in this area. Also, there existed a very strong negative relationship between air temperature and groundwater ($r = –.716^{**}$) at 99 % confidence level. Chen et al. [2002] also reported a negative correlation between annual average groundwater level and annual air temperature in the carbonate rock aquifer of the southern Manitoba, Canada. This negative relationship shows that there is an inverse relationship between monthly air temperature and groundwater. When the air temperature is high in any particular month, there is reduction in groundwater level which can be attributed to the rate of evaporation, because groundwater occurrence in this area is shallow. However, a very strong positive relationship was revealed between monthly rainfall and monthly groundwater level ($r = .815^{**}$) at 99 % confidence level. Chen et al. [2002] in their research discovered a positive correlation between annual average groundwater level and annual precipitation. This strong positive relationship shows that groundwater level increases and decreases at the same frequency with the amount of rainfall occurrence. This is expected since the study area is underlain by basement complex rock where recharge is solely from rainfall. This is in agreement with Sekhar et al. [1994] and Nyagwambo [2006] that recharge in a basement complex aquifer is solely from rainfall. This therefore shows that groundwater level is subjected to the degree of rainfall variability in this area, which the results of the rainfall anomalies, percentage change in rainfall of this area have clearly shown.

The results of the multiple regression analysis in Table 6 has an R^2 of .673 which is an indication that rainfall and air temperature accounted for 67.3 % of variability in monthly groundwater level in Ilara-mokin and its

environs. The model in equation 9 revealed that for every 1 % increase in rainfall in any month, there is 0.163 % increase in monthly groundwater level, and for every 1 % increase in temperature in any month, there is –1.63 % decrease in monthly groundwater level. This is an indication that groundwater respond positively to rainfall occurrence but negatively to air temperature incidence. This also supported the result of the multiple correlations. While the stepwise multiple regression has an R^2 of .664 which is an indication that monthly rainfall in the study area accounted for 66.4 % of variability in the monthly groundwater level in the area. The model in equation 10 revealed that for every 1 % increase in monthly rainfall there is 0.195 % increase in monthly groundwater level. This is also in agreement with Sekhar et al. [1994] and Nyagwambo [2006] that recharge in a basement complex aquifer is solely from rainfall. However, the remaining 33.6 % variability in groundwater level can be attributed to the type of overburden on which the monitored well are located. Chen et al. [2002] though carried out their research on a shallow carbonate aquifer, their results also revealed variability in groundwater response to rainfall, which they attributed to differences in recharge characteristics and the permeability of overlying sediments. The study area is generally underlain by thin weathered basement rocks which has produced thin and marginally thick overburden [Oladapo et al., 2009] but areas with thick and sandy overburden which are high groundwater potential zones [Bala and Ike, 2001] are absent from the study area [Oladapo et al., 2009]. This is an indication that the groundwater is highly exposed to the vagaries of climate especially rainfall because of the shallow overburden aquifer in the study area.

CONCLUSION

Having established the climatic scenarios of this area looking at the trend, anomalies and changes in climate, especially rainfall and air temperature. It is clear that while air temperature is on the increase, though at a very slow rate, the rainfall received in this area is highly varied from year to year and on decadal basis. The relationship between groundwater and air temperature is negative, while there existed a positive relationship between groundwater and rainfall. This is an indication that increasing monthly temperature will greatly affect the groundwater of this area and the change (positive or negative) in rainfall received will also have significant effect on groundwater resources of the area. This may be the reason for water supply shortages reported by previous study in this area. Hence, there will be enormous challenges facing the inhabitant of this area as they depend mainly on shallow groundwater which respond to the vagaries of climate (rainfall and temperature). Though the study focused on the response of groundwater to rainfall and temperature as if they were the only two variables that affect recharge in a shallow aquifer based on the suggestions of Sekhlar et al [1994] and Nyagwambo [2006]. It is however a good starting point in understanding how groundwater will respond to climate variability in a shallow aquifer of a tropical basement rock to enhance adaptation and management of the groundwater resources of the area. ■

REFERENCES

1. Aizebeokhai, A.P. (2011). Potential impacts of climate change and variability on groundwater resources in Nigeria, African Journal Environmental Science & Technology, 5 (10), 760–768.

2. Allen, M.R. and Ingram, W.J. (2002). Constraints in future changes in climate and the hydrologic cycle. Nature. 419, 224–232.

3. Ashaolu, E.D. and Adebayo, M.O. (2014). Characterizing groundwater level and flow pattern in a shallow overburden aquifer: a study of Ilara-mokin and its environs, Southwestern Nigeria. Momona Ethiopian Journal Science, 6 (2), 55–72.

4. Bala, A.N. and Ike, E.C. (2001). The aquifer of the crystalline basement rocks in Gusau area, North-western Nigeria. Journal of Mining & Geology, 37 (2), 177–184.

5. Bowleg, J. and Allen, D.M., (2012). Effects of storm surges on groundwater resources, North Andros Island, Bahamas. In: Triedel, H., Martin-Bordes, J.L. and Gurdak, J.J. (Eds), Climate Change Effects on Groundwater Resources: A Global Synthesis of Findings and Recommendations. CRC Press/Balkema, Taylor and Francis Group, London, Uk.

6. Chaves, H.M.L., Camelo. A.P.S. and Mendes, R.M., (2012). Groundwater discharge as affected by land use change in small catchments: a hydrologic and economic case study in central Brazil. In: Triedel, H., Martin-Bordes, J.L. and Gurdak, J.J. (Eds), Climate Change Effects on Groundwater Resources: A Global Synthesis of Findings and Recommendations. CRC Press/Balkema, Taylor and Francis Group, London, Uk.

7. Chen, Z., Grasby, S.E. and Osadetz, K.G., (2002). Predicting average annual groundwater levels from climatic variables: an empirical model. Journal of Hydrology, 260 (2002), 102–117.

8. Chen, Z., Grasby, S.E. and Osadetz, K.G., (2004). Relation between climate variability and groundwater levels in the upper carbonate aquifer, southern Manitoba, Canada. Journal of Hydrology, 290 (1–2), 43–62.

9. Green, T.R., Taniguchi, M., Kooi, H., Gurdak, J.J., Allen, D.M., Hiscock, K.M., Treidel, H. and Aureli, A., (2011). Beneath the surface of global change: Impacts of climate change on groundwater. Journal of Hydrology, 405 (2011), 532–560.

10. Henry, M.H., Demon, H., Allen, D.M. and Kirste, D., (2012). Groundwater recharge and storage variability in southern Mali. In: Triedel, H., Martin-Bordes, J.L. and Gurdak, J.J. (Eds), Climate Change Effects on Groundwater Resources: A Global Synthesis of Findings and Recommendations. CRC Press/Balkema, Taylor and Francis Group, London, Uk.

11. Holman, I.P., (2006). Climate change impacts on groundwater recharge-uncertainty, shortcomings, and the way forward? Hydrogeology Journal. 14 (5), 637–647.

12. Ifabiyi, I.P. and Ashaolu, E.D. (2013). Analysis of the Impacts of Rainfall Variability on Public Water Supply in Ilorin, Nigeria, Journal of Meteorology and Climate Science 11 (1), 18–26.

13. IPCC, 2007. Climate change (2007): the physical science basis. Contribution of working group I to the fourth assessment report of the intergovernmental panel on climate change. In: Solomon, S., et al. (Eds.), Cambridge University Press, Cambridge, UK, and New York, USA, pp. 996.

14. MacDonald, A.M., Davies, J., Calow, R.C. and Chilton, P.J. (2005). Developing groundwater – a guide to rural water supply. Rugby, UK, Practical Action Publishing. 358 pp.

15. Makanjuola, O.R., Salami, A.W., Ayanshola, A.M., Aremu, S.A. and Yusuf, K.O., (2010). Impact of Climate Change on Surface Water Resources of Ilorin, 2nd Annual Civil Engineering

Conference, University of Ilorin, Nigeria. 26–28 July, 2010, International Conference on Sustainable Urban Water Supply in Developing Countries: 284–297.

16. Marechal, J.C., Dewandel, B. and Subrahmanyam, K., (2004). Use of hydraulic tests at different scales to characterize fracture network properties in weathered fractured layer of a hard rock aquifer. Water Resources Research, 40, 1–17.

17. Nyagwambo, N.L., (2006). Groundwater recharge estimation and water resources assessment in a tropical crystalline basement aquifer. Dissertation submitted in fulfilment of the requirements of the board for Doctorates of Delft University of Technology and of the Academic Board of the Unesco-Ihe Institute for Water Education, Delft, The Netherlands. 182 p.

18. Oladapo, M.I., Adeoye-Oladapo, O.O. and Mogaji, K.A., (2009). Hydrogeophysical study of the groundwater potential of Ilara-Mokin Southwestern Nigeria. Global Journal of Pure & Applied Science, 15 (2): 195–204.

19. Olaniran, O.J. (2002). Rainfall anomalies in Nigeria: the contemporary understanding. 55th inaugural lectures, University of Ilorin, Ilorin, Nigeria. 55 pp.

20. Olanrewaju, R.M. (2009). The climate effect of urbanization in a city of developing country: The case study of Ilorin, Kwara Sate, Nigeria. Ethiopian Journal of Environmental Studies & Management, 2 (2), 67–72.

21. Salami, A.W., Raji M.O., Sule, B.F., Abdulkareem, Y.A. and Bilewu, S.O., (2010). Impacts of Climate Change on the Water Resources of Jebba Hydropower Reservoir, 2nd Annual Civil Engineering Conference, University of Ilorin, Nigeria. 26–28 July, 2010, International Conference on Sustainable Urban Water Supply in Developing Countries: 298–312.

22. Sandstorm, K., (1995). Modelling the effects of rainfall variability on groundwater recharge in semi-arid Tanzania. Nordic Hydrology, 26, 313–330.

23. Sekhar, M., Kumar, M.S.M. and Sridharan, K., (1994). A leaky aquifer model for hard rock aquifers. Applied Hydrogeology, 3 (94), 32–39.

24. Taylor, R.G. and Howard, K.W.F., (2000). A tectono-geomorphic model of the hydrogeology of deeply weathered crystalline rock: evidence from Uganda. Hydrological Journal, 8, 279–294.

25. Taylor, R.G. and Tindimugaya, C., (2012). The Impacts of Climate Change and rapid Development on Weathered Crystalline Rock Aquifer Systems in the Humid Tropics of Sub-Saharan Africa: Evidence from South-Western Uganda, In: Triedel, H., Martin-Bordes, J.L. and Gurdak, J.J. (Eds), Climate Change Effects on Groundwater Resources: A Global Synthesis of Findings and Recommendations. CRC Press/Balkema, Taylor and Francis Group, London, Uk.

26. Trenberth, K.E., Dai, A., Rasmussen, R.M. and Parsons, D.B., (2003). The changing character of precipitation. Bulletin of the American Meteorology Society, 84, 1205–1217.

27. White, I. and Falkland, T. (2012). Reducing groundwater vulnerability in Carbonate Island countries in the pacific. In: Triedel, H., Martin-Bordes, J.L. and Gurdak, J.J. (Eds), Climate

Change Effects on Groundwater Resources: A Global Synthesis of Findings and Recommendations. CRC Press/Balkema, Taylor and Francis Group, London, Uk.

28. World Metrological Organization, (2009). Flood management in a changing climate: A tool for Integrated Flood Management, APFM technical document No. 13, flood management tools series.

29. World Metrological Organization, (2007). The role of climatological normals in a changing climate, world climate data and monitoring programme No. 61, Geneva March, 2007.

Eniola D. Ashaolu received a Bachelor of Science degree and Masters of Science degree in Geography from University of Ilorin, graduating top of his classes. He is currently on his PhD degree in the same university. He is an independent researcher and research analyst. His research interest is in the fields of climatology, hydrology and water resources management. He has published five research articles, in reputable national and international journals. He is a member of International Hydrological Sciences.

Akhmetkal R. Medeu
Institute of Geography, Kabanbai Batyr / Pushkin st. 67/99, Almaty, 050010, Republic of Kazakhstan, Tel: (8-727) 291-81-29, 291-88-69, Fax: (8-727) 291-81-02, e-mail: ingeo_2009@mail.ru

THE METHODOLOGY OF NATURAL HAZARDS MANAGEMENT IN KAZAKHSTAN

ABSTRACT. Over the last 10 years, more than 4,000 natural disasters have been recorded around the world; they resulted in death of more than half a million people, which is 1.5 times greater than in the previous decade. Similarly, in the Republic of Kazakhstan, there has been an increase in occurrence of natural and technogenic disasters, leading to human casualties and substantial material loss. The paper demonstrates that risk management is one of the promising ways for providing safety of human activities. The methodology of risk management described in the paper is based on scientific and technological achievements and involves assessment of risks of natural and technogenic emergency situations (ES) emergence and associated damage. The paper provides systematization of natural hazards with isolation of geological, geomorphological, hydrological, climatic, and other processes. The characteristics of spatial distribution are identified; the level of hazard and risk of adverse impacts is shown; and a series of thematic maps at various scales, spatial coverage, and content is compiled for the Republic of Kazakhstan territory with consideration given to goals, objectives, and level of risk management. The paper demonstrates that natural and technogenic hazards are discrete in terms of emergence and their onset is of short duration. Risk management is broken into the following phases:
1. Before the onset of ES;
2. During the immediate threat of ES and their onset;
3. After ES.
The methodology suggests that all efforts of risk-management implementation should be directed towards achieving acceptable level and safety.

KEY WORDS: natural and technogenic disasters, risk management, risk of emergence of natural and technogenic hazards, maps of natural hazards and risks

OCCURRENCE OF NATURAL HAZARDS IN THE WORLD

According to the Center for Research on the Epidemiology of Disasters [CRED...] and other sources, in the last century and the beginning of the current century, i.e., in 1900–2013, there have been about 21 thousand disasters[1] in the world[2], including 13 thousand natural disasters[3] and 8 thousand caused by humans[4]. They killed approximately 33 million people, of which 32.5 million were victims of natural disasters. Natural disasters amounted to 2.5 trillion dollars out of 2.6 trillion of the total loss. The largest number of disasters is caused by floods (32 %), storms (28 %), epidemics (10 %),

[1] Catastrophe – the death toll of more than 10 people, the number of victims is more than 100 people.
[2] World – continents Asia, America, Africa, Europe, Oceania.
[3] Natural disasters – droughts, earthquakes, epidemics, extreme temperatures, floods, insect infestation, avalanches, landslides, storms, volcanic eruptions, wildfires.
[4] Man-made disasters – industrial, technological and transportation accidents.

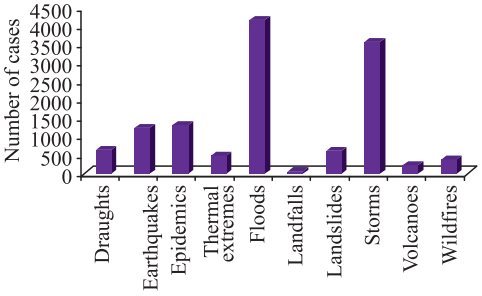

Fig. 1. Distribution of natural disasters by types.

and earthquakes (9 %) (Fig. 1). The maximum damage was inflicted by storms (940 billion dollars), earthquakes (760 billion dollars), floods (590 billion dollars), and droughts (126 billion dollars.). Drought, epidemics, floods, and storms led to the death of 11, 9.6, 6.9, and 1.4 million people, respectively.

Analysis of the temporal distribution of accidents shows that, during the XX and XXI centuries, there has been an increase (with minor fluctuations) of their numbers. The most intense growth of both natural and man-made disasters began in the second half of the XX century.

The period 1965–2013 was associated with 92 % (12.8 thousand of cases) of natural and 95 % (7.3 thousand) of technogenic disasters. This may be explained by both technical and natural factors. Technical factors include creation and improvement of systems for monitoring, collection, and analysis of data, and enhanced information and the volume of data included in the CRED database. Natural factors include industrial revolution, industrialization, and climate change. This period practically accounts for the entire loss associated with disasters; however, the number of victims of these disasters is only 16 % (5.3 million) of all cases that happened in 1900–2013.

Analysis shows that in 2000–2010, the number of natural disasters, their victims, and the damages rose 1.4, 1.3, and 1.6 times, respectively, compared with 1990–1999. The number of man-made disasters increased 1.6 times; the number of deaths and the loss increased 1.2 and 3.5 times, respectively.

The dynamics of disasters over 1900–2013 (Fig. 2–4) shows that while the second half of the XX century is associated with the growing number of disasters and losses caused by them, the number of casualties is declining. Thus, at the beginning of 1900–1965, there were 29 million deaths compared with 5.1 million in 1966–2013. There has been the continuous growth of the number of man-made disasters and associated losses; the maximum number of casualties – 283 thousand – is recorded in 1966–2013 compared with 56 thousand recorded in 1900–1965.

Such multidirectional temporal distribution of the tragic consequences of disasters can be attributed to several reasons, the most important of which are different capabilities of their occurrence and impact risk management.

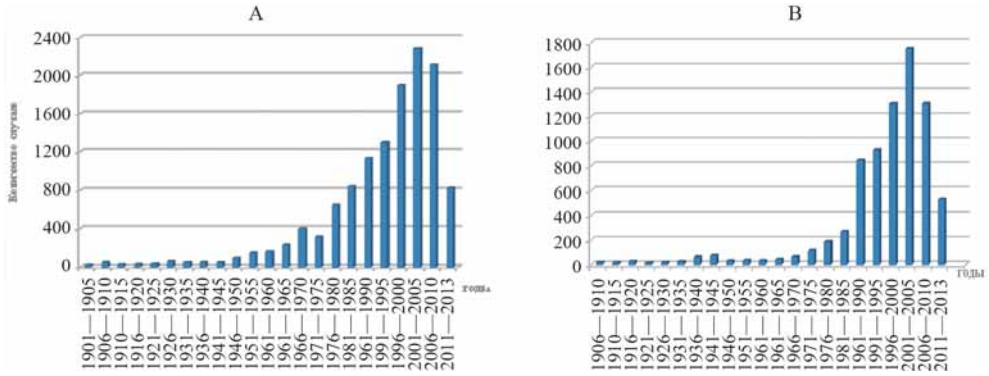

Fig. 2. The number of natural (a) and man-made (b) disasters in the world in 1901–2013.

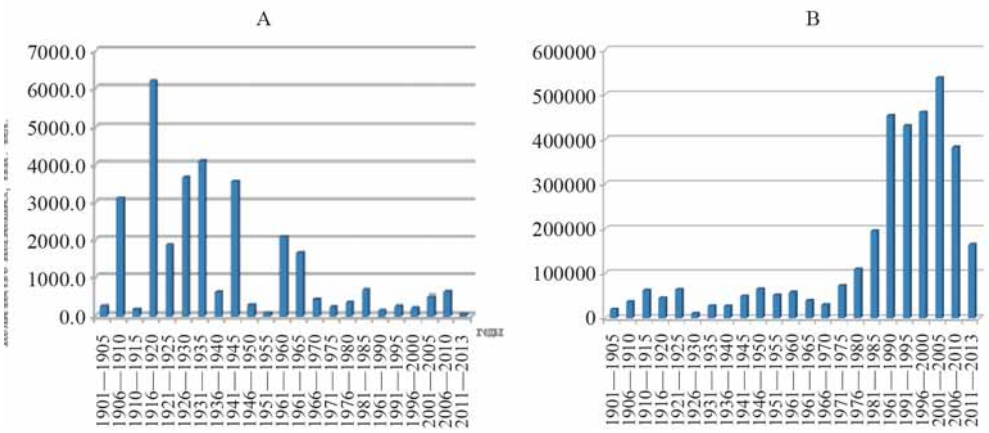

Fig. 3. The number of casualties (thou people) due to natural (a) and man-made (b) disasters in 1901–2013.

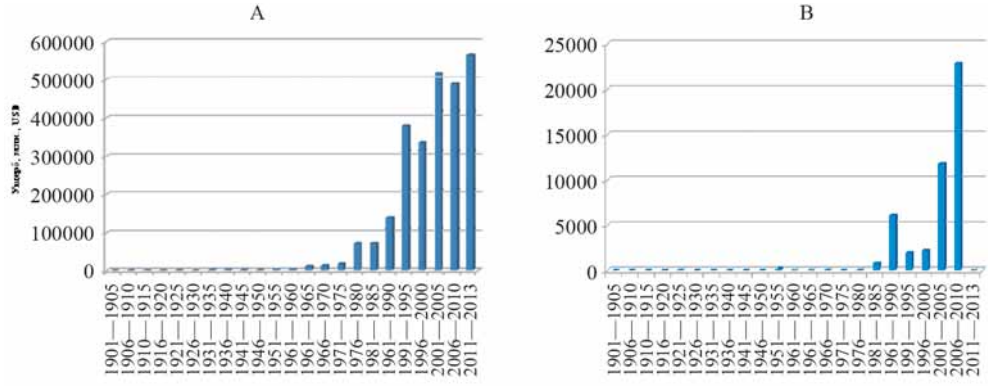

Fig. 4. The loss (mln USD) due to natural (a) and man-made (b) disasters in 1901–2013.

Measures to reduce and prevent damage are being consistently incorporated in the fight against natural hazards in the second half of the XX century: monitoring the impact factors, forecast of occurrence, warning of the population, timely protective measures; these measures have led to the reduction of human casualties. At the beginning of the XX century, the death toll of man-made disasters does not correlate with the scale of production, but it increases with the volume and technological complexity of the latter, together with the number of employees and allocation of facilities in densely populated areas. Despite the development of safety systems, it is practically impossible to forecast the outcomes of technogenic disasters because of a large number of people that they impact.

NATURAL HAZARDS IN KAZAKHSTAN

Accidents in the Republic of Kazakhstan are accounted for in the global statistics beginning in 1991 – the year of obtaining the independence. According to the CRED criteria, the database for the period from 1991 to 2013 includes 19 cases of natural and 15 man-made disasters with the total number of 574 people killed, and the loss of 280 million dollars. The Ministry of Emergency Situations (PK emer.gov.kz) provides synthesis of information about disaster by using more detailed criteria that allow obtaining a more complete picture. According to the Ministry, every year in Kazakhstan, there are about 5,000 emergency situations (ES), natural and man-made, that impact more than 6,000 people; more than 1,500 people died. The average annual loss from disasters reaches 25 billion tenge.

In Kazakhstan, dangerous natural processes and phenomena that can harm human health, economy, and environment are widespread. In some years, material damage from natural disasters exceeded 20 billion tenge alone. Although natural disasters account for 20 % of all ES, the share of affected people reaches 73 %, which is more than 6,000 people per year with 460 fatalities (30 % of those killed in ES).

The most detailed data on natural disasters exist for the period 2004–2008; we will consider this period below. During this period, the number of natural disasters per year for Kazakhstan as a whole ranged from 3,900 to 5,500. The annual material damage amounted to more than 5 billion tenge (47 % of the total damage caused by ES). The largest number of natural disaster was noted in the Almaty, Aqtobe, East Kazakhstan, and South Kazakhstan regions

The number of victims of natural disaster ranged from 3,200 to 15,500 people. The greatest number of people were affected by dangerous infections (49 %), hydro-meteorological and geological processes and phenomena, and by accidents on water. Most of the victims were recorded in the South Kazakhstan, Zhambyl, and Kyzylorda regions. The death toll from natural disasters in Kazakhstan in those years ranged from 410 to 620. Most of the victims drowned in accidents on water. Deaths from hydro-meteorological and geological events occupy the second position. On average, 3.1 persons, per thousand, die from ES per year. In the Almaty and Aqtobe regions, the figure is close to 6, while in the cities of Astana and Almaty and the Kostanai region, it is less than 1.

Most losses (90 %) are attributed to hydro-meteorological and geological factors. They are followed by wildfires. The damage caused by natural disaster varies greatly from year to year. In 2004, 2006, and 2007, the loss amounted to less than 1 billion tenge, while in 2005, the loss reached almost 8 billion tenge. In 2008, in 8 months only, the loss exceeded 16 billion tenge. The average annual damage from natural disasters in 2004–2007 was 0.027 % of GDP. This parameter varies by region, from less than 0.001 % in the Almaty, Karaganda, and Aqtobe regions to more than 0.5 % in the South Kazakhstan and Zhambyl regions, where in some years damage from natural disasters reaches 2.2 % of GDP (Fig. 5–8).

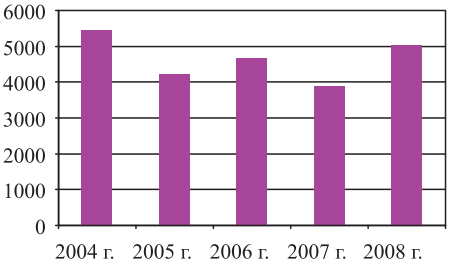

Fig. 5. The number of natural ES.

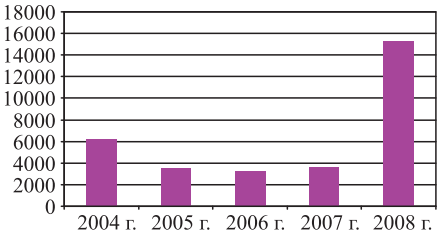

Fig. 6. The number of people affected by natural ES.

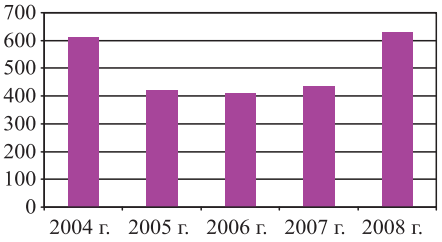

Fig. 7. The number of dead as a result of natural ES.

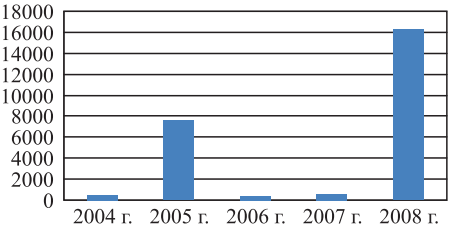

Fig. 8. Damage caused by natural disasters (mln tenge).

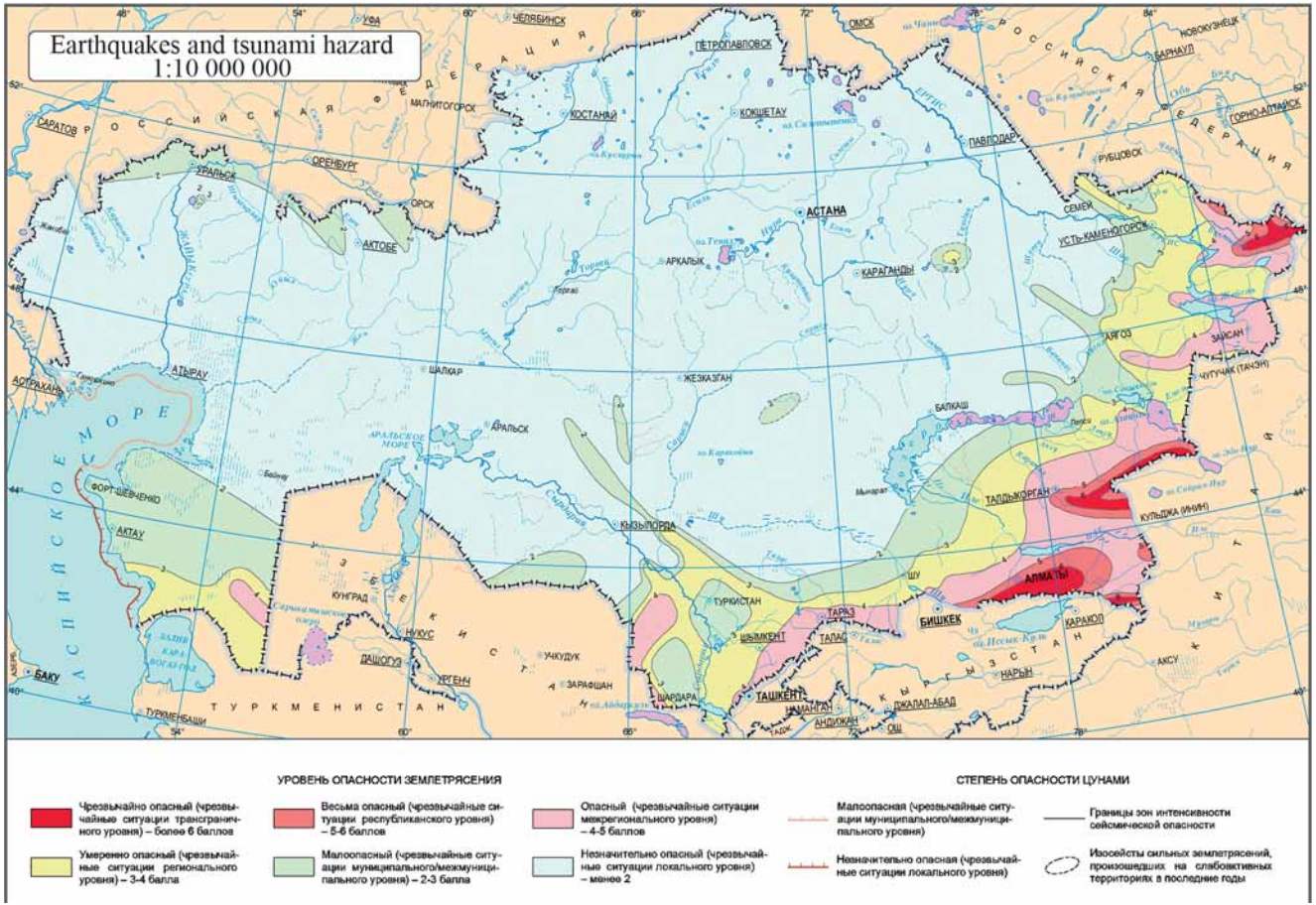

Fig. 9. Map of earthquakes and tsunami hazard (from the "Atlas of natural and man-made hazards and risks of emergency situations" Almaty, 2012). The earthquake danger decreases from red to green and light blue areas.

Fig. 10. Destruction of houses in the Lugovskoy earthquake in 2004.

Fig. 11. Aftermath of the Lugovskoy earthquake in 2004.

The greatest damage is caused by earthquakes, extreme floods, droughts, and weather (heavy snowfalls and heavy rains, snowstorms, high winds, etc.) phenomena. In the mountain and foothill areas, mudslides, landslides, and avalanches represent continuous danger. Their disastrous manifestation consistently increases, including the number of cases caused by inadequate human activities.

In Kazakhstan, the most earthquake-prone regions are the eastern and southern mountainous areas. The earthquake-prone areas, with the magnitude of 8–9 points, occupy nearly 10 % of the territory. The earthquake-prone area includes the cities of Almaty, Taldykorgan, Ust-Kamenogorsk, Shymkent, and Taraz (Fig. 9, 10, 11).

Susceptibility of the territory of Kazakhstan to dangerous exogenous geological processes and phenomena is the highest in the eastern and southern regions with mountainous terrain. Landslide-prone areas occupy about 20 % of the area of Kazakhstan. Landslides are common in the low mountain and foothill areas of Altai, Zhetysu Alatau, and Tien Shan, as well as in the valleys of major rivers: Yertys, Tobyla, Yesil, and Zhaiyk, and cliffs of the Ustyurt Plateau (Fig. 12, 13, 14).

Avalanche areas cover an area of over 100 sq. km. Avalanches happen in Altai, on the Kalbinskiy Ridge, in Sauyre, Tarbagatai, in Zhetysu, Ile, Kung, and Terskey Alatau, and on the Uzynkar, Kyrgyz, Ugam, and Tau Ridges (Fig. 15–17).

Mudflows affect about 30 % of the territory of Kazakhstan; in particular, mountain regions of Altai, Zhetysu Alatau, and Tien Shan. Less exposed to the danger of mudflow are the Kalba, Sauyr, Tarbagatai, Karatau, and Mangistau Ridges. Suspended mud-like floods are possible on the Kazakh Upland (Fig. 18–21).

Weather natural hazards: strong winds, snowstorms, dust storms, heavy rains, snow, thunderstorms, hail, fog, and sudden variations in temperature, are observed throughout Kazakhstan. They can paralyze the economic activity within wide areas. Their damage can reach 16 billion tenge per year, and the death toll is more than 100 people. The most part of the territory of Kazakhstan is subject to atmospheric and soil drought, which causes great damage to agriculture (Fig. 22).

Among hydrological processes, the greatest danger is associated with snowmelt floods and high water. They occur annually in spring in all the rivers of Kazakhstan. There is winter high water on the Syrdarya River associated with water releases from the Shardarinsky Reservoir (Fig. 23, 24).

Wild forest, steppe, and forest-steppe fires are particular frequent in the northern, eastern, and south-eastern regions of Kazakhstan, where they cause considerable damage to forest- and farmland.

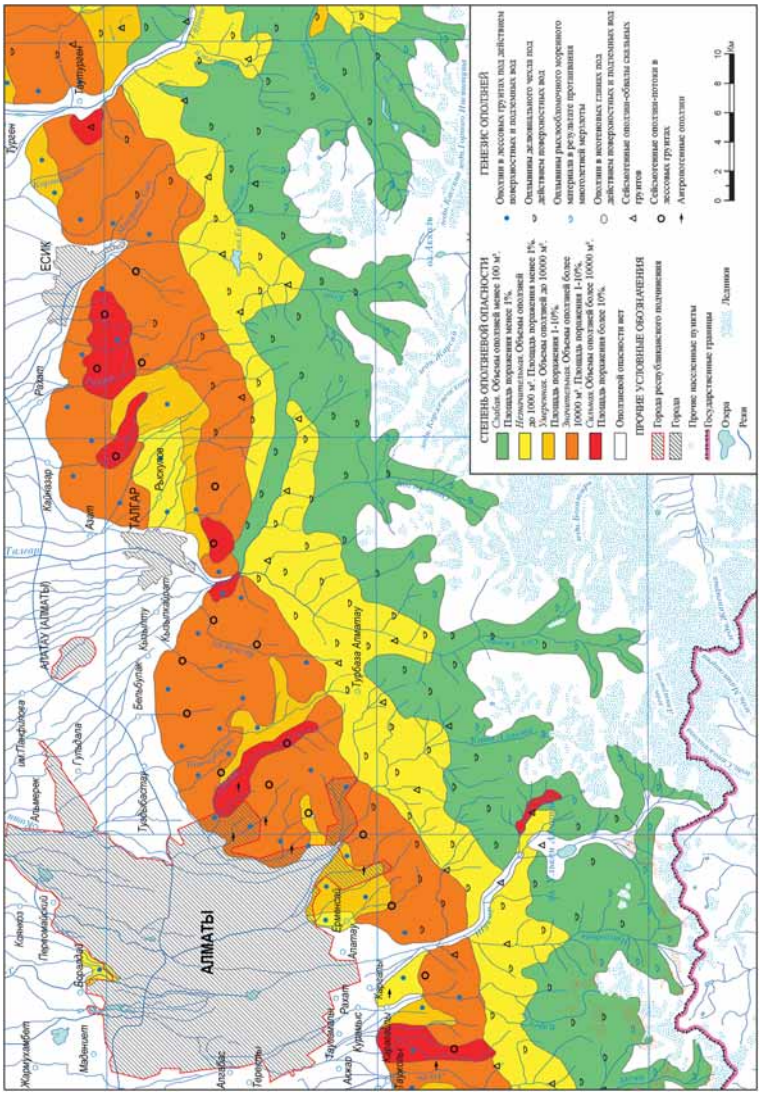

Fig. 12. Landslide hazard map of the northern slope of Ile Alatau (from the "Atlas of natural and man-made hazards and risks of emergency situations" Almaty, 2012). The degree of landslide hazard increases from green to red areas.

Fig. 13. Landslide in the basin of the Taldybulak River in Ile Alatau that destroyed buildings and claimed the lives of 30 people.

Fig. 14. Landslide in the basin of the Kargaly River in Ile Alatau that destroyed buildings and claimed the lives of 3 people.

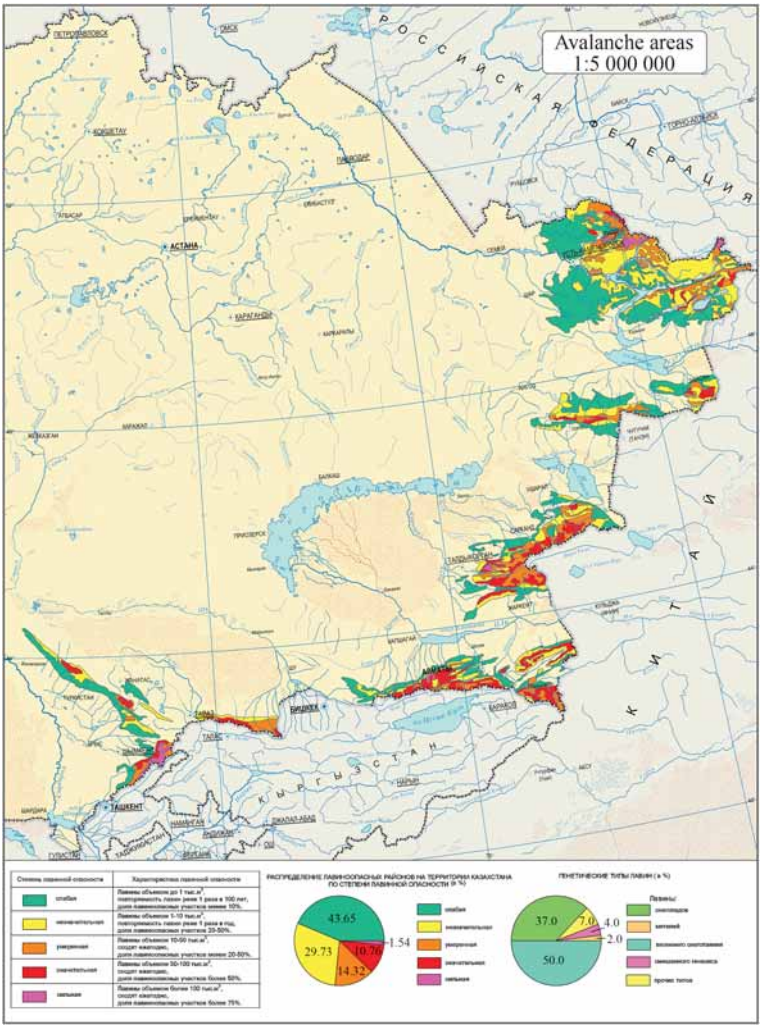

Fig. 15. Map of avalanche areas of Kazakhstan (from the "Atlas of natural and man-made hazards and risks of emergency situations" Almaty, 2012). The degree of avalanche hazard increases from green to red and pink areas.

Fig. 16. Large wet avalanche in the basin of the Koturbulak River in Ile Alatau, 2010.

Fig. 17. Wet avalanche in the Kimasar tract in Ile Alatau, 2010.

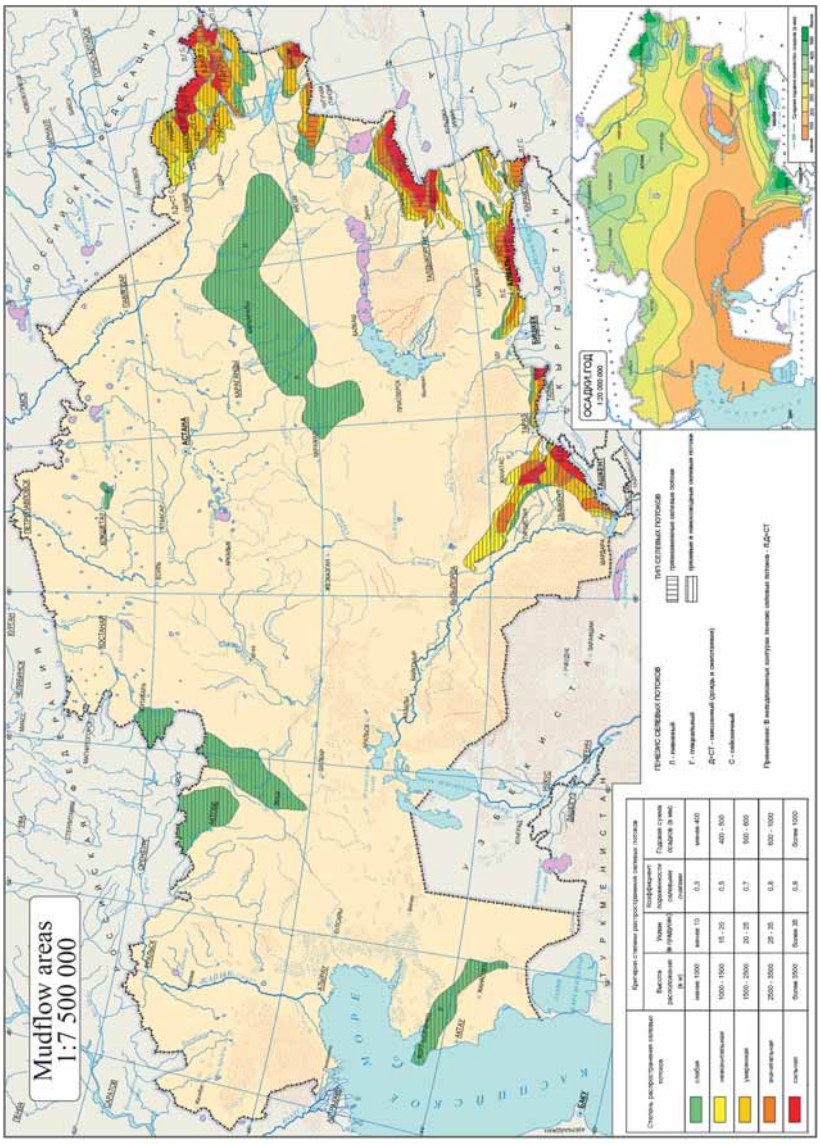

Fig. 18. Map of mudflow areas in Kazakhstan (from the "Atlas of natural and man-made hazards and risks of emergency situations" Almaty, 2012). The occurrence of mudflows increases from green to red areas.

Fig. 19. Passage of mudflow in Esik (Ile Alatau) in 1963.

Fig. 20. Mudflow in the basin of the Kishi Almaty River (Ile Alatau) in 1973.

Fig. 21. Traces of the passage of mudflow in the Ulken Almaty River basin (Ile Alatau) in 2006.

Fig. 22. Dust storms in the Aqtobe region (image from space).

IMPROVEMENT OF MEASURES TO COMBAT NATURAL HAZARDS

The inevitable result of natural and man-made disasters is worsening of the socio-economic issues, particularly in intensively cultivated and densely populated regions. According to experts, if the trend of growth continues, in the next decade, an increase in economic losses from them will be comparable with the growth of GDP. Therefore, the world community is revising its attitude towards disasters as inevitable phenomena and is treating them with more of confidence that it is possible to prevent them, mitigate, reduce human losses, and material damage through greater and active use of scientific and technological achievements.

Adopted at the UN Conference on Environment and Sustainable Development (Rio de Janeiro, 1992), the principle of pre-emption (precautionary) clearly defines priorities in dealing with security issues. The provisions of the concept of sustainable development with respect to natural disasters have been developed in the materials of the UN Conference on Disaster Risk Reduction in 1994 (Japan). Its declaration states that the effort for the reduction of damage from natural disasters should be an important element of the government strategy of all countries of the world. The Declaration of the Habitat II Conference in Istanbul (Turkey, 1996) adopted the Agenda – the principles, commitments, and plan of action related to the protection of human settlements. Two years later, in Moscow (Russia, 1998), the International Conference "Global problems as a source of emergency situations," was held during the International Decade for Natural Disaster Reduction. The conference participants expressed concern about the vulnerability of people to natural disasters.

In January 2004, Kobe (Japan) hosted the UN World Conference on Disaster Reduction, which adopted the Hyogo Declaration and Framework for Action 2005–2015 that stipulates building the resilience of nations and communities to disasters. The following priority items, among others, are listed in the program: identification (including inventory), assessment, monitoring disaster risks, early warning alerts, use of innovative knowledge to reduce underlying risk factors, and disaster preparedness.

Despite this well-founded proposal, the number and the damage caused by natural disasters have not been reduced; this was noted in the resolution of the UN conference "Rio + 20" (2012) which explicitly states that over the past 20 years after the adoption of the Declaration on Sustainable Development, the progress in protection against natural disasters has not been as effective as expected.

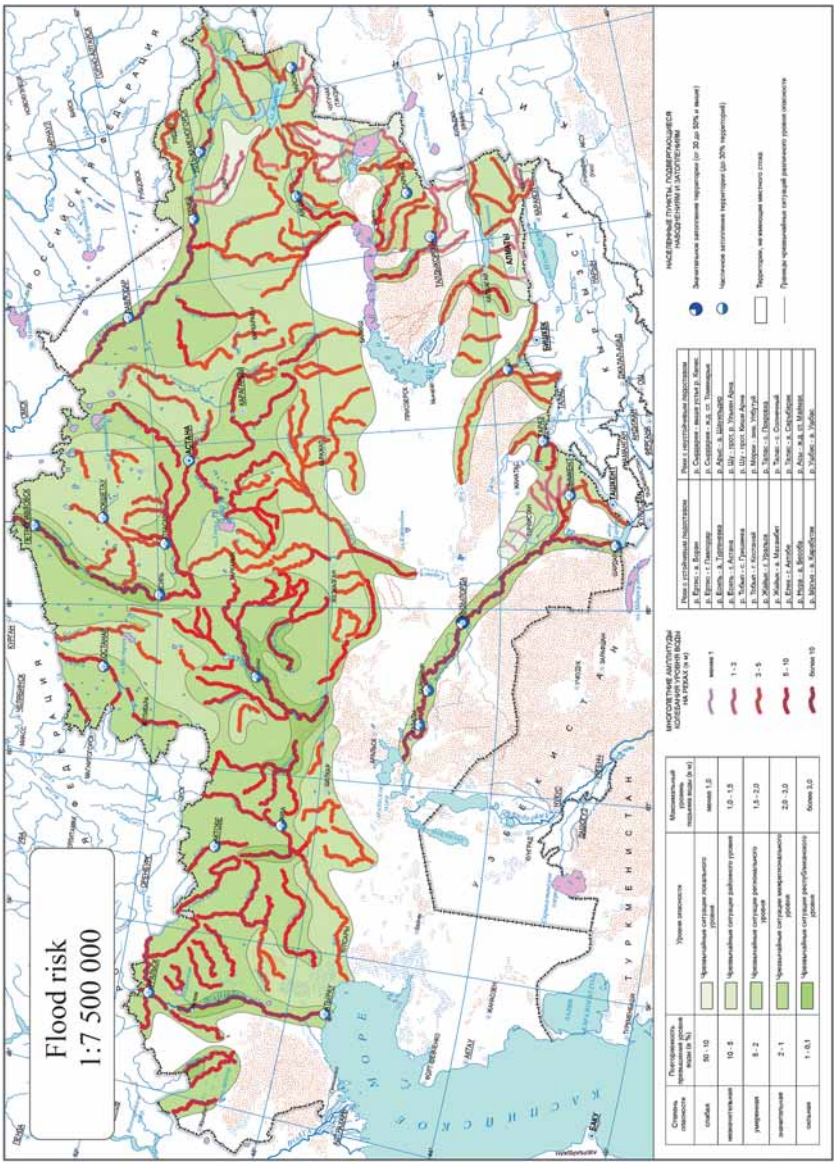

Fig. 23. Map of flood risk in Kazakhstan (from the "Atlas of natural and man-made hazards and risks of emergency situations" Almaty, 2012).
The flood risk becomes higher (local-regional-national) from light to darker green areas.

Fig. 24. Flooding in the Syrdarya River basin.

THE NEW STRATEGY AGAINST NATURAL HAZARDS

The system of proposals discussed above demonstrates that in the studies of assessment and risk management, the priority goal is safety. It is clear that in order to achieve this goal, a new Paradigm should be implemented: measures for providing safety of the population and socio-economic facilities, which have been founded earlier based on the concept "react and manage," should give place to a new principle "forecast and prevent." The new quality of relations should realize a new pragmatic approach, i.e., effective risk management, which is associated with organization of human activities and society in a way that prevents reaching the upper limit level of impact of natural processes; exceeding this limit may lead to catastrophic consequences. Of course, the main problem in dealing with the prevention and reduction of the damage is a well-thought, responsible, and effective policy of public authorities, based on the legislative and regulatory documents.

THE SYSTEM OF NATURAL HAZARDS MANAGEMENT

The establishment and functioning of the risk management system requires a system of focused activities, including scientific and applied research on the development of methodologies and management practices and the creation of schemes and projects to protect specific objects.

Solving the problem of natural risks management is largely determined by the choice of methodology. As is known, the development of the methodology is an important step in any field of knowledge. The fist step should include formulation of scientific ideology, philosophical approach, and outlook in the study area; the second step involves development of a set of rules and regulations and methods and tools that provide for the solution. The Institute of Geography of the Ministry of Education and Science (MES) of the Republic of Kazakhstan has developed methodological framework for management of natural risks: it has formulated the conceptual framework, suggested a synergetic approach to the problem in general and ways of solving particular problems; and conducted tests using empirical evidence that supports the study objective and its connection reality, its nature, and the laws of development and functioning; the framework has been partly implemented in the course of scientific research [Medeu, 2008, 2011].

Under this framework and in the course of development of the new ideology and new paradigm for providing security, an algorithm for natural risk management has been also developed. The algorithm means management of identified and assessed natural risks using the principle of reasonable efficiency and the division of responsibility between the state, the population, and economic entities. It was proposed to treat management as a system that includes processes for formulation of problems, missions, and goals, identification and assessment of risks, selection of risk management strategies and of best practices and ways of risk reduction, and implementation of administrative decisions (Fig. 25).

The mission of natural risks management is to contribute to sustainable development of the Republic by ensuring protection of the vital interests of all categories of the population, industrial and economic systems, and material and spiritual values of the environment in areas prone to the adverse effects of natural hazards. The fundamental (strategic) objectives of the management of natural risks that define its general direction is safety, which is achieved by taking into account the ways of socio-economic development and investment intentions of the state and using innovative technologies. Tactical management objectives include the choice of optimal solutions and acceptable methods of reducing the likelihood of hazards and the damage by increasing security of the recipients. Operational objectives include the most effective way to

achieve practical implementation of the objectives of a higher level (Fig. 26).

The solution of basic and individual issues of risk management is not possible without **the creation of the information foundation**, i.e., a database on natural phenomena. The creation of a database includes analysis, interpretation, and systematization of information about the natural phenomena, the use of which is necessary for the development of management solutions to reduce and prevent damage. The structure and composition of the data must provide for the achievement of the ultimate objective of the study and its components should address the sub-goals of a lower hierarchical level. It should reflect the connection of phenomena "part – whole" and "cause and effect," as well the connection between groups of data corresponding to pieces of information about these phenomena.

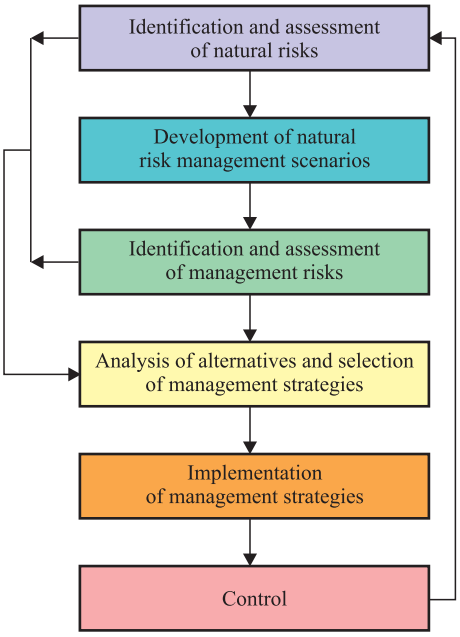

Fig 25. Algorithm for natural risks management.

The data may have different levels of generality. The minimum level of generality should allow identification of the phenomena in a studied aspect, while the maximum level should ensure the generation of particular objectives. In the latter case, it is possible to establish associative (non-hierarchical) relations between data groups; information models for evaluation of natural risks should be developed.

All information collected must be analyzed to determine its relevance and adequacy. The significance of the data is established by comparing them with a set of goals. After determining the value of the data, the data are either saved (memory formation) for later use, or are used directly. At the same time, adequacy of the data for risk management is assessed; the subsequent steps to obtain the missing information (increase in the depth of retrospection, specialized survey of the territory, etc.) are planned and implemented. As a result, the database must contain the interpreted, structured, relevant, and sufficient information for the development of administrative decisions: information about the past events, conditions of their formation, and characteristics of the recipient areas of impact damage. Databases should be created with the use of GIS technologies for cartographic representation of information considering the possibility of using the data in interactive mode (Fig. 27).

An important aspect of developing this methodology is the clear definition of **the notion of assessment of natural risks**, because to date, various interpretations of it exist; they can be divided into two groups. In the first group, risk means hazard and probability of an adverse event or a process; in the second group, risk means potential consequences and loss. In developing this methodology for natural risks management, the risk caused by any natural phenomenon is determined by a combination of the risk of its occurrence and the risk of damage that it inflicted. Often, risk is the product of these parameters

$$R = P_{phen} Y,$$

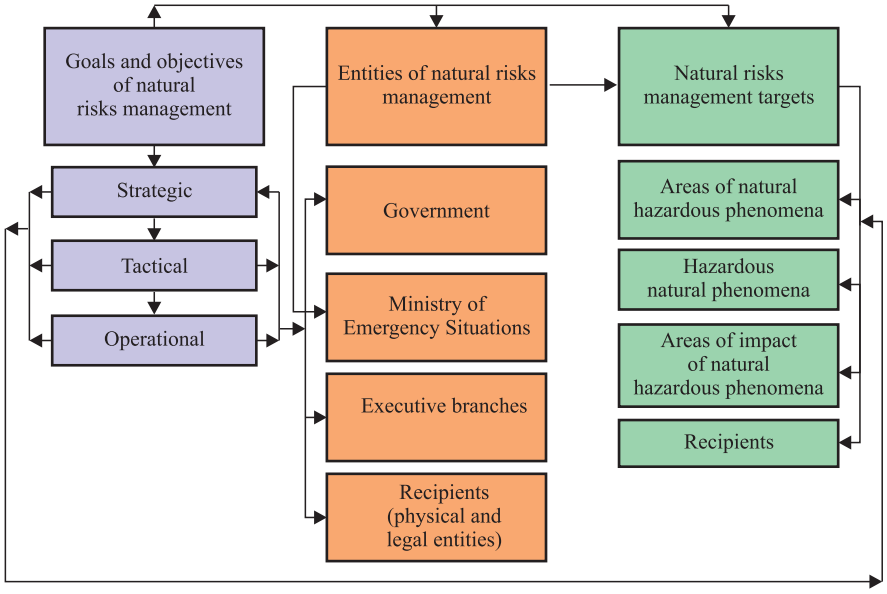

Fig. 26. Structural and functional schematic for risk management.

where R – the risk of negative consequences of a natural phenomenon; P – probability of occurrence of the phenomenon, Y – the value of the damage caused by the phenomenon.

However, since the factors in the above expression may be determined in various terms, including qualitative, in the most general form, the magnitude of risk is better represented as a function

$$R = F(R_{emergence}, R_{imact}),$$

where R – the risk of negative consequences of a natural phenomenon; $R_{emergence}$ – recurrence, probability, or distribution of events of various strength and scale; R_{impact} – damage caused by the phenomenon in sociological, technological, and environmental spheres considering the vulnerability and safety of the recipients.

We have developed a **method for natural hazard risks assessment** that contains, according to the definition stated above, the blocks for assessment of emergence of a phenomenon and of risk of the phenomenon impact, and the integral assessment of the risk of adverse consequences of the natural phenomenon in general.

The block of assessment of the risk of a phenomenon includes the following:

A). The stage of identification includes determination of a phenomenon that can destabilize the situation at a facility, area, or region; a general model (image) of the phenomenon is created; the model, with a certain level of adequacy, reflects its physical nature and the demands of management; it identifies factors that cause a dangerous evolution of events, their potential, and regulatory role. The analyzed factors cover the factors that have directly caused the formation and development of the phenomenon, as well as the subsequent factors or the "chain of causation." Choosing the horizon in this chain, and therefore the identification of the characteristics that describe the conditions of occurrence of a hazard, depends on the purpose and scope of the assessment; various scenarios of risk situations in the emergence and development of phenomena of different scales are developed; their critical thresholds, beyond which a dangerous phenomenon develops, are identified; the characteristics of

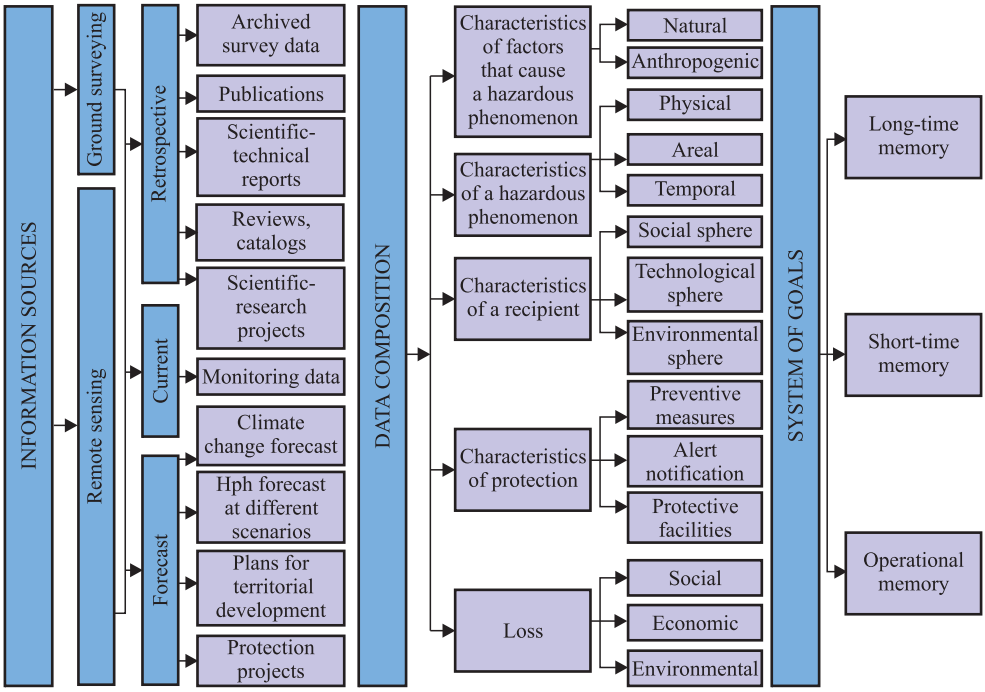

Fig. 27. Information model of natural hazardous phenomena (HPh).

the phenomenon under different scenarios of its emergence and development are identified. The implementation of the risk scenarios is shown in the example of mudflows (Fig. 28, 29, 30).

B). The evaluation stage includes assessment of the probability of occurrence and development of hazard; it is either the probability of achieving the critical values of the factors shaping the phenomenon, or the likelihood of manifestation of various characteristics of the phenomenon itself in the course of implementation of various scenarios of its emergence. In quantitative assessment from the data on the shaping factors, the statistical nature of which is known, it is possible to use the composite method for determining the probability distribution function of the phenomenon under study by calculating the probability density of the combinations of various factors determining the phenomenon. If the theoretical distribution functions of the characteristics that form the shaping factors are not known, the risk of the phenomenon can be calculated as the probability of co-occurrence of critical values in all shaping factors using Bayes' formula. The characteristics of mudflows are determined from the frequency curves for their characteristics; the curves are, in turn, determined from empirical data or from mathematical models. Qualitative assessment of the numerical values of the emergence criteria, thus, of the phenomenon itself, and of the factors' frequency is substituted with the linguistic definition of the categories identified with the various levels of detail (high, medium, low, etc.). Procedures for quality assessment use the methods of qualitative analysis, i.e., fuzzy logic, qualimetry, etc.

C). The forecast assessment of natural risk is based on the information about the expected under global warming changes of the factors that lead to the emergence of a phenomenon and the possible changes of the actual characteristics of a natural phenomenon.

The block of impact risk assessment includes the following:

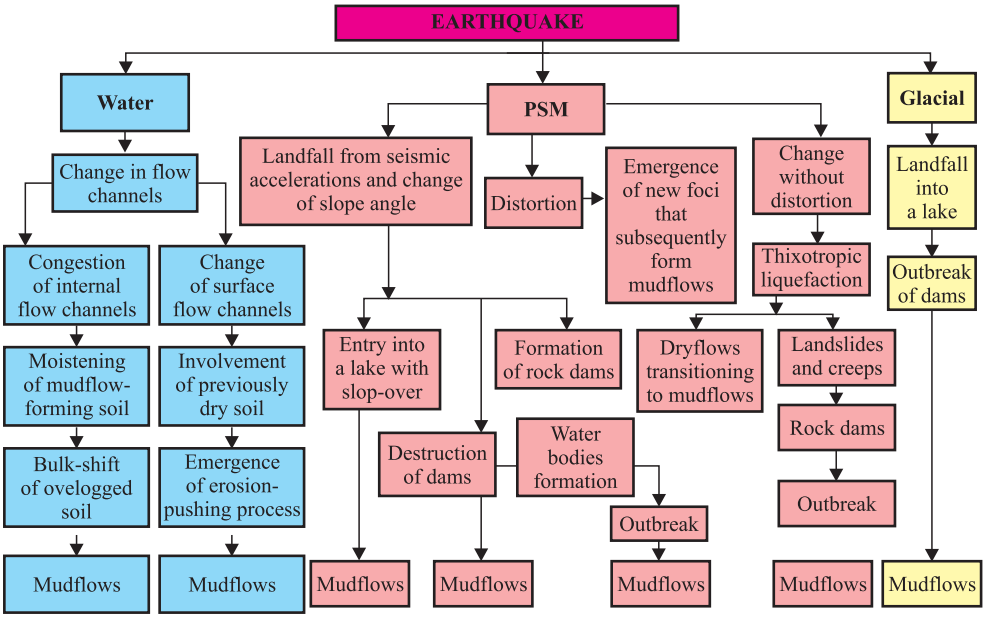

Fig. 28. Scenarios of risk evolution in the course of mudflow development.

- The stage of identifying the source of impact involves determination of the characteristics of the analyzed hazardous phenomenon, causing devastating effects; the areas of its impact are identified using historical data about the areal distribution of the phenomenon using mathematical models for the phenomenon (if any); the recipients of the direct exposure to the hazard are

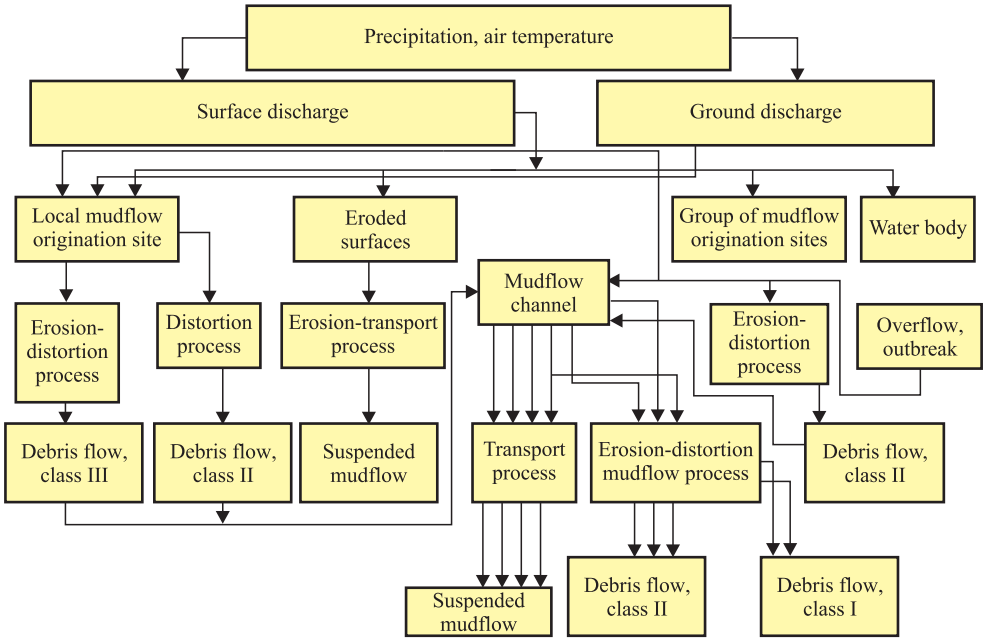

Fig. 29. Scenarios of risk evolution in the course of cloudburst mudflows development.

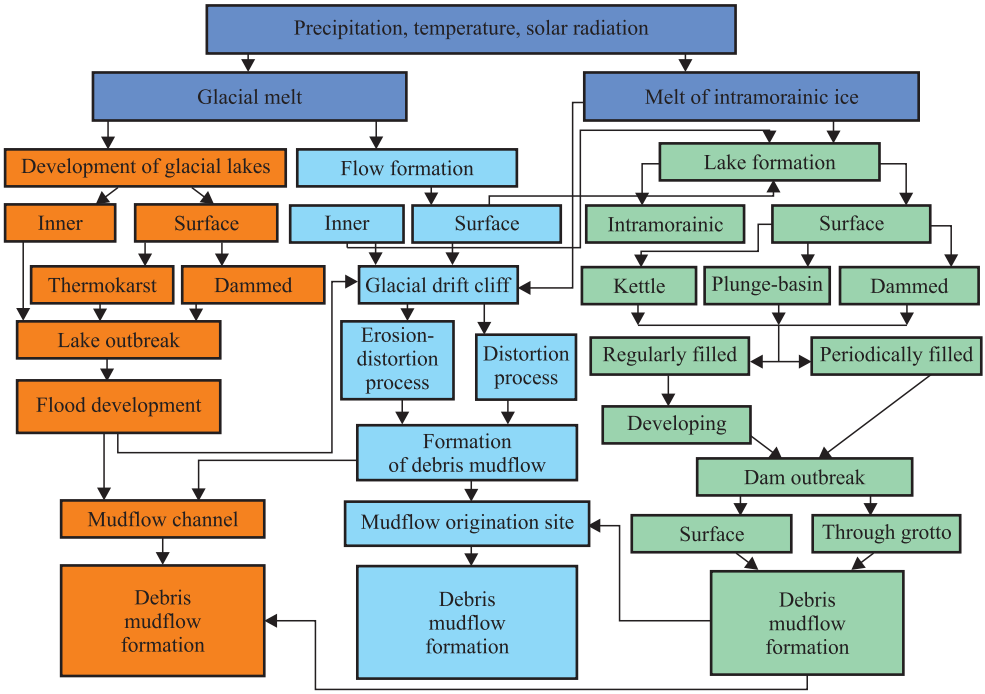

Fig. 30. Scenarios of risk evolution in the course of development of glacial mudflows.

identified in the socio, technological, and environmental spheres (the methods include development of short lists, networks, GIS); scenarios are developed – the scenarios provide for direct and indirect negative impact, forward and backward linkages, the chain reactions in the development of the phenomenon and its negative effects (a graphical representation of the impact scenario in a "tree-diagram" is useful), and a common list of recipients of the direct and indirect effects is formed; such characteristics of the recipients as their social, humanitarian, economic, etc., importance are identified together with vulnerability due to the characteristics of the recipient (permanent of temporal location, adaptation to the impact, etc.), protection by facilities, security systems, etc. The latter (vulnerability and security) reflect the probability of socio, technological, and environmental spheres of truly becoming the recipients of the negative impact of the phenomenon.

- Evaluation of the impact risk is carried out in a qualitative and quantitative manner. Since the recipients are objects of a different nature (socio-sphere, environmental sphere, techno-sphere), the qualitative assessment of the impact of the classifying criteria is based on the same, for all objects and systems, characteristics, i.e., stability; the impact classes define the extent of its breach and the consequences. The main classes of impacts are identified: a) acceptable risk – when system components have time to assimilate the effects due to self-restoration and self-regulation; b) critical risk – recovery is possible in the implementation of relevant activities; c) catastrophic – the limit of stability is exceeded and there are changes even with irreversible consequences, unrecoverable damage; there are also a number of intermediate classes describing the degree of approximation to the effects of the main classes. The description of the degree of impact uses linguistic variables (high, low, substantial, moderate, etc.);

assessment procedures are carried out with the use of quality control, fuzzy logic, etc. The quantitative (economic) impact assessment of natural phenomena is a monetary evaluation of the negative effects of development of hazardous processes described at the steps of the qualitative analysis and expressed in physical units. The quantitative assessment of the impact for socio-, techno-, and environmental spheres is based on market prices and takes into account damage, restoration costs, and losses using the probability theory and mathematical statistics methods.

- Forecast assessment of the risk exposure is based on information about changes in the composition and the number of recipients, their importance, vulnerability, and safety in accordance with the development plan and the development of the territories.

The block of the integrated risk assessment of the negative effects of any natural phenomenon includes the aggregate risk assessments of emergence and impact (Fig. 31).

Qualitative assessment is performed using methods of qualitative analysis, i.e., qualimetry, fuzzy logic, etc. Quantitative assessment is done using methods of mathematical statistics and the probability theory. The assessments are compiled with a different period of pre-emption according to the goals and objectives of management (annual risk, 5–10 years, and long-term perspective). The long-term assessment is based on the input forecast information on risk emergence and impact.

The research results yield spatial-temporal forecast a natural phenomenon adverse impact risk – mapping. A set of specialized maps is generated; the maps have different scales, meet certain objectives, cover varying areas, and have different content, depending on the goals, objectives, and the level of risk management. Such maps are the maps of factors causing the emergence of a natural hazardous phenomenon, of recipients with identification of their basic characteristics and protection, of risk of emergence and development of a hazardous phenomenon (Fig. 32)[5], and of integrated risk of adverse consequences of development of a natural phenomenon (Fig. 33)[6]. The maps should reflect the current and forecast condition of the mapped parameters. The system of such maps is a clear representation of research material and allows (through the use of GIS) simulation of various risk situations.

The obtained data on occurrence and frequency of natural disasters and associated risks allow identification of the structure of safety management systems with determination of responsibilities and relations of its elements.

Natural risks management is classified by objective, scope, objects, and subjects of management, and the timing of implementation of management activities. It is subdivided into national, regional, local, and facility, according to the scale of management. The subjects of risk management are the state bodies, regional and local authorities, and legal entities and individuals; the objects are hazardous natural and anthropogenic phenomena and recipients that are subjected to their negative effects and consequences.

The authorities must define strategy, tactics, and ways to solve urgent problems. These risk-management efforts should be aimed at achieving an acceptable level of safety. The criteria for the acceptable risk should be: the absolute primacy of the preservation of human life and minimization of the possibility of damage to a level not exceeding the cost of risk management. Decisions must be based on evidence-based scientific procedures. The most commonly used methods for this purpose are linear programming, simulation models, network models, queuing theory, decision-tree, game theory, etc. There is a widely suggested scenario that included analysis, the steps of determining the purpose of the formation of the scenarios, development of scenarios,

[6] The maps of mudflows are given as the examples.

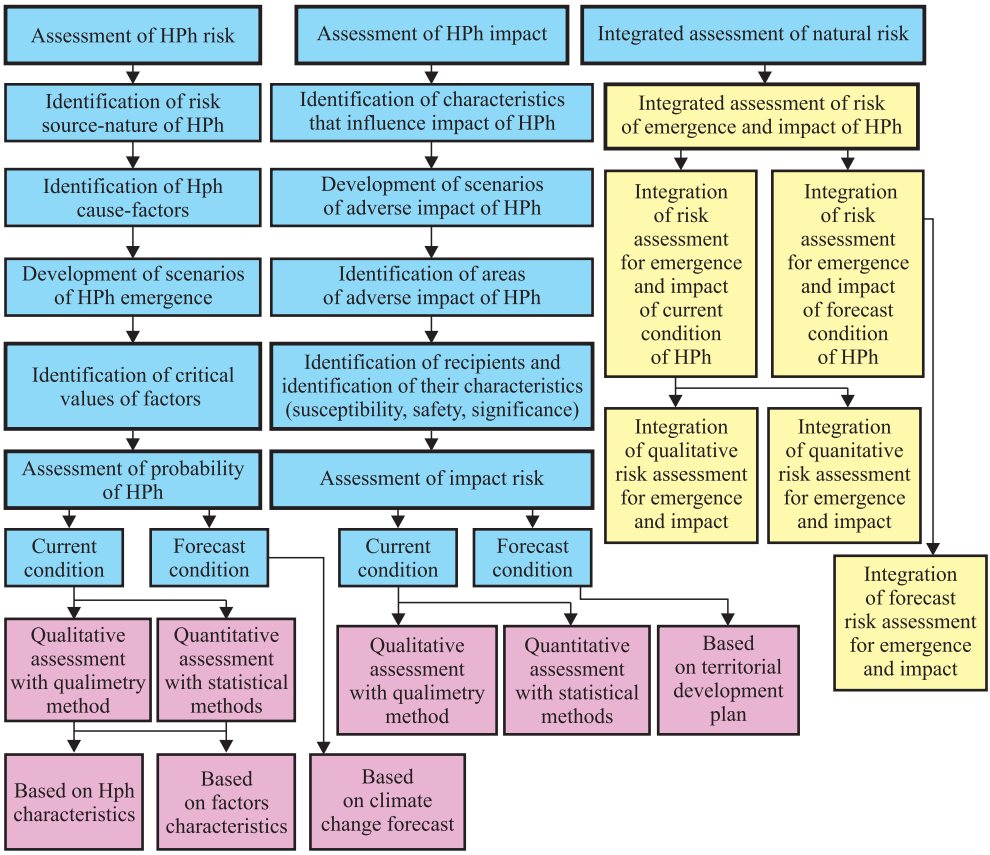

Fig. 31. Natural risk assessment algorithm.

determination of their characteristics, analysis and optimization scenario, and conversion of selected scenario into programs and plans. Solution of the problems of risk management widely utilizes the so-called method of decision-tree. Among its advantages are the convenience and clarity of graphical presentation and ease of calculations. The method of decision-tree is particularly effective when a complex problem can be split into relatively simple tasks, each of which is addressed separately and then brought back for synthesis in complex solutions. Thus, the decision-tree comprises a trunk and branches of different sizes, and they all form a single process run by the laws of probability.

Since natural and man-made ES are characterized by a discrete occurrence and short duration, risk management is carried out: (Fig. 34).

1. prior to the emergence of a disaster;
2. during the period of the threat and emergence of a disaster;
3. after the events.

During the period of stable situations, prior to the emergence of ES, the main areas of management are risk assessment, expert-analytical and consulting work, monitoring of ES factors, analysis of monitoring information for disaster risk assessments in real time, selection of the object, design and construction of protective structures, introduction of safe technologies, implementation of preventive measures that reduce the risk of hazardous processes, implementation of measures of recipients' adaptation to the dangerous impacts (including insurance), establishment of warning systems, emergency response, and control.

In the period of an ES threat, management activities consist of the emergency notification

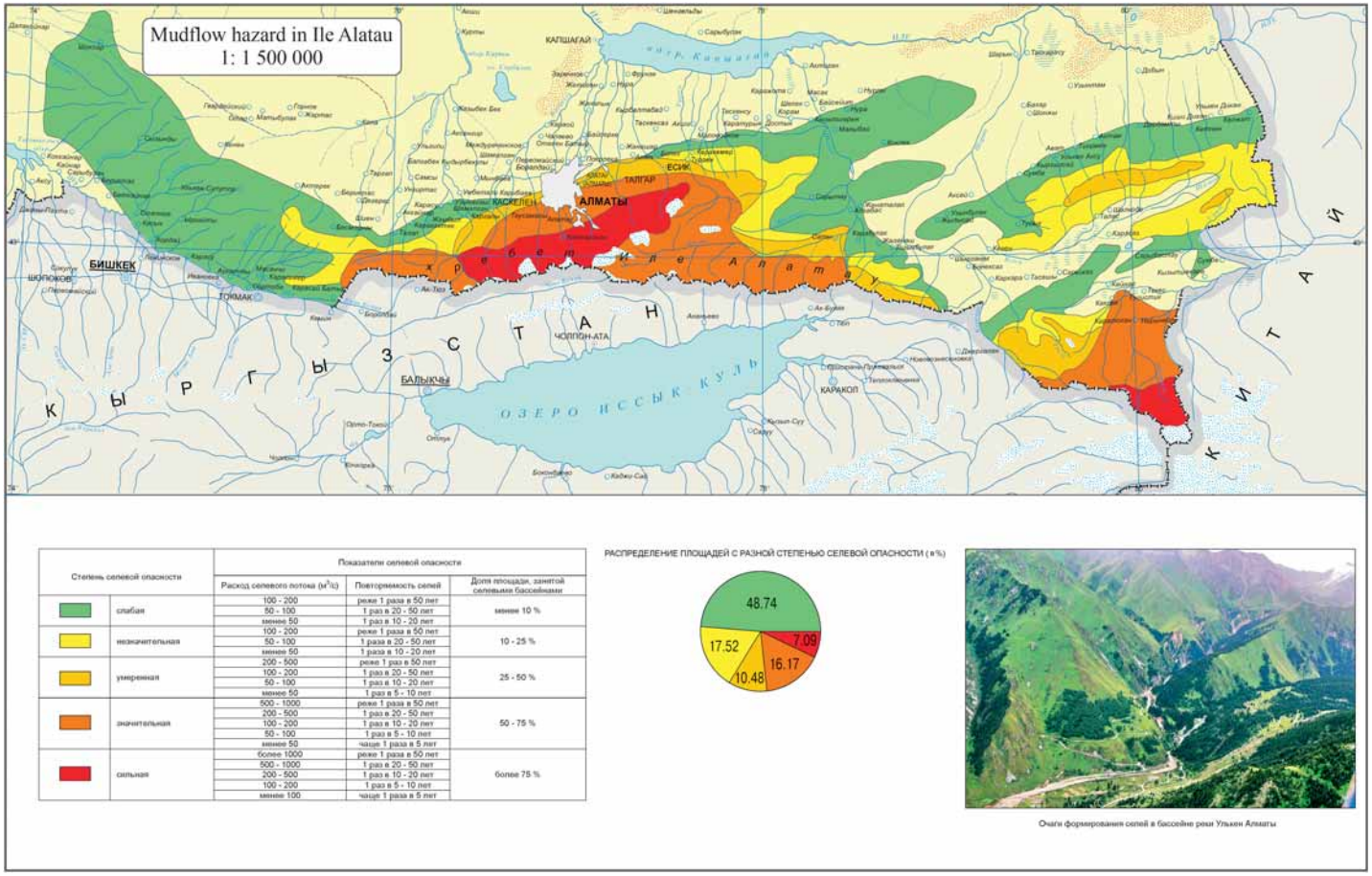

Очаги формирования селей в бассейне реки Улькен Алматы

Fig. 32. Map of mudflow hazard in Ile Alatau (from the "Atlas of natural and man-made hazards and risks of emergency situations" Almaty, 2012). The degree of mudflow hazard increases from green to red areas.

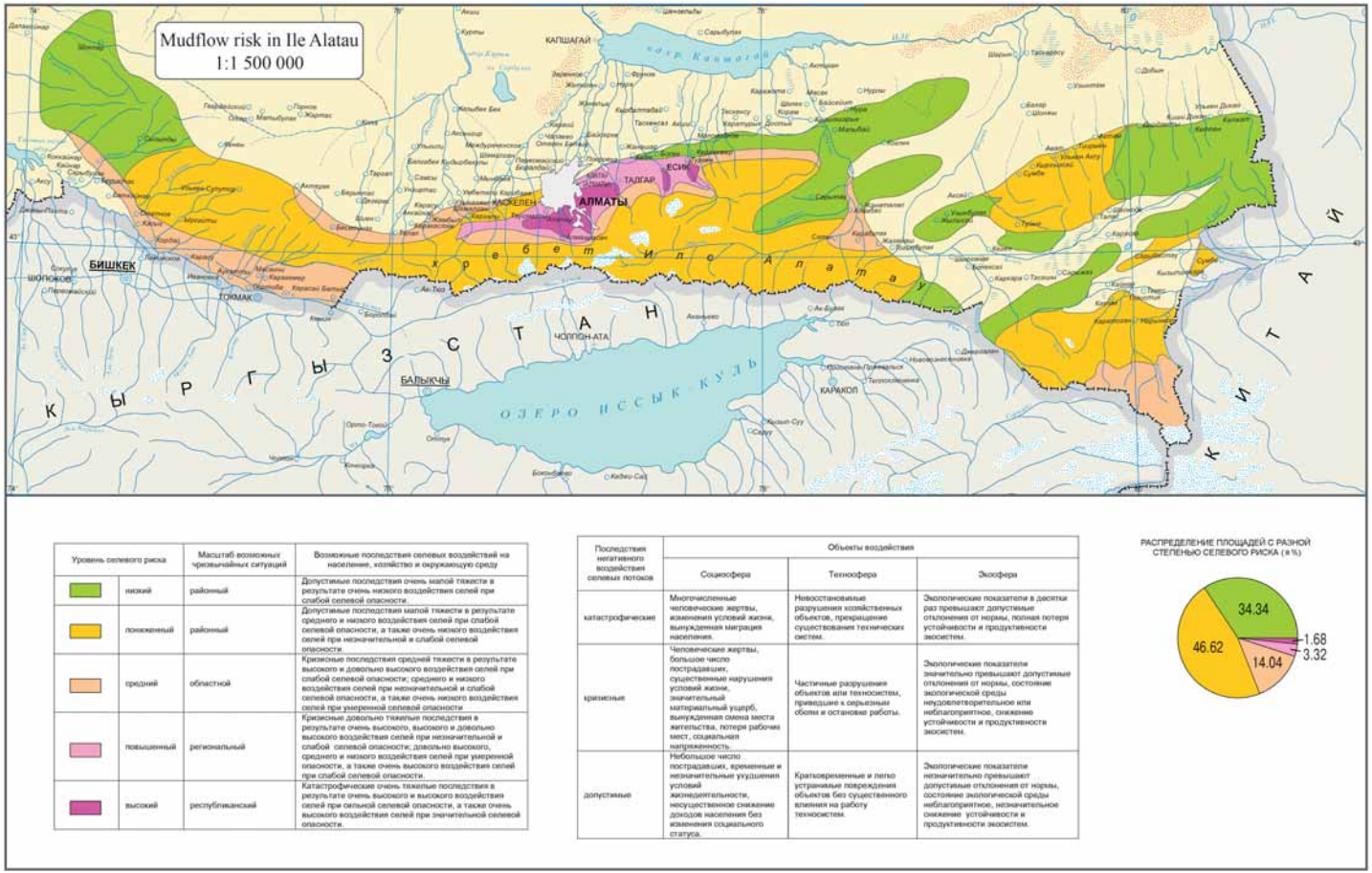

Уровень селевого риска		Масштаб возможных чрезвычайных ситуаций	Возможные последствия селевых воздействий на население, хозяйство и окружающую среду
	низкий	районный	Допустимые последствия очень малой тяжести в результате очень низкого воздействия селей при слабой селевой опасности.
	пониженный	районный	Допустимые последствия малой тяжести в результате среднего и низкого воздействия селей при слабой селевой опасности, а также очень низкого воздействия селей при незначительной и слабой селевой опасности.
	средний	областной	Кризисные последствия средней тяжести в результате высокого и довольно высокого воздействия селей при слабой селевой опасности; среднего и низкого воздействия селей при незначительной и слабой селевой опасности, а также очень низкого воздействия селей при умеренной селевой опасности
	повышенный	региональный	Кризисные довольно тяжелые последствия в результате очень высокого, высокого и довольно высокого воздействия селей при незначительной и слабой селевой опасности; довольно высокого, среднего и низкого воздействия селей при умеренной опасности, а также очень высокого воздействия селей при слабой селевой опасности.
	высокий	республиканский	Катастрофические очень тяжелые последствия в результате очень высокого и высокого воздействия селей при сильной селевой опасности, а также очень высокого воздействия селей при значительной селевой опасности.

Последствия негативного воздействия селевых потоков	Объекты воздействия		
	Социосфера	Техносфера	Экосфера
катастрофические	Многочисленные человеческие жертвы, изменения условий жизни, вынужденная миграция населения.	Невосстановимые разрушения хозяйственных объектов, прекращение существования технических систем.	Экологические показатели в десятки раз превышают допустимые отклонения от нормы, полная потеря устойчивости и продуктивности экосистем.
кризисные	Человеческие жертвы, большое число пострадавших, существенные нарушения условий жизни, значительный материальный ущерб, вынужденная смена места жительства, потеря рабочих мест, социальная напряженность.	Частичные разрушения объектов или техносистем, приведшие к серьезным сбоям и остановке работы.	Экологические показатели значительно превышают допустимые отклонения от нормы, состояние экологической среды неудовлетворительное или неблагоприятное, снижение устойчивости и продуктивности экосистем.
допустимые	Небольшое число пострадавших, временные и незначительные ухудшения условий жизнедеятельности, несущественное снижение доходов населения без изменения социального статуса.	Кратковременные и легко устранимые повреждения объектов без существенного влияния на работу техносистем.	Экологические показатели незначительно превышают допустимые отклонения от нормы, состояние экологической среды неблагоприятное, незначительное снижение устойчивости и продуктивности экосистем.

Fig. 33. Map of mudflow risk in Ile Alatau (from the "Atlas of natural and man-made hazards and risks of emergency situations" Almaty, 2012). The mudflow risk becomes higher from green to red and pink areas.

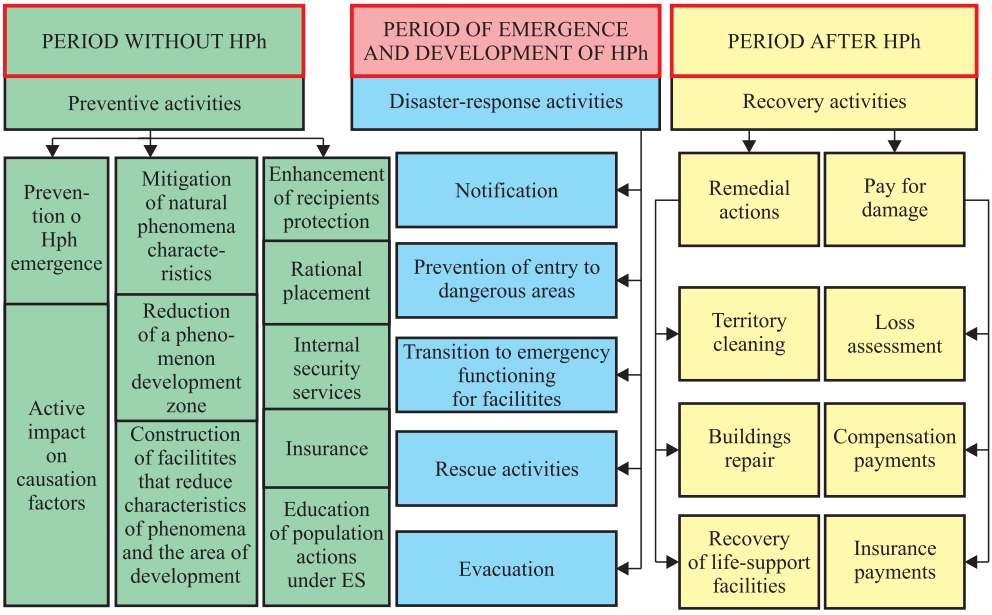

Fig. 34. Types of natural risks management.

of the recipients of its onset, emergency evacuation from the area of impact, and emergency measures to protect the objects from the damaging impact.

In the period of development of Es, management activities include emergency notification of recipients about the onset, urgent evacuation of the population out of the impact area, and emergency response activities for facilities protection from the destruction impact.

CONCLUSION

Summing up the above said, we can state that all over the world, including the Republic of Kazakhstan, there has been an increase of natural and man-made disasters involving loss of life and extensive material damage. Evidence-based scientific approach has been employed in accordance with the strategy of the international community to prevent and reduce the adverse impacts of disasters. One promising way to achieve security is to manage natural and man-made risks. The methodology of risks management developed by the MES Institute of Geography provides the science-based and integrated use of both existing methods for providing safety of the people and property and new activities insuring completeness, effectiveness, and adequacy. The practical implementation of the methodological foundations of risks management can make a significant contribution to the sustainable economic and social development of the country. ■

REFERENCES

1. Centre for Research on the Epidemiology of Disasters – CRED www.emdat.be/data base
2. Medeu, A.R. (2008) Geographicheskiye osnovy obespecheniya bezopasnosti zhiznedeyatelnosti v zonakh opasnykh prirodnykh i tekhnogennykh protsessov (Geographic fundamentals for life safety in the areas of natural hazards and man-made processes) // geographicheskiye problemy ustoichivogo razvitiya. Teoriya i praktika. / Trudy mezh-

dunarodnoy nauchno-practicheskoy konferentsii, posvyashchennoy 70-letiyu Instituta geografii. Almaty, Kazakhstan JSC TsNZMO, RK. pp. 8–16 (In Russian).

3. Medeu, A.R. (2011) Selevye yavleniya Yugo-Vostoka Kazakhstana. Osnovy upravleniya (Mudflows of the Southeast Kazakhstan. Management Basics). Almaty, 2011, Vol. 1, 284 p (In Russian).
4. The Ministry of Emergency Situations of the Republic of Kazakhstan. emer.gov.kz.

Akhmetkal R. Medeu, Professor (2009), Corresponding Member of the National Academy of Sciences of the Republic of Kazakhstan (NAS RK). He graduated from the Al-Farabi Kazakh National University in geography (1977). He is Doctor of Geographic Sciences (the title of his dissertation is "Scientific Fundamentals of Mudflow Processes Management in Seismic Mountain Geosystems of Kazakhstan," 1994). From 2001, he has been Director of the Institute of Geography, NAS RK. He has developed a scientific area with two priority directions: 1) modern geomorphogenesis and geomorphological and environmental-geomorphological mapping and 2) scientific and technological fundamentals of natural hazards protection and emergency risk management. He was scientific advisor of five Doctors of Sciences and 13 Candidate of Sciences. He is Editor-in-Chief and Principle Investigator of the "National Atlas of the Republic of Kazakhstan" (in 3 volumes), the "Atlas of the Mangistauskaya Oblast (in Kazakh, Russian, and English; 2010), and the "Atlas of Natural Hazards and Emergency Risks in the Republic of Kazakhstan." Under his management and with his direct participation, for the first time ever in Kazakhstan, the project "Water Resources of Kazakhstan" was conducted; the results were published in a 30-volume monograph. He is the author of over 150 scientific works, including six monographs and two dictionaries of geographic place-names.

Varvara V. Akimova[1*], Irina S. Tikhotskaya[2]
[1] Faculty of Geography, Lomonosov Moscow State University, Moscow, Russia; Leninskie Gory, 1, 119991; Tel.: + 7 495 9393621, e-mail: atlantisinspace@mail.ru
***Corresponding author**
[2] Faculty of Geography, Lomonosov Moscow State University, Moscow, Russia; Leninskie Gory, 1, 119991; Tel.: + 7 495 9393621, e-mail: iritiro@gmail.com

A WAY TO A SUSTAINABLE FUTURE: THE SOLAR INDUSTRY IN JAPAN

ABSTRACT. Solar energy is considered one of the most promising and rapidly growing sectors of the world economy. In line with the international trend of switching to renewable energy sources, particularly solar, and because of the tragic events at the Fukushima nuclear power station, Japan is experiencing a real "solar boom." However, despite all obvious advantages of using solar power (ensuring national energy security, overcoming concerns about environmental consequences of using fossil energy sources, etc.), Japan is facing several problems in its development. The most important one is the fact that technological and social progresses in Japan do not match each other as a result of a unique history of the nation. In order to promote renewable technology, the emphasis should be made on the role of the governmental policy and the effects of built-in tariffs for renewable energy sources. Considering dynamics and character of solar energy development in Japan, new energy strategy, and megasolar plants construction, the conclusion might be drawn that in the nearest future Japan will keep its place among the leaders in this field.

KEY WORDS: solar energy; photovoltaics in Japan; "solar boom" in Japan; solar panels; new energy strategy; megasolar power plants.

INTRODUCTION

The Sun is a powerful inexhaustible (and free!) source of renewable clean energy. If the total energy flux from the Sun during a year is to be converted into conventional fuel for oil, then this figure will be about 100 trillion tons that is ten thousand times more than the total current energy consumption of the Earth.

Not surprisingly, the solar energy industry is developing rapidly and steadily. At the end of 2010, there were 27.2 GW of solar photovoltaic power (PV) installed in the world and the growth rate in their capacity in just one year totaled 118 %. At the end of 2011, the installed capacity of photovoltaics in the world reached 69 GW and in 2012 – 103 GW, i.e. during 2010–2012, it increased by 3.8 times [Masson et al, 2013]. No other industry in the world, including telecommunications and computers, had such impressive growth. This is the most promising renewable energy industry; its growth rate is more than twice higher than that of its main competitor – the wind.

At present, solar energy is used in more than 60 countries, and in some countries is able to cause the most serious competition for conventional energy, especially in achieving grid parity (when the price of 1 kW • h produced using renewable energy sources is equal to or less than the cost of 1 kWh produced by conventional sources of energy).

The great potential of the solar industry development is the reason that many countries aim to ensure national energy security and are concerned about ecological consequences of fossil energy sources use and the volatility of their prices.

Among the factors that increase the attractiveness of solar energy is constant price reduction of electricity generated by solar power systems as a result of innovation and technological advancement. If 20 years ago 1 kWh cost 1 euro, now it costs 10 cents and sometimes even less [Masson et al, 2013]. Solar power systems are modular and allow creating power-generating stations of any capacity. They can work either connected to the public main electric networks (on-grid, or grid-connected), or standalone (off-grid).

At the same time, the solar industry development faces such problems as dependence on weather and time of a day, difficulties of energy accumulation, high cost of facilities, and the need for cleaning dust from reflecting surfaces, although all of them are gradually becoming technically solvable. For example, photovoltaic systems can operate using both direct and scattered solar radiation. And energy specific storage technologies are applied to ensure operation of the solar power around the clock, usually molten salt, or battery, or diesel generator adding to photovoltaic systems.

The vast majority of works dedicated to the solar industry have mainly economic or technical context and cannot be applied to geographical matters, which makes this study unique. This paper is based on the official statistical data and annual reports from international organizations involved in the solar energy field such as the International Energy Agency, the European Photovoltaic Industrial Association (EPIA), etc. The methods used are statistical and comparative analysis allowing studying the problem from different angles.

SOLAR ENERGY IN JAPAN

Japan is among the five leading countries developing solar energy (accounting for about 11 % of the world capacity (Fig. 1.)), which is partly due to a very high level of insolation in the country – 4.3–4.8 kW*h/m^2 per day.

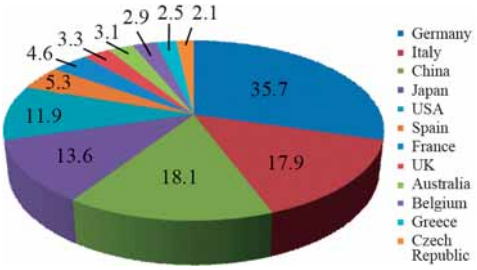

Fig. 1. Total photovoltaic capacity in 2013 (by leading countries).

At the beginning stage of the industry development, an important role in enhancing competitiveness and investment attractiveness is played by the state policy and governmental support measures including soft loans, grants, loans, and tax incentives. Japan was the first country to begin the development of solar energy at the legislative level. In 1994, the Ministry of Economy, Trade and Industry (METI) has adopted a program to subsidize individual solar installations and originally they covered 50 % of the photovoltaic systems cost. Precisely since then the solar industry has begun to develop rapidly. After the introduction of the renewable energy portfolio standards in 2003, the renewables share in the electricity production in Japan doubled and solar power gained a new impetus towards increasing capacity; though it is still extremely low and accounts for 2.4 % [International energy…, 2014]).

In 2004, Japan became the first country in the world to overcome the mark of 1 GW of solar power (Fig. 2), but remained the most powerful solar power generator (38 % of the world's installed photovoltaic capacity) only until 2005 [Japan lags behind…, 2007], when Germany has outstripped and is still leading in the photovoltaics field.

Japan's early leadership was achieved due to the above-mentioned measures of stimulating the solar industry. However, in the mid-2000s, its development has slowed down somewhat, for some time, partly because of the adoption of a new energy program in

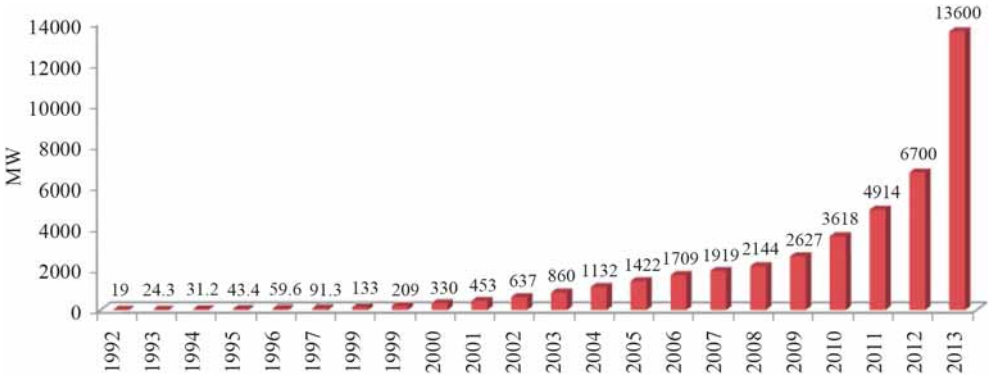

Fig. 2. Dynamics of photovoltaics' development in Japan, 1992-2013.

2002 aimed at further expansion of nuclear power to a capacity equivalent to 17.5 GW.

In accordance with METI Plan of innovative energy technologies "Cool Earth 50" adopted in 2008, by 2100, the share of nuclear energy in the primary energy mix was to be increased from 10 % to 60 % and the share of renewable resources from 5 % to 10 % (while the share of fossil fuel reduced from 85 % to 30 %). This scenario was developed by Nuclear Regulation Authority for the purpose of reducing carbon emissions by 2100 by 90 %, with half of this to be achieved by increasing the contribution of nuclear energy [Cool Earth…, 2008]. In June 2010, in order to ensure energy security and reduce carbon emissions, METI decided to increase self-sufficiency in terms of energy sources up to 70 % by 2030, mainly due to nuclear energy [Nuclear Power in Japan…, 2011].

However, the Great East Japan Earthquake in March 2011 has led to the revision of the national energy strategy, not least under public pressure, from increasing nuclear capacity to its abandonment and significant increase of the share of renewables in the energy mix.

In 2012, the Japanese government imposed an unprecedentedly high tariff on electricity generated by solar power systems: 42 yen per kWh (at that time an equivalent of about $0.53). In April 2013, it was decreased to 37.8 yen, or about $0.38 per kWh due to falling prices of solar cells. In accordance with this policy, the price of solar electricity is fixed for 20 years ahead. As a result, in just one year, the country of the rising sun joined the world "solar club," the group of the countries that have a total capacity of solar energy over 10 GW.

Immediately after the approval of the new tariff, in July 2012, Japanese homeowners installed capacity of 300 MW (i.e., about 10 MW per day), and in February 2013 – 837 MW, or 30 MW per day; industrial power stations commissioned 53 MW and 420 MW, accordingly [Masson et al, 2013]. A boom like that has not been seen anywhere else in the world. Thus, a doubling of this energy sector happened again in just one year. Its share in all of the country's generating capacity also doubled – up to 5 %.

As for solar cells and solar panels, in 2012 its total production in Japan was 2286 MW – slightly less than in 2011 (2497 MW). However, imports of solar cells actually tripled up to 776 MW (in 2011 – 263 MW) [Yamada, Ikki, 2013].

The distinctive feature about solar energy in Japan is the absolute predominance of individual photovoltaic installations (70 % of solar power in 2012 [Burger, 2012]), which differs Japan from Europe and America. They cover 900 thousand houses (overall there are 27 million houses in Japan). In the period ahead, through the use of battery chargers and "smart" meters, photovoltaic systems

in Japan are expected to turn into a regular "household appliance." Such orientation is quite natural as the country lacks large vacant spaces required for the power stations of industrial scale operation. Land-based power plants and other local sources not included in the overall grid accounted for only 20 % in 2011, although next year their share already rose to 30 % [Feed-in Tariff Scheme in Japan…, 2012], in line with the global trend towards solar megaprojects.

There are 40 solar parks in Japan. Basically, they were built due to existing subsidies for the purpose of experimental research, and now are going through the transition stage to commercialization. Their cost is still high, 400–500 thousand yen per kWh (while in other countries, there are cases when it is less than 300 thousand yen). With the release of China's solar panels to market, their value decreased; so in terms of international competitiveness, the cost of installing holders and auxiliary equipment comes to the forefront, as well as power drives.

One of the proposed megaprojects in Japan, the solar power station Kagoshima Nanatsujima (70 MW), in Prefecture Kagoshima, was launched in November 2013 by Kyocera. It is the largest sea-based solar power plant in Japan. Clean energy generated by this power station is fed into the national grid through a local utility company [Kyocera starts…, 2013]. The site is located close to the shore without disturbing the existing sea and land routes. In Tahara, on the peninsula Atsumi, a large solar power plant with capacity of 77 MW was expected to be built in 2014 [One of Japan's largest…, 2013].

Therefore, we can conclude that the factors of solar energy development in Japan are, on the one hand, the lack of free space, which prevents wide industrial implementation of it, and, on the other hand, the existence of the consumers who are aware of the profitability of individual photovoltaic installation from economic as well as from environmental perspective.

Corporate structure of the solar industry.

An early emergence of the photovoltaic market in Japan has had an evident influence on the development of high-tech industries and the production of solar cells and solar panels. Companies that gained from the state preferences at the first stage and are now leading the photovoltaics development in the country are Sharp, Sanyo, and Kyocera. Specifically these Japanese companies helped keeping development and production of solar panels worldwide afloat when, in 1990, the U.S. government decided to cancel funding of this industry.

The Sharp Company accounts for 3 % of the world solar panels market. Its products are used in various projects in the field of alternative energy: from electrifying satellites and lighthouses to powering industrial and residential facilities. Sharp's first research in the field of solar panels dates back as early as to 1959 and only in four years the company achieved mass production. In 1966, solar panels made by Sharp Solar Co. were installed on the largest lighthouse at that time. Ten years later, their products were installed on the Japanese satellite as well.

Since 1994, photovoltaic systems of this company have been used by homeowners. In 2005, Sharp Solar increased its annual production capacity to 400 MW and started mass production of thin film solar cells that can be used as a replacement to windows and building materials. In 2008, Sharp Solar was the first to hit the mark of 2 GW of power-generating capacity. Two years later, the company began mass production of solar photovoltaic systems with an efficiency of over 32.5 %, and its annual production capacity grew to 2.8 GW, which allowed it to become the number one producer of photovoltaic cells, in terms of revenues [Sincerity and creativity…, 2012].

Sharp Solar has three facilities in Japan: a production factory of photovoltaic cells and solar panels in Katsuragi, and plants in Tochigi

and Yao (Osaka), that produce end solar products. Apart from Japan, this company has facilities in the USA and in Europe: production of photovoltaic modules in the state of Memphis and in Wrexham, United Kingdom, that began in 2003.

In 2012, twelve Japanese companies were engaged in the production of solar panels: Sharp, Kyocera, Sanyo Electric Co., Ltd., Mitsubishi Electric (MELCO), Kaneka, Fuji Electric, Honda Soltec (a member of the Honda Motor Group), Solar Frontier (a part of Showa Shell Sekiyu Group), Clean Venture 21, PVG Solutions, Hi-nergy, and Choshu Industry Co. Most companies produce the first generation silicon solar cells, principally from the single-crystal silicon.

Obstacles and opportunities for solar energy development

Although Japan remains a tough market for "non-Japanese" companies, as Japanese consumers prefer to buy solar panels, like everything else, produced at home and not abroad, the country is really interested in attracting foreign companies to its market to accelerate the supply of photovoltaic components and, therefore, power stations construction.

It is even harder for foreign companies to get through to the customer on the Japanese market of inverters (power converters) because of the strict rules of certification, which are also constantly being tightened. It is not rare when a product needs to be upgraded before it can pay off. Therefore, today the market of inverters is the "bottleneck" that hinders the industry development in whole.

There is also an additional problem in Japan preventing the full implementation of solar installations into the existing grid that has roots in its history. Since the Meiji era, the electrical grid of Japan has a unique "Euro-American" structure: in the northeast, the current frequency is 50 Hz (as in Europe), and in the south-west – 60 Hz (as in the U.S.). This happened because in 1885, Tokyo Electric Light Co bought electrical equipment in Germany for the installation in the eastern part of Japan, where it had solid position and strong connections; Osaka Electric Lamp, in turn, purchased equipment from General Electrics to be used in the western part of the country. At the moment, there is only one frequency converter with a total capacity of 1 GW between these two power systems, which is far less than the existing electricity demand in Japan [Gordenker, 2011].

In order to be able to shift electricity to another part of the country, it is necessary to separate the electricity transportation capacity from its generation and sales. Thereby it will put an end to a more than a century of the fragmentation of the electricity grid.

In October 2013, Abe Government revised the law aimed at the liberalization of the energy market in 2015–2020 to create the monitoring service of electricity demand and supply in different regions of the country. This service will have the authority to order utility companies to supply more energy in case of deficit and, if necessary, even at the expense of increasing power generation. It will also be responsible for planning the highly variable production of renewable energy in order to distribute it more widely and effectively [Monitor power…, 2013].

However, creation of such an organization and considering the interests of all stakeholders, needs time, especially in Japan, where achieving a consensus after many discussions and consultations is a lengthy process. In this regard, energy companies may face certain problems. During the day, many consumers will be using the energy generated by their own solar panels, and selling expensive grid generated energy (due to the growing share of solar energy its price will inevitably raise) to them seems unreal. As a result, there will be underutilization of photovoltaic capacities.

And if the share of solar energy in the electricity generation in the country reaches

20 %, it will be impossible to sell the major part of this energy to consumers, as no one will be storing it for the night use.

Despite the current rapid development of solar energy in Japan, the existing subsidizing policy raises concern among members of the Japanese business groups. As experts rightly believe that supporting alternative energy may result in rising utility bills and slowdown in the domestic economy recovery, in connection with which, the new energy program of Japan once again appeals to the nuclear energy return as a temporary forced measure.

At the end of 2013, Keidanren announced that stopping nuclear power generation in Japan costs 3.6 trillion yen annually [A proposal for future…, 2013] that leave the country, as domestic investments are becoming extremely unprofitable. In addition, economic growth, of course, requires affordable energy that is also a powerful argument for keeping nuclear energy.

At the end of October 2014, only two reactors operated in Japan. Ccommissioning of the other 48 is only possible after they fully comply with the new requirements. The requirements include providing special countermeasures in case of critical emergency situations, such as the meltdown of the reactor core occurred in the 2011. For example, according to the Nuclear Regulation Authority, in September 2014, two reactors at the plant «Sendai» in Kagoshima Prefecture received a permit for commissioning, but only if the population of that area agrees.

Under the influence and pressure of all these circumstances, Japan, which has the complete nuclear fuel cycle (it includes enrichment and reprocessing of spent nuclear fuel for recycling), is turning back to the past. Contrary to the public expectations of a total abandonment of nuclear power plants, the new basic plan, released by the government in May 2014, not only turned back to nuclear power, but, in spite of the Kyoto Protocol, to the use of coal.

Despite certain difficulties named above (the lack of solar cells, the crisis of overproduction in other industrial segments of solar power system, the fragmentation of the country's electricity network), it can be assumed that Japan will continue to increase photovoltaic and solar thermal capacity, as incentives for the solar energy development have not disappeared, and a certain reserve, which was established in 2012, is the guarantee of the competitiveness of this sector. In support of this idea there are examples of large, sometimes seemingly incredible, solar projects.

"Luna Ring." Japanese construction company Shimizu, which has longer than 200-year history, has developed an original concept of "Luna Ring." Its goal is to generate solar energy on the Moon and transmit it to the Earth with the help of advanced space technologies [The energy paradigm shifts…, 2009]. Implementation of this project (the company hopes to accomplish it by 2035) would allow the clean energy production without interruption, regardless of weather conditions, and its use anywhere in the world.

In accordance with this plan, a ring of solar panels, producing a steady stream of energy, will be installed along the entire length of the equator of the Moon (11 thousand km). This stream of energy will go to the transmitting stations located on the front side of the Moon. Those will convert it into microwave energy and the laser light beams, and by using antenna 20 km in diameter, will pass it in the direction of the Earth.

The conversion of received energy into electrical one will be performed on the Earth and then supplied to the electricity grid or used for obtaining hydrogen (for storage or use as fuel).

"Space solar power." Japan Aerospace Exploration Agency (JAXA) has proposed an idea of building the space station to collect solar energy.

The basic concept of orbital solar park, which can meet the energy needs of humanity,

involves the creation of a giant photovoltaic platform in the Earth orbit. This platform will be used to collect solar energy with its subsequent direction in the form of microwaves to receiving stations located on our planet. Thereafter, the received energy will be converted into electricity.

For the realization of this project, the Japanese Aerospace Exploration Agency has developed a complicated scheme. Road map, compiled by Japanese experts, describes the creation of a commercial system consisting of a series of ground-based and orbiting stations with a total capacity of 1 GW by 2030. This is comparable with a standard nuclear power plant.

The project, presented in the journal IEEE Spectrum, involves the construction of an artificial island of 3 kilometers in length, where a huge network of 5 billion tiny antennas will be rolled out to convert the microwave frequency radio waves into electricity [Sasaki, 2014]. A substation on the island will be used for the transmission of electricity via underwater cable to Tokyo to support the industrial zones and urban neighborhoods. Collection of solar energy will be carried out at an altitude of 36 thousand kilometers above the Earth's surface.

Experts emphasize that it will be difficult and expensive, but the result is worth it, not only from the economic point of view. Throughout human history the appearance of each new energy source, starting with wood, continuing with coal, oil, gas, and ending with nuclear energy, was associated with the revolution. If the humanity masters collecting solar energy in space, satellites in the orbit could provide its almost infinite energy, putting an end to conflicts occurring as a result of the struggle for energy resources of the Earth. Placing an increasing number of equipment in space will give rise to the development of a prosperous and peaceful civilization beyond the Earth.

"Village of the Future." In the coastal town of Minamisoma, Fukushima Prefecture, contaminated in 2011 as a result of the accident at the nuclear power plant, a real, on the contrary, down-to-Earth project is being developed, that is a model of the village of the future. This project is being performed in the area, two-thirds of agricultural land of which is in the evacuation zone due to nuclear contamination. There are already 120 photovoltaic panels that produce 30 kilowatts of power in the proposed village.

The centerpiece of the project is what the Japanese call "solar sharing" (i.e., joint use of solar energy), which allows growing crops under elevated solar panels. The project is supported by generous tariffs set by the government. Income from yields and energy will be reinvested in the project.

Its proponents hope that this model will be used by farmers, whose livelihood had been undermined because of nuclear contamination that occurred in the 2011 after the Fukushima accident. The model of the village of renewable energy offers a way out of a difficult situation. It could help save the Earth and the settlements, and by generating revenue from two sources at the same time could even lead to higher returns than in the past.

CONCLUSION

Due to the revision of the subsidy program for solar energy and the introduction of the feed-in tariff in 2012, four times the world average, there is a rapid progress in the solar industry development in Japan. As a result, it overtook Germany to become the world leader in photovoltaics in terms of value.

Obviously, the real breakthrough in solar energy in Japan has already occurred, although a complete substitution of fossil fuels is possible only with the exponential technological, social, and political development. However, given its high dependence on energy recourses import and the problems caused by the disaster in 2011, Japan will definitely be among the leaders hereafter as well. Possible

return to nuclear energy and coal in accordance with the new energy strategy can be regarded as an emergency temporary measure to support the national economy. In terms of this transition, a cut in government subsidies for solar energy will result in nothing else but the decrease in price of solar electricity, which, in turn, will help solar energy to achieve grid parity. As a result, in years to come, the industry will become self-sufficient, and the prospects of its development will be even more favorable. ■

REFERENCES

1. A proposal for future energy policy (2013). Keidanren, Japan Business Federation [online]. Available from: http://www.keidanren.or.jp/en/policy/2013/089.html [Accessed 01.10.2014].

2. Burger S. (2012) The Reign of Residential PV in Japan [online]. Greentechmedia. Available from: http://www.greentechmedia.com/articles/read/the-reign-of-residential-pv-in-japan [Accessed 01.10.2014].

3. Cool Earth-innovative energy technology program (2008). Ministry of Economy, Trade and Industry (METI) [online]. Available from: http://www.meti.go.jp/english/newtopics/data/pdf/031320CoolEarth.pdf [Accessed 01.10.2014].

4. Feed-in tariff scheme in Japan (2012). Ministry of Economy, Trade and Industry (METI) [online]. Available from: http://www.meti.go.jp/english/policy/energy_environment/renewable/pdf/summary201207.pdf [Accessed 01.10.2014].

5. Gordenker A. (2011). Japan's incompatible power grids [online]. The Japan Times. Available from: http://www.japantimes.co.jp/news/2011/07/19/reference/japans-incompatible-power-grids/#.VCvOhmd_uSp [Accessed 01.10.2014].

6. International energy statistics (2014). U.S. Energy Information Administration [online]. Available from: http://www.eia.gov/countries/cab.cfm?fips = ja [Accessed 01.10.2014].

7. Japan lags behind Europe in solar power (2007). EcoEarth (Environmental Portal&Search Engine) [online]. Available from: http://www.ecoearth.info/shared/reader/welcome.aspx?linkid = 74644 [Accessed 01.10.2014].

8. Kyocera starts operation of 70MW Solar Power Plant, the largest in Japan (2013). Kyocera news releases [online]. Available from: http://global.kyocera.com/news/2013/1101_nnms.html [Accessed 01.10.2014].

9. Masson G., Latour M., Rekinger M., Theologitis I.-T., Papoutsi M. (2013) Global market outlook for photovoltaics 2013–2017, EPIA [online]. Available from: http://www.epia.org/fileadmin/user_upload/Publications/GMO_2013_-_Final_PDF.pdf [Accessed 01.10.2014].

10. Monitor power industry reform (2013). The Japan news. Available from: http://www.japantimes.co.jp/opinion/2013/11/24/editorials/monitor-power-industry-reform/#.UvkRqWJ_s8o [Accessed 01.10.2014].

11. Nuclear power in Japan (2014). World Nuclear Association [online]. Available from: http://www.world-nuclear.org/info/Country-Profiles/Countries-G-N/Japan/ [Accessed 01.10.2014].

12. One of Japan's largest mega solar projects to be built in Aichi (2013). Mitsubishi Corporation [online]. Available from: http://www.mitsubishicorp.com/jp/en/pr/archive/2013/html/0000018356.html [Accessed 01.10.2014].

13. Sasaki S. (2014). JAXA wants to make the sci-fi idea of space-based solar power a reality [online]. IEEE Spectrum. Available from: http://spectrum.ieee.org/green-tech/solar/how-japan-plans-to-build-an-orbital-solar-farm [Accessed 01.10.2014].

14. Sincerity and creativity (2012). Sharp [online]. Available from: http://sharp-world.com/corporate/img/info/his/h_company/pdf_en/all.pdf [Accessed 01.10.2014].

15. The Energy paradigm shift opens the door to a sustainable society (2009). Shimizu corporation [online]. Available from: http://www.shimz.co.jp/english/theme/dream/lunaring.html [Accessed 01.10.2014].

16. Yamada H., Ikki O. (2013). National survey report of PV power application in Japan 2013, International Energy Agency photovoltaic power systems programme [online]. Available from: http://www.iea-pvps.org/index.php?id = 93&no_cache = 1&tx_damfrontend_pi1[showUid] = 2099&tx_damfrontend_pi1[backPid] = 93 [Accessed 01.10.2014].

Varvara V. Akimova studied Social and Economic Geography at the Lomonosov Moscow State University. She graduated with honors in 2014 and obtained her Specialist's degree (Diploma). From October 2014, she is a Ph. D student of the Department of Social and Economic Geography of Foreign Countries of the Faculty of Geography, Moscow State University. The focus of her studies is in alternative energy, solar energy complex, and oil and gas sector.

Irina S. Tikhotskaya is Associate Professor of the Faculty of Geography, Lomonosov Moscow State University, since 1999; she was previously Senior Researcher at the Institute of Oriental Studies, the Russian Academy of Sciences, where she received her Ph. D. in Economics in 1982. Her research interests relate to social and economic geography and regional studies of Japan. She writes extensively and is the author of several textbooks (e.g., Social and Economic Geography of the Foreign World, in co-authorship, ed. by V.V. Volskii, 2005), books (e.g., The Raw Materials Problem of Modern Japan, 1987), and a number of articles (e.g., Economic and Geographical Problems of Waste Utilization in Japan: Towards Sound Material Cycle Society 2010

INSTRUCTIONS FOR AUTHORS CONTRIBUTING TO "GEOGRAPHY, ENVIRONMENT, SUSTAINABILITY"

AIMS AND SCOPE OF THE JOURNAL

The scientific English language journal "GEOGRAPHY, ENVIRONMENT, SUSTAINABILITY" aims at informing and covering the results of research and global achievements in the sphere of geography, environmental conservation and sustainable development in the changing world. Publications of the journal are aimed at foreign and Russian scientists – geographers, ecologists, specialists in environmental conservation, natural resource use, education for sustainable development, GIS technology, cartography, social and political geography etc. Publications that are interdisciplinary, theoretical and methodological are particularly welcome, as well as those dealing with field studies in the sphere of environmental science.

Among the main thematic sections of the journal there are basics of geography and environmental science; fundamentals of sustainable development; environmental management; environment and natural resources; human (economic and social) geography; global and regional environmental and climate change; environmental regional planning; sustainable regional development; applied geographical and environmental studies; geo-informatics and environmental mapping; oil and gas exploration and environmental problems; nature conservation and biodiversity; environment and health; education for sustainable development.

GENERAL GUIDELINES

1. Authors are encouraged to submit high-quality, original work: scientific papers according to the scope of the Journal, reviews (only solicited) and brief articles. Earlier published materials are accepted under the decision of the Editorial Board.

2. Papers are accepted in English. Either British or American English spelling and punctuation may be used. Papers in French are accepted under the decision of the Editorial Board.

3. All authors of an article are asked to indicate their **names** (with one forename in full for each author, other forenames being given as initials followed by the surname) and the name and full postal address (including postal code) of the **establishment(s)** where the work was done. If there is more than one institution involved in the work, authors' names should be linked to the appropriate institutions by the use of 1, 2, 3 etc superscript. **Telephone and fax numbers and e-mail addresses** of the authors could be published as well. One author should be identified as a **Corresponding Author**. The e-mail address of the corresponding author will be published, unless requested otherwise.

4. The GES Journal style is to include information about the author(s) of an article. Therefore we encourage the authors to submit their photos and short CVs.

5. The optimum size of a manuscript is about 3 000–5 000 words. Under the decision (or request) of the Editorial Board methodological and problem articles or reviews up to 8 000–10 000 words long can be accepted.

6. To facilitate the editorial assessment and reviewing process authors should submit "full" electronic version of their manuscript with embedded figures of "screen" quality as a **.pdf file.**

7. We encourage authors to list three potential expert reviewers in their field. The Editorial Board will view these names as suggestions only. All papers are reviewed by at least two reviewers selected from names suggested by authors, a list of reviewers maintained by GES, and other experts identified by the associate editors. Names of the selected reviewers are not disclosed to authors. The reviewers' comments are sent to authors for consideration.

MANUSCRIPT PREPARATION

Before preparing papers, authors should consult a current issue of the journal at http://www.geogr.msu.ru/GESJournal/index.php to make themselves familiar with the general format, layout of tables, citation of references etc.

1. Manuscript should be compiled in the following **order**: authors names; authors affiliations and contacts; title; abstract; key words; main text; acknowledgments; appendices (as appropriate); references; authors (brief CV and photo)

2. The **title** should be concise but informative to the general reader. The **abstract** should briefly summarize, in one paragraph (up to 1,500 characters), the general problem and objectives, the results obtained, and the implications. Up to six **keywords**, of which at least three do not appear in the title, should be provided.

3. The **main body** of the paper should be divided into: (a) **introduction**; (b) **materials and methods**; (c) **results**; (d) **discussion**; (e) **conclusion**; (f) **acknowledgements**; (g) **numbered references**. It is often an advantage to combine (c) and (d) with gains of conciseness and clarity. The next-level subdivisions are possible for (c) and (d) sections or their combination.

4. All **figures** (including photos of the authors) are required to be submitted as separate files in original formats (CorelDraw, Adobe Photoshop, Adobe Illustrator). Resolution of raster images should be not less than 300 dpi. Please number all figures (graphs, charts, photographs, and illustrations) in the order of their citation in the text. **Composite figures** should be labeled A, B, C, etc. Figure captions should be submitted as a separate file.

5. Tables should be numbered consecutively and include a brief title followed by up to several lines of explanation (if necessary). Parameters being measured, with units if appropriate, should be clearly indicated in the column headings. Each table should be submitted as a separate file in original format (MS Word, Excel, etc.).

6. Whenever possible, total number of **references** should not exceed 25–30. Each entry must have at least one corresponding reference in the text. In the text the surname of the author and the year of publication of the reference should be given in square brackets, i.e. [Author1, Author2, 2008]. Two or more references by the same author(s) published in the same year should be differentiated by letters a, b, c etc. For references with more than two authors, text citations should be shortened to the first name followed by et al.

7. References must be listed in alphabetical order at the end of the paper and numbered with Arabic numbers. References to the same author(s) should be in chronological order. Original languages other than English should be indicated in the end of the reference, e.g. (in French), (in Russian) etc.

Journal references should include: author(s) surname(s) and initials; year of publication (in brackets); article title; journal title; volume number and page numbers.

References to books should include: author(s) surname(s) and initials; year of publication (in brackets); book title; name of the publisher and place of publication.

References to multi-author works should include after the year of publication: chapter title; "In:" followed by book title; initials and name(s) of editor(s) in brackets; volume number and pages; name of the publisher and place of publication.

All references in Cyrillic should be transliterated (please use http://www.translit.ru); English translation of the name of publication is given in square brackets after its transliteration.

8. Authors must adhere to SI units. Units are not italicised.

9. When using a word which is or is asserted to be a proprietary term or trade mark, authors must use the symbol ® or TM.

10. As Instructions for Authors are subjected to changes, please see the latest "Example of manuscript style" at http://www.geogr.msu.ru/GESJournal/author.php

MANUSCRIPT SUBMISSION

Authors are encouraged to submit their manuscripts electronically. Electronic submissions should be sent as e-mail attachments to GESJournal@yandex.ru

ISSN 2071-9388

SOCIALLY SCIENTIFIC MAGAZINE "GEOGRAPHY, ENVIRONMENT, SUSTAINABILITY"

No. 03(v. 08) 2015

FOUNDERS OF THE MAGAZINE: Faculty of Geography, Lomonosov Moscow State University and Institute of Geography of the Russian Academy of Sciences

The magazine is published with financial support of the Russian Geographical Society.

The magazine is registered in Federal service on supervision of observance of the legislation in sphere of mass communications and protection of a cultural heritage. The certificate of registration: ПИ МФС77-29285, 2007, August 30.

EDITORIAL OFFICE
Lomonosov Moscow State University
Moscow 119991 Russia
Leninskie Gory,
Faculty of Geography, 2108a
Phone 7-495-9392923
Fax 7-495-9328836
E-mail: GESJournal@yandex.ru

DESIGN & PRINTING

Advertising and Publishing Agency "Advanced Solutions"
Moscow, 119071 Russia,
Leninskiy prospekt, 19, 1
Phone 7-495-7703659
Fax 7-495-7703660
E-mail: om@aov.ru

DISTRIBUTION

East View Information Services
10601 Wayzata Blvd, Minneapolis, MN 55305-1526 USA
Phone +1.952.252.1201 Fax +1.952.252.1202
E-mail: periodicals@eastview.com
www.eastview.com

Sent into print 26.09.2015
Order N gi315

Format 70 × 100 cm/16
8.45 p. sh.
Digital print
Circulation 850 ex.